Expression of microRNAs and their Precursors

in Synaptic Fractions

of Adult Mouse Forebrain

BY

GIOVANNI LUGLI
M.S., Universita' di Modena, Italy, 1994

THESIS

Submitted as partial fulfillment of the requirements
for the degree of Doctor of Philosophy in Neuroscience
in the Graduate College of the
University of Illinois at Chicago, 2011

Chicago, Illinois

Defense Committee:

Neil R. Smalheiser, Chair and Advisor
John Larson
Yogesh Dwivedi
Michael Ragozzino, Psycology
Thomas Park, Biological Sciences
Peter Penzes, Northewestern University Feinberg School of Medicine

ACKNOWLEDGMENTS

I would like to thank my thesis advisor, Neil R. Smalheiser, and my thesis committee (John Larson, Yogesh Dwivedi, Michael Ragozzino, Thomas Park and Peter Penzes) for their support and assistance. They provided guidance in all areas that helped me accomplish my research goals.

I would also like to thank Maryann Martone and Ying Jones for performing electron microscopy study, and Michael Demars for the immunohistochemistry study.

I would like to acknowledge Chris Adams and Bradley Love (Invitrogen) for supervising the microarray labeling and hybridizations and for helpful discussions.

GL

TABLE OF CONTENTS

TABLE OF CONTENTS (continued)

LIST OF TABLES

LIST OF FIGURES

LIST OF FIGURES (continued)

FIGURE PAGE

LIST OF FIGURES (continued)

LIST OF ABBREVIATIONS

aa	amino acids
AGO	Argonaute
AMPA	2-amino-3-(5-methyl-3-oxo-1,2- oxazol-4-yl)propanoic acid
APT1	acyl protein thioesterase 1
BDNF	brain-derived neurotrophic factor
Bp	base pairs
BrdU	Bromodeoxyuridine
C. elegans	Caenorhabditis elegans
co-IP	co-immunoprecipitation
CREB	cAMP response element-binding
DGCR8	Di George syndrome critical region 8
DUF283	Domain of unknown function 283
dFMR1	Drosophila FMRP
dsRBD	double stranded RNA binding domain
dsRNA	double stranded RNA
EM	electron microscopic immunocytochemistry
FMRP	Fragile X mental retardation protein
IHC	immunohistochemistry
kDa	kilo Dalton
KHC	Kinesin heavy chain
KIF	Kinesin protein

LIST OF ABBREVIATIONS (continued)

KLC	Kinesin light chain
LM	light microscopic immunocytochemistry
LTP	long term potentiation
MAGUK	membrane-associated guanylate kinase
Mg	magnesium
miR-	microRNA
miRNA	microRNA
mRNA	messenger RNA
NMDA	N-methyl D-aspartate
Nt	nucleotides
PACT	protein activator of PKR
PAZ	Piwi Argonaute Zwille
pre-miRNA	microRNA precursor
pri-miRNA	microRNA primary transcript
PRR	Proline rich region
PSD	post-synaptic density
RISC	RNA-induced silencing complex
RNAi	RNA interference
RS	Arginie/Serine domain
qRT-PCR	quantitative (real time) reverse transcriptase polymerase chain reaction
siRNA	small interfering RNA

LIST OF ABBREVIATIONS (continued)

SynN	Synaptoneurosome
TRBP	transactivating response RNA-binding protein
UTR	untranslated region

SUMMARY

The expression of microRNAs and selected microRNA precursors and primary microRNA transcripts have been characterized within several synaptic fractions of adult mouse forebrain, including synaptoneurosomes, synaptosomes and isolated postsynaptic densities, using methods of microRNA microarray, real time qRT-PCR, Northern blotting and immunopurification using anti-PSD95 antibody. The majority of brain microRNAs (especially microRNAs known to be expressed in pyramidal neurons) are detectably expressed in synaptic fractions, and a subset of microRNAs is significantly enriched in synaptic fractions relative to total forebrain homogenate. MicroRNA precursors and primary microRNA transcripts are also detectable in synaptic fractions at levels that are at least comparable to whole tissue. Whereas mature microRNAs are predominantly associated with soluble components of the synaptic fractions, microRNA precursors and primary microRNA transcripts are predominantly associated with postsynaptic densities.

I characterized a new Drosha antibody, and proved to be suitable for immunoprecipitation studies in vivo. To confirm the specificity of the Drosha antibody Drosha was silenced in N2a cells using siRNA and found that Drosha 160kDa immunoreactive band was specifically decreased.

Through subcellular fractionation study, affinity purification of the postsynaptic densities and immunohistochemistry analyses of adult mouse hippocampus, I showed that Drosha and DGCR8 are localized where PSD-95 is detected. Moreover, Drosha and DGCR8 are also associated in vivo with KIF5.

These findings support the proposal that microRNAs may be formed, at least in part, via processing of primary microRNA transcripts and/or microRNA precursors locally, within dendritic spines. Drosha, DGCR8 and Dicer are expressed in postsynaptic densities, whereas Dicer is enzymatically inactive until conditions that activate Calpain cause its liberation. Since Dicer is able to process primary-like microRNA transcripts and microRNA precursors, I propose that synaptic stimulation may lead to local processing of microRNA precursor-forms (pre and pri) in proximity to the synapse.

I. INTRODUCTION

1. Discovery of microRNAs

In 1993, Lee (1993), discovered that lin-4 RNA, a gene known to control the timing of *Caenorhabditis elegans* (*C. elegans*) larval development, does not code for a protein but instead produces a pair of small RNAs and negatively regulates the translation of LIN-14 protein. This discovery can be considered the first evidence of the existence of what we now know as microRNAs. They then suggested that because the lin-4 sequence had complementarity to the lin-14 3'UTR region, a possible mechanism of action to be an antisense RNA-RNA interaction. They also noted that the steady state levels of the Lin-14 mRNA were not altered in the lin-4 mutant background. And they suggested some possible explanations for the antisense regulation mechanism. The inhibition of translation could be caused by a post-transcriptional modification of the mRNA by the short lin-4 RNA or by the relocation of the mRNA to a different subcellular compartment, making it not accessible to the ribosomes. Finally, the antisense RNA binding to the mRNA could prevent the ribosomes from accessing the mRNA and translating it (Lee, 1993).

A few years later, in 1998, Fire (1998) showed that the use of short double-stranded RNA (dsRNA) sequences injected in the C. elegans, were shown to selectively inhibit the translation of the complimentary mRNA. Injected animals with a synthetic dsRNA sequence homologous to unc-22 mRNA resulted in almost completely undetectable endogenous mRNA levels and the phenotype created was highly specific. Even the progeny of injected animals showed loss of function mutation in unc-22. Fire (1998) further confirmed the target

specificity of dsRNA with three other genes with a well-characterized phenotype. From then on, it was clear that dsRNA was highly effective in RNA interference. This exogenous perfectly matching double-stranded RNA sequence is called small interfering RNA (siRNA) and is a useful tool to study gene function. Only a couple of years later, Zamore (2000) showed that longer exogenous dsRNA could be processed in the Drosophila lysate in RNA fragments of about 21-23 nucleotides (nt) of length in an ATP dependent manner. Also, the mRNA was cleaved in the corresponding binding site of the short dsRNA.

In 2001, the mechanism of posttranscriptional regulation produced by microRNAs, previously thought to be limited to lin-4 and let-7 microRNAs, was discovered to be more general than previously anticipated. Lagos-Quintana (2001) showed that these endogenous 22 nt. long RNAs were not only present in invertebrates and vertebrates, but their sequences, which are similar to let-7 microRNA, were also highly conserved in them. They also offered valuable predictions about the genomic organization of some microRNA gene clusters and their predicted precursor structures. A more detailed tissue-specific cloning in mice opened up the possibility that some of these newly discovered microRNAs could have a distinctive expression pattern in different tissues. For example, microRNA 124a (miR-124a) was found to be clearly brain dominant whereas microRNA 122 (miR-122) liver dominant (Lagos-Quintana, 2002). By cloning strategies both in plants, invertebrates and vertebrates, more and more microRNAs have been discovered (Lagos-Quintana, 2003). Today, the actual microRNA database has more than 10,000 entries as a result of deep-sequence techniques (Ryu, 2011).

2. The microRNA pathway

2.1. From primary transcripts to mature microRNAs

The first evidence that microRNAs were processed from a longer sequence was shown by Lee (1993), while demonstrating that in C. elegans Lin-4 encodes for a short RNA. Shortly afterwards, Pasquinelli (2000) predicted that these longer precursor sequences could actually arise from a stem loop structure, which was later labeled as microRNA precursor (pre-miRNA) (Grishok, 2001). These precursor hairpin structures of about 70 nt. long arise from longer transcripts, which are named primary microRNAs (pri-miRNAs) (Lee, 2002).

Analysis of the genomic positions of some known human and mouse microRNAs led Lagos-Quintana (2003) to predict that at least half of these transcripts are localized in intergenic regions. Of the remaining microRNAs, some were found in sense orientation within introns of coding transcripts, others in sense orientation within introns of noncoding genes, and others in the reverse orientation within an intronic region. The conclusion from this study was that microRNAs can be either transcribed from their own promoters or derived from a pre-mRNA that frequently codes for an additional gene product (Lagos-Quintana, 2003). One of the features of microRNAs is that they can occur in clusters that are co-expressed (Lagos-Quintana, 2001, 2002; Lau, 2001; Lee, 2002). The microRNA genes that have been found in close proximity, suggesting that they are expressed as a single transcriptional unit, are called polycistronically expressed (Lee, 2002). Cai (2004) found out that the intergenic human pri-miRNAs, that they analyzed, had a 3' poly(A) tail and a 5' 7-methil guanylate (m7G) cap, which are specific characteristics of most of the eukaryotic mRNAs. They also showed that a small amount of the full length pri-miRNAs that they tested reach the cytoplasm in HeLa cells. This data supports the microRNA stepwise

processing and subcellular localization model proposed by Lee (2002) in which the generation of the pre-miRNAs (~ 70 nt long) from the longer transcripts pri-miRNA takes place primarily in the nucleus and the processing of the pre-miRNAs into mature miRNAs takes place into the cytoplasm.

The mature microRNA, about 22 nt. long can reside on either arm of the precursor, but its features, or those of its precursor, must determine which side of the fold-back contains the stable product (Lau, 2001). The presence of 5′ phosphate and 3′ hydroxyl termini suggests that the dsRNA could be processed by an enzymatic activity similar to *Escherichia coli* RNase III (Nicholson, 1999). MicroRNAs can be distinguished from most other RNA oligonucleotide fragments by three criteria: a length of about 22 nt., a 5′-terminal monophosphate, and a 3′-terminal hydroxyl group (Elbashir, 2001; Bernstein, 2001; Hutvágner, 2001).

2.2. The microRNA pathway.

In a very short period of time, researchers uncovered key protein components involved in the microRNA pathway (Figure 1). In mammals, the majority of endogenous microRNA genes are transcribed initially as pri-miRNAs by RNA polymerase II (Lee, 2004; Cai, 2004). The enzyme Drosha together with "Di George syndrome critical region 8" (DGCR8), which both belong to the RNase III family, initiate the microRNA processing (Lee, 2003; Han, 2004), cleaving both strands near the base of the primary stem-loop and yielding the pre-miRNA. Mirtrons are alternative precursors for microRNA biogenesis that were recently described in invertebrates. These short hairpin introns use splicing to bypass

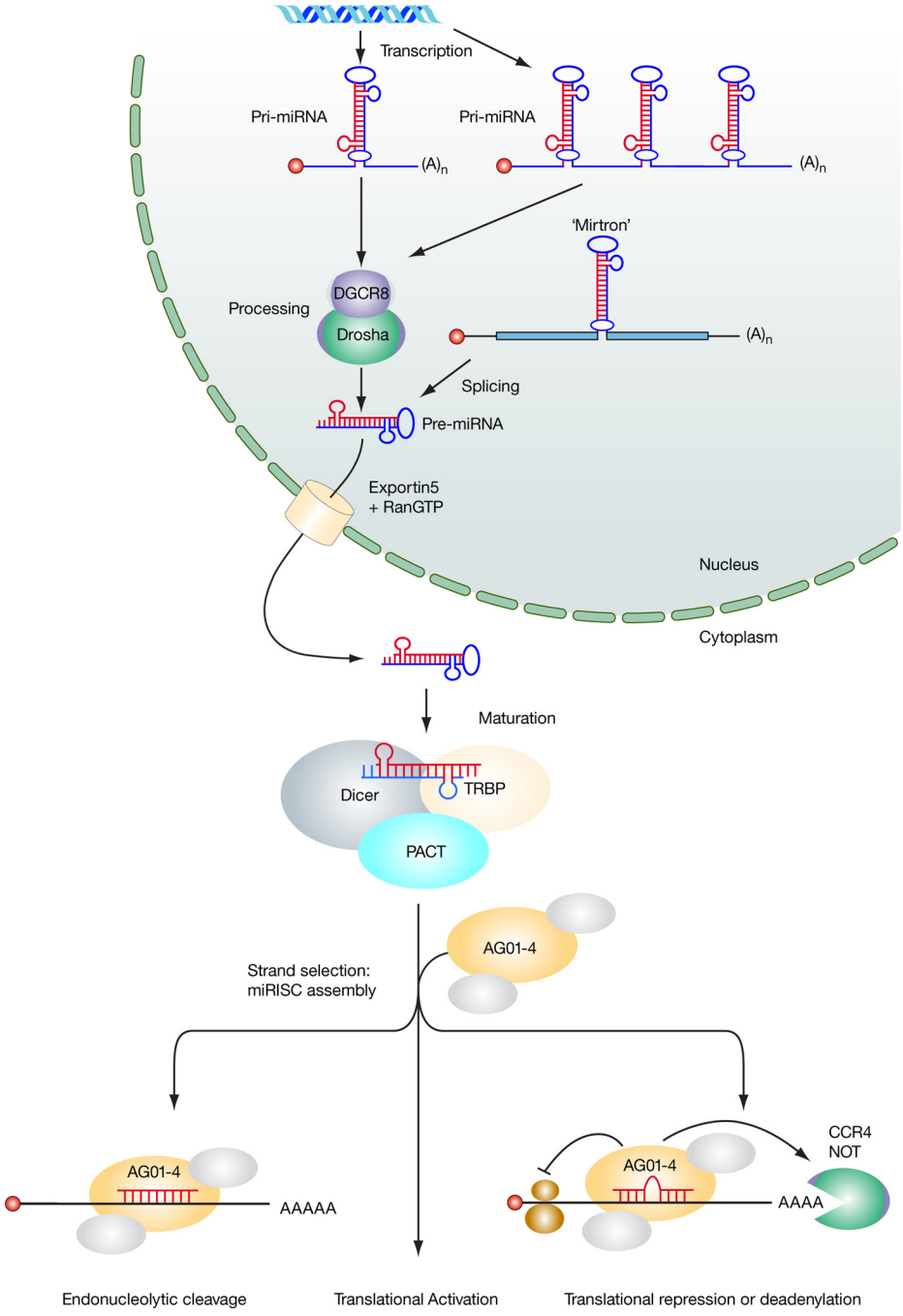

Figure 1. The microRNA pathway
Adapted by permission from Macmillan Publisher Ltd.: [Nature Reviews Genetics] (9, 1002-1114), copyright (2008).

Drosha cleavage, which is otherwise essential for the generation of canonical animal microRNAs (Berezikov, 2007).

RNase III proteins are double-stranded RNA (dsRNA) endonucleases, which were first discovered and characterized in *E.Coli* and whose enzymatic activity is dependent on either the divalent cations magnesium or manganese, but not calcium nor zinc (Li, 1993).

Drosha polypeptide, which contains 1373 amino acids (aa) (160 kDA), exhibits in the C-terminal a single dsRNA-binding domain (dsRBD) and two catalytic domains. A Proline-rich region (PRR) and an Arginine/Serine domain (RS) are present in the N-terminal portion, suggesting protein-protein interactions, even though weak and reversible, which are important for its function (Fortin, 2002). In HeLa cells, Drosha was shown to be localized mainly in the nucleus (Wu, 2000). In addition, phosphorylation of Serine 300 or Serine 302 was shown to be required for its nuclear localization and microRNA processing in Hek293T cells (Tang, 2010).

DGCR8 protein is composed of 773 aa (100 kDa) and it possesses two dsRBDs and a WW domain, which is a protein module with two highly conserved tryptophanes that bind proline-rich regions (PRR) (Landthaler, 2004). The two dsRBDs of DGCR8 are crucial for RNA recognition and binding, since the single dsRBD of Drosha is insufficient (Han, 2004). The model proposed for their cooperative function is that DGCR8 anchors the pri-miRNAs and directs Drosha to cleave it (Han, 2006). Pre-miRNAs are exported to the cytoplasm by exportin-5, a member of the karyopherin family (Yi, 2003). Like other known transport receptors, Exportin-5 binds specifically to RanGTP and shuttles between the nuclear and the cytoplasmic compartment. Interestingly, exportin-5 also associates with dsRNA binding

proteins through their dsRBD in a RanGTP-dependent manner, and the dsRBD is the limiting sequence required for this interaction (Brownawell, 2002).

Once exported into the cytoplasm, the pre-miRNAs are handed to and processed by Dicer into mature microRNAs. Dicer was first identified as the enzyme responsible for processing long double-stranded RNA to siRNA-like RNA structures in S2 cells (Bernstein, 2001). It turned out that Dicer was also involved in the formation of microRNAs (Ketting, 2001). Based on these findings, it appeared that Dicer was involved both in posttranscriptional gene regulation, through the microRNA pathway, and RNA interference (RNAi). The first pathway (microRNA pathway) leads to translation suppression via interaction between the endogenous microRNAs and their mRNA targets. The second pathway (RNAi) leads to mRNA degradation via the RISC (RNA-induced silencing complex) complex (Hammond, 2000).

Dicer is a multidomain dsRNase III endonuclease (218 kDa) that produces 21-23 nt long fragments in a magnesium-dependent manner from dsRNA (Provost, 2002), leaving a 3′ overhang of 2 nt (Elbashir, 2001). Dicer has in its C-terminal portion a dsRBD and two RNase III catalytic domains. These are followed by a PAZ domain, a DUF283 domain, and a Helicase N-terminal domain (Welker, 2011). It was recently discovered that the N-terminal Helicase domain, also known as the DExD/H-box domain, inhibits the single-turnover of dsRNA cleavage rate, which is stimulated by its association with the human immunodeficiency virus transactivating response RNA-binding protein (TRBP) (Ma, 2008). Limited proteolysis enhances Dicer catalytic activity (Zhang, 2002). Both Provost (2002) and Zhang (2002) found that Dicer catalytic activity is stronger at a pH of around 6.8 and an optimum potassium or sodium salt concentration between 50-100mM.

Dicer activity is enhanced by two co-factors, TRBP (Chendrimada, 2005) and the Protein activator of PKR (PACT) (Lee, 2006). Both TRBP and PACT are dsRNA-binding proteins, which contain three dsRBD domains. Even though both TRBP and PACT are able to regulate and enhance Dicer catalytic activity, they are not required for it (Lee, 2006). TRBP seems to be required to recruit the Dicer complex to Argonaute 2 (Ago2), which is the catalytic engine of the RNA-induced silencing complex (RISC) for microRNA processing (Doi, 2003, Chendrimada, 2005).

Ago2, a member of the Argonaute family, was the first enzyme discovered in the posttranscriptional gene silencing pathway (Hammond, 2000), and the following year Ago2 was shown to be part of the bigger RISC complex (Hammond, 2001). Argonaute proteins contain a Piwi Argonaute Zwille domain (PAZ) and a PIWI domain (Carmell, 2002). The PAZ domain is an RNA binding domain that recognizes the characteristic 2-nt 3' overhang and is found in Argonaute proteins and Dicer (Song, 2003). The PIWI domain (named for the protein piwi) is similar to ribonuclease H, with a conserved active site aspartate-aspartate-glutamate motif, strongly implicating Argonaute as "Slicer" for its endonuclease activity. The architecture of the molecule and the placement of the PAZ and PIWI domains define a groove for substrate binding and suggest a mechanism for siRNA-guided mRNA cleavage (Song, 2004).

The RISC is a large and heterogeneous multiprotein complex. The core components of the RISC include Dicer, TRBP, PACT and Argonaute 2 protein (AGO2); of these, AGO2, which was identified as the sole protein required for mRNA-cleaving RISC activity (Slicer activity), is the key RISC component (Figure 1) (Li, 2007).

Many other proteins have been shown to be associated to the RISC complex in vivo, such as Gemini 3 and 4 in humans (Mourelatos, 2002) and Fragile X mental retardation protein (FMRP) in Droshopila (Caudy, 2002, Ishizuka, 2002) and in mammals (Jin, 2004; Lugli, 2005). Interestingly, the activity of FMRP in translational repression is dependent on phosphorylation (Ceman, 2003), and its phosphorylation inhibits association with Dicer causing an increase of pre-miRNA association to Dicer (Cheever, 2009).

3. MicroRNA function in general

MicroRNAs, formed by Dicer, comprise a large family of small ~ 21-nucleotide-long noncoding RNAs that have emerged as key posttranscriptional regulators of gene expression in metazoan animals, plants, and protozoa. In mammals, microRNAs are thought to control the activity of more than 60% of all protein-coding genes (Friedman RC, 2009) and to participate in the regulation of almost every cellular process investigated to date, such as apoptosis, cell proliferation and organ development, cell signaling, control of development timing, haematopoietic cell differentiation, stem cells differentiation and proliferation, cancer and many other diseases (reviewed in Bartel, 2009; Bushati, 2007; Ghildiyal, 2009). Moreover, microRNAs function has also been linked to many neurological disorders such as Autism (Abu-Elneel, 2008; Talebizadeh, 2008), Rett syndrome (Klein, 2007), Schizophrenia (Perkins, 2007; Beveridge, 2008), DiGeorge syndrome (Stark, 2008; Wang, 2007) and major depression (Smalheiser, 2011; review in Dwivedi, 2011).

The current state of knowledge is that microRNAs regulate protein synthesis by base-pairing to target mRNAs. In animals, most studied microRNAs form imperfect hybrids with sequences in the mRNA 3′-untranslated region (3′ UTR), with the microRNA 5′-proximal

"seed" region (positions 2–8) providing most of the pairing specificity (Bartel, 2009; Bushati, 2007; Ghildiyal, 2009; Filipowicz, 2008). Generally, microRNAs inhibit protein synthesis either by repressing translation and/or by causing deadenylation and subsequent degradation of mRNA targets (Chekulaeva, 2009). More recently, however, some microRNAs have been reported to activate mRNA translation (Vasudevan, 2007, 2008; Orom, 2008). These microRNAs can also bind to the 5' UTR of some mRNAs and enhance their translation (Orom, 2008; Henke, 2008). MicroRNAs function in the form of ribonucleoprotein complexes (RISC) (Fabian, 2009).

4. M**icroRNA functions in mature neurons**

The pioneering work of Lagos-Quintana (2002) identified some microRNAs that appeared to be extremely tissue specific, suggesting a critical role for some of them, especially in the mouse brain. Since then, many more microRNAs have been discovered that are expressed in the adult brain (Dostie, 2003; Krichevsky, 2003; Kim, 2004; Miska, 2004; Sempere, 2004). And still very little is known about the function of the many neuronal specific microRNAs in the adult nervous system. The first microRNA shown to play a role in post-mitotic neurons was miR-132 (Vo, 2005). This study was also the first report that some of the cAMP-response-element-binding protein (CREB) functions are mediated by a microRNA (Fiore, 2007). MiR-132 is enriched in neurons and, like many neuronal CREB targets, is highly induced by neurotrophins. Expression of miR-132 in cortical neurons induced neurite outgrowth. Conversely, inhibition of miR-132 function attenuated neuronal outgrowth. These data revealed that a CREB-regulated microRNA regulates neuronal morphogenesis by responding to extrinsic trophic cues. Also miR-124 has been shown to be

implicated in neurite outgrowth in mouse primary cortical neurons (Yu, 2008). Interestingly, both miR-132 and miR-124 exert their growth-promoting effect by regulating the activity of small Rho GTPases, which are crucial regulators of the dendritic actin cytoskeleton (Schratt, 2009). More intriguing is the evidence that miR-134 is localized in the synapto-dendritic compartment of rat hippocampal neurons and that it negatively regulates the size of dendritic spines. The effect is mediated by the inhibition of the translation of the protein kinase Limk1 mRNA that controls spine development. Exposure of neurons to extracellular stimuli, such as brain-derived neurotrophic factor (BDNF), relieves miR-134 inhibition of Link1 translation, and may in this way contribute to synaptic development, maturation and/or plasticity (Schratt, 2006).

Successively, by performing a functional screen, miR-138 was discovered to control the dendritic spine structure in rat hippocampal neurons. Mir-138 is highly enriched in the brain, localized within dendrites and negatively regulates the size of dendritic spines. It seems that miR-138 controls the expression of acyl protein thioesterase 1 (APT1) which is an enzyme regulating the palmitoylation status of proteins that are known to function at the synapse, including the α_{13} subunits of G proteins ($G\alpha_{13}$). RNA-interference-mediated knockdown of APT1 and the expression of membrane-localized $G\alpha_{13}$ both suppress spine enlargement caused by inhibition of miR-138, suggesting that APT1-regulated depalmitoylation of $G\alpha_{13}$ could be an important downstream event of miR-138 function (Siegel, 2009).

Very recently, it was shown that post-transcriptional regulation of CREB expression by the brain-specific miR-134 was able to activate the "NAD-dependent deacetylase sirtuin-1" (SIRT1). SIRT1 normally functions to limit expression of miR-134 via a repressor

complex containing the transcription factor YY1, and unchecked miR-134 expression following SIRT1 deficiency results in the down-regulated expression of CREB and BDNF, thereby impairing synaptic plasticity (Gao, 2010).

Interestingly, because miR-124 is an evolutionary conserved miRNA it has also been studied in the nervous system in invertebrates species. In *C. elegans* miR-124 is encoded by only one gene, unlike vertebrate genomes. Clark (2010) showed that miR-124, expressed in a subset of sensory neurons in *C. elegans*, contributes to defining cell-type-specific gene activity by repressing a diverse set of co-expressed genes. In *Drosophila*, it has been shown that miR-124 steady-state level in the nervous system is regulated by dFMR1 (Xia-Lian, 2008), providing novel mechanistic insights into the role of dFMR1 in the miRNA pathway and neuronal development. Recently, still in *Drosophila*, the miR-310 cluster was shown to negatively regulate synaptic strength at the neuromuscular junction (Tsurudome, 2010). More fascinatingly, Rajasethupathy (2009) showed that in *Aplysia* miR-124 responds to serotonin by derepressing CREB, providing a role for miR-124 in long-term plasticity of synapses in the mature nervous system. A few years before Ashraf (2006) showed, in *Drosophila,* that Armitage protein, a component of the RISC complex, was modified by proteolysis during long-term olfactory learning, and that learning was impaired in an armitage mutant.

5. The microRNA pathway in adult mouse brain

5.1. Dicer and eIF2c are enriched at postsynaptic densities in adult mouse brain

A significant amount of knowledge of the microRNA pathway has been achieved in cell culture systems. In my previous work, I provided evidence that in the adult mouse brain

Dicer, the rate-limiting enzyme in formation of small RNAs, is expressed in the somatodendritic domain of projection neurons, including the dendritic spines, and is enriched at postsynaptic densities (PSDs) (Lugli, 2005). Using immunocytochemistry at both LM (Figure 2) and EM levels (Figure 3), which was performed by Martone M.E. and Jones Y., we showed that Dicer and eIF2c (Argonaute homologue) were expressed mainly in the somatodendritic compartment of neurons, and were detectable as well within dendritic spines. Electron microscopy immunocytochemistry, using peroxidase-based detection, confirmed that Dicer-like immunoreactivity was present within dendritic spines and appeared to be particularly associated with PSDs (Figure 2). eIF2c was also prominent in spines (Figure 2) (Lugli, 2005).

5.2. Dicer has RNase III activity that is enhanced by Calpain

Recombinant Dicer and immunoprecipitated brain Dicer both exhibited typical Dicer-like RNase III activity that was Mg-dependent and resulted in formation of 22 nt. products. Previous reports demonstrated that brief proteinase K treatment of recombinant Dicer increases its RNase III activity (Provost, 2002, Zhang, 2002). Because Calpain participates in neuronal responses to synaptic activation (Lynch and Baudry, 1987; Chan and Mattson, 1999), we asked whether Calpain might also cleave Dicer and activate Dicer RNase III activity. Calpain I treatment of recombinant Dicer markedly increased RNase III activity, which lasted at least 24 h (Figure 4)

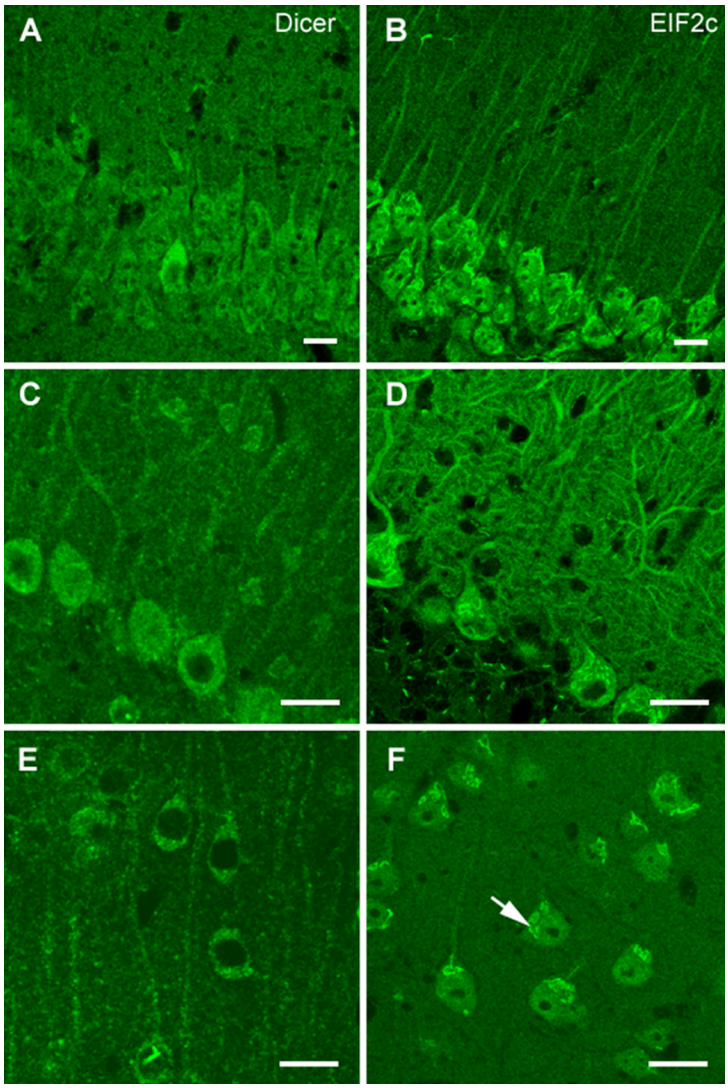

Figure 2. Immunolabeling for Dicer and eIF2c in adult mouse brain.
(a, c, e) Anti-Dicer antibody, (b, d, f) anti-eIF2c antibody labeling. (a, b) hippocampal area CA1, (c, d) cerebellar cortex and (e, f) neocortex. Although labeling for the two proteins was generally found in the same cells and subcellular locations, labeling for eIF2c was much stronger than for Dicer, cortex, where Purkinje cells were particularly in cerebellar (d) intensely labeled throughout the dendritic tree and dendritic spines. Labeling for Dicer was more uniform in the various cell layers of the cerebellar cortex (c). eIF2c exhibited a prominent subcellular localization that likely corresponded to the Golgi apparatus (arrow in f). In contrast, Dicer showed a punctate distribution more uniformly in the cytoplasm. Scale bars = 20 μm.

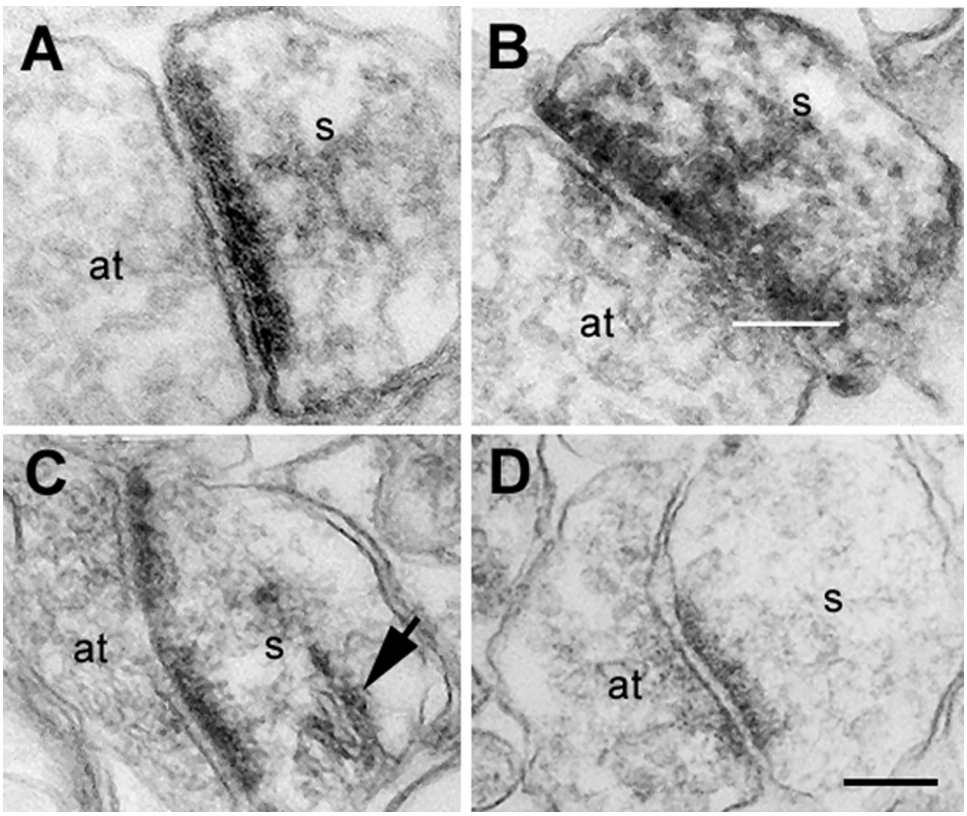

Figure 3. Electron microscopy localization of Dicer and eIF2c in dendritic spines in cortex and hippocampal area CA1.
The distribution of Dicer (a, c) tended to be more discrete than eIF2c. In the cortical spine in (c), a deposit of label can be seen surrounding the spine apparatus (arrow). Post-synaptic densities were heavily labeled for both proteins, much greater than the slight contrast due to heavy metal staining that can be seen in tissue labeled without the primary antibody (d). s, spine head; at, axon terminal. Scale bar = 200 nm.

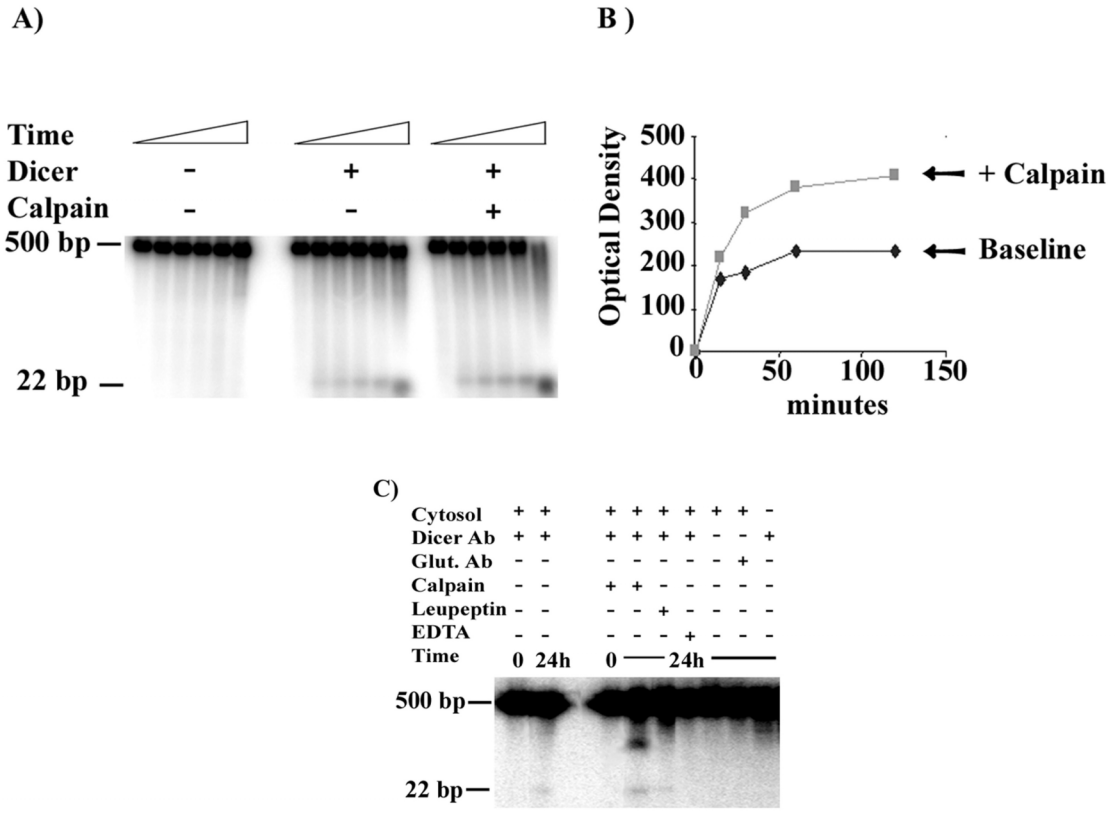

Figure 4. Calpain I stimulates Dicer RNAse III activity.
(A) Recombinant Dicer was assayed for RNAse III activity. Reactions were stopped after 0, 15, 30, 60, 120 min, and 24 h by adding gel loading buffer, separated on a 4–20% Criterion-TBE gel, and autoradiographed. Panel at left: when Dicer was omitted, no activity was detected. Middle panel: baseline Dicer assay shows progressive formation of 22 nt products over time. Panel at right: calpain I (3 U/mL) treatment caused a greater loss of 500 bp substrate, and more formation of 22 nt product, relative to the baseline assay. Calpain alone had no RNAse III activity (not shown). (B) Optical density measurements of the 22 nt products (from the autoradiograms in A) are plotted for the first 2 h of incubation. (C) Brain Dicer was immunoprecipitated from cytosol using anti-Dicer antibody and assayed for RNAse III activity. As negative controls, no activity was detected when anti-Dicer antibody was omitted, or when rabbit anti-glutamate antibody was used instead for immunoprecipitation. Also, no RNAse III activity was observed in the absence of Mg, or in the presence of excess EDTA. Calpain treatment increased the amount of 22 nt product observed; this increase was blocked in the presence of the Calpain inhibitor leupeptin.

5.3. Cryptic Dicer is activated in postsynaptic densities by Calpain

It is intriguing that no detectable RNase III activity was detected in purified PSDs (Figure 5a). However, after treating purified PSDs with Calpain I for 10 min, the preparation was subsequently quite active in cutting the dsRNA template (Figure 5b). This result indicates that much of the Dicer protein associated with the PSD is cryptic (not active or not accessible to dsRNA) until acted upon by Calpain. When purified PSDs were incubated directly with Calpain I, Dicer disappeared from the PSDs, whereas Dicer-immunoreactive bands at 220 kDa and fragments at 150, 140, 75 and 50 kDa were liberated into the supernatant (Figure 5a, top). Treating purified PSDs with Calpain I caused the disappearance of the eIF2c 140 kDa band, concomitant with the appearance of eIF2c 94 kDa in the supernatant (Figure 5a, bottom).

Treating synaptoneurosomes with calcium (Figure 6), and treating acute hippocampal slices with NMDA (50 μM, 15 min) caused the appearance of a discrete fragment of Dicer, which was blocked by the cell-permeable Calpain inhibitor calpeptin (Figure 7). This shows that Dicer is cleaved (and presumably activated) by stimuli that raise intracellular calcium and activate Calpain. Calpain is of interest since, as mentioned above, it is activated by the same trigger, Calcium, that allows long term potentiation (LTP) to occur. Calpain is thought to process many different components of the synapse, including AMPA receptors and cytoskeletal elements, thus making structural elements available and permitting plasticity to occur (Lynch, 2007).

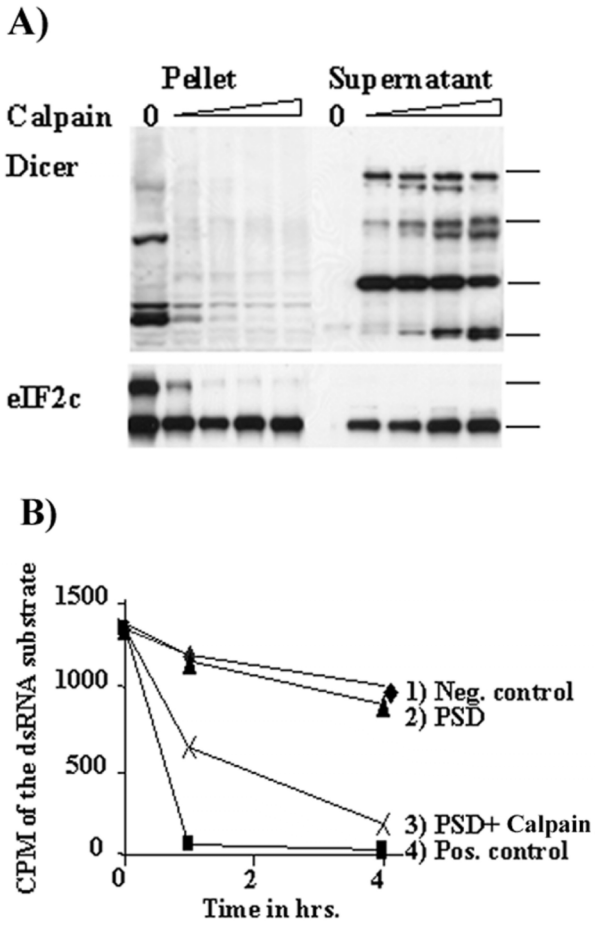

Figure 5. Calpain I liberates Dicer and eIF2c from postsynaptic densities (PSDs) and uncovers cryptic RNAse III activity. (A) Purified PSDs were treated with increasing concentrations of Calpain I for 30 min at 37°C, and spun down at 20 000 *g*, 30 min, 4°C. Pellet and supernatant were loaded on 4–20% gradient polyacrylamide gels (equal fractions per lane) and immunoblotted with anti-Dicer antibody (top) or anti-eIF2c (bottom). Top: Calpain digestion caused the loss of nearly all of the Dicer associated with the PSD and liberated a number of Dicer-immunoreactive bands into the supernatant, including a band that co-migrated with full-length Dicer (220 kDa) and smaller discrete bands. Marks indicate the position of molecular mass standards at 250, 150, 75, and 50 kDa. Bottom: the eIF2c 140 kDa band associated with the PSD is cleaved by Calpain, occurring in parallel with the release of a eIF2c 94 kDa band into the supernatant. Marks indicate 140 and 94 kDa. (B) Purified PSDs were treated with or without Calpain I for 30 min, 37°C, then leupeptin was added to stop residual Calpain activity before conducting a RNAse III assay. As a negative control, a tube was run with no PSDs added, and as a positive control, an extra tube was assayed using recombinant Dicer. Whereas purified PSDs were no different than the negative control group, the Calpain-treated PSDs showed significant RNase III activity.

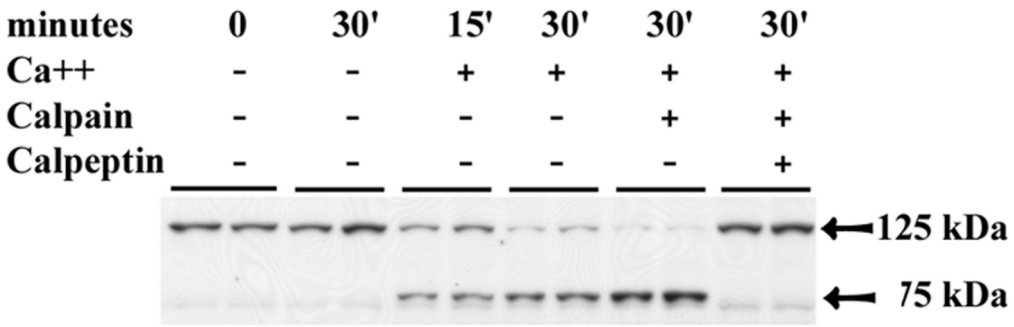

Figure 6. Calpain-dependent cleavage of Dicer in synaptoneurosomes.
Synaptoneurosomes were incubated in HB buffer (lacking EDTA and protease inhibitors) at 37°C in the presence of $CaCl_2$ 2.5 mm, Calpain I (3 U/mL), or the specific Calpain inhibitor calpeptin (100 μg/mL). Reactions were stopped at 15 or 30 min by methanol precipitation; samples were resuspended in sodium dodecyl sulfate–polyacrylamide gel electrophoresis buffer under reducing conditions and immunoblotted with anti-Dicer antibody. Experiments were run in duplicate (each lane is a separate sample). Calcium treatment caused a rapid decrease in a 125 kDa fragment with the appearance of a new fragment at 75 kDa. Decreases were also observed in Dicer 220 and 50 kDa (not shown).

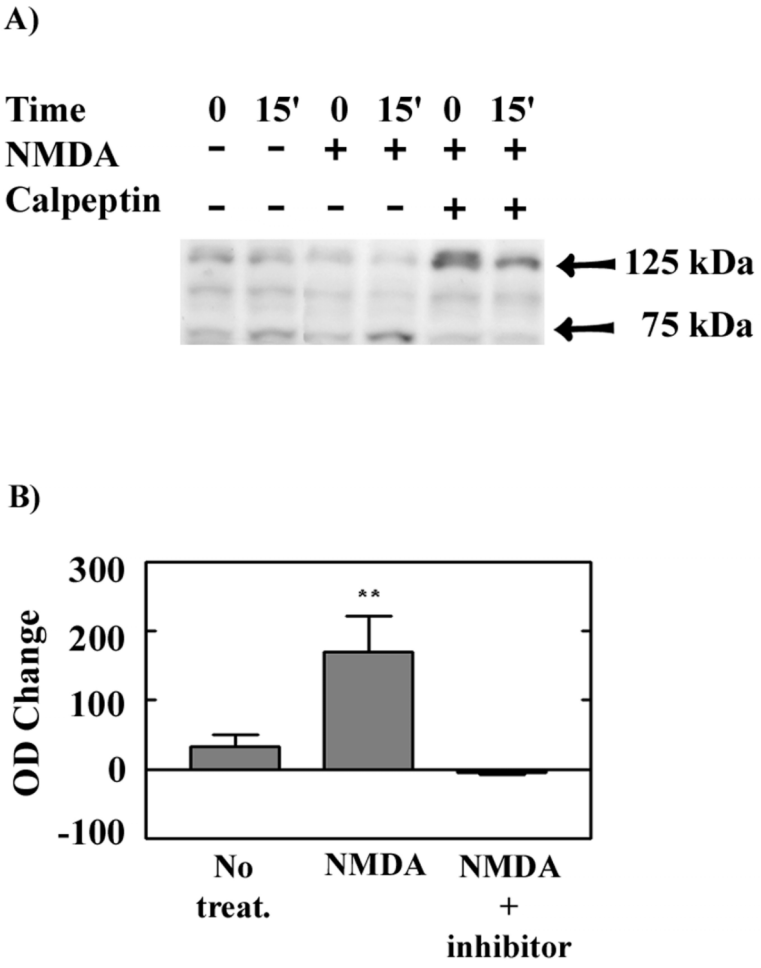

Figure 7. Calpain-dependent cleavage of Dicer in NMDA stimulated hippocampal slices. (a) Hippocampal slices (six slices pooled per sample) were pre-incubated with or without calpeptin (100 μg/mL) for 1 h and treated with or without NMDA (50 μM) for 15 min. Pooled slices taken either before (time 0) or after treatment were homogenized in HB, spun (20 000 *g*, 20 min, 4°C), and supernatant was precipitated in methanol, dissolved in SDS–polyacrylamide gel electrophoresis buffer plus dithiothreitol and loaded for immunoblotting using anti-Dicer antibody. (b) Changes in the 75 kDa band after no treatment, NMDA treatment, or NMDA plus calpeptin. In each experiment, the optical density (OD) of the 75 kDa bands was normalized to the value of the 'No treatment at $t = 0$' lane. Histogram shows the mean change in OD (± SEM) from $t = 0$ to $t = 15$ min for each condition in five independent experiments. **anova indicated a significant effect of treatment ($F_{2,8} = 10.29$, $p < 0.01$); Newman–Keuls tests showed that the NMDA group was significantly higher than both the No Treatment and NMDA + inhibitor groups ($p < 0.01$), which did not differ from each other.

6. RNA localization and synaptic plasticity

RNA localization is an important mechanism to sort proteins to specific subcellular domains. In neurons, several mRNAs (*i.e.* CamKIIa, ARC, beta-actin) (Sanches-Carbente, 2008) and polyribosomes have been detected within dendrites. Polyribosomes have been shown to be translocated within dendritic spines (especially after stimuli that elicit long-term potentiation) (Ostroff, 2002; Bourne, 2007), and mRNAs and translational regulatory components have also been detected in proximity to PSDs (Asaki, 2003; Suzuki, 2007). Cytoplasmic bodies, such as RNA granules, stress bodies and P-bodies (no ribosomes) have also been identified within dendrites (Ferrari, 2007; Krichevsky, 2001; Sossin, 2006; Vessey, 2006). Some mRNAs, such as CaMKIIa and Arc mRNAs, are transported to dendrites in large granules (>1000S) by KIF5 (Kanai, 2004), while others are transported by KIF3c through the binding of FMRP (Davidovic, 2007). In dendrites, the transport of NMDA receptors is mediated by the molecular motor KIF17 (Hirokawa, 2006; Guillaud, 2003). In contrast, AMPA receptors are transported by the conventional motor KIF5 (Setou, 2002). The polarity of microtubules in proximal dendrites is mixed, while in the distal dendrites the polarity is the same as in axons. Some dendritic motors, such as KIF17, sense the difference between the two types of neurites and exist predominantly in dendrites, while other motors, such as KIF5 proteins, transport cargoes in both dendrites and axons (Hiorkawa, 2008). There is a clear indication that local translation plays a key role in synaptic plasticity (Weiler, 1997; Eberwine, 2001; Sutton, 2005, Todd, 2003). Long-lasting changes at synapses are at the core of brain activities, such as learning and memory, and rely on enduring changes in synaptic efficacy (Eyman, 2007, Ju, 2004). A large body of evidence indicates that synaptic

plasticity, dendritic spine growth, and learning are critically dependent upon regulation of specific protein synthesis near or within dendritic spines.

II. HYPOTHESIS

Despite these great advances, it is neither clear whether a diverse population of microRNAs is expressed in dendrites and/or in dendritic spines, nor whether they are as abundant near synapses as within the cell body compartment. Nor is it understood how microRNAs arrive at the synaptic compartment(s). There are at least three possible ways that microRNAs may arrive at dendrites (Tai, 2006; Kosik, 2007; Fiore, 2008). First, mature microRNAs may passively diffuse into dendrites, which seems to be the predominant mode within neurons that are still maturing (Kye, 2007). Second, mature microRNAs may be processed from precursors in the neuronal cell body and then actively transported to dendrites, either by themselves or by 'piggybacking' onto their mRNA targets as the latter become transported to dendrites. Third, primary microRNA gene transcripts (pri-miRNAs) or small hairpin precursors (pre-miRNAs) may be actively transported to dendrites and then processed locally to microRNAs. These scenarios are not mutually exclusive. However, because Dicer, the RNase III enzyme that cleaves precursors into mature microRNAs, is expressed within dendritic spines and is highly enriched at PSDs (Lugli, 2005), I hypothesized that microRNA precursors would be expressed in synaptic fractions of adult mouse forebrain and locally processed into mature microRNAs.

III. RESULTS

1. Expression of microRNAs and their precursors in synaptoneurosomes

1.1. Synaptoneurosomes

Synaptoneurosomes are small vesicular structures that are prepared by filtration of total forebrain homogenate through mesh of progressively decreasing size, followed by low-speed centrifugation (discarding the pellet) and higher-speed centrifugation (keeping the pellet). This fraction is thought to be enriched in dendritic spines. The synaptoneurosomes were prepared by a modification of Weiler (1997) as described in my previous study (Lugli, 2005), by adding a cocktail of RNase inhibitors to preserve RNA species.

Synaptoneurosomal preparations were characterized by Western blotting of PSD95 and by real-time RT-PCR measurements of BC1 and CAMK2a to verify that these components were enriched relative to total forebrain homogenate (see below).

1.2. MicroRNAs expression in synaptoneurosomes

In the experiments reported here, each sample (Synaptoneurosomes "SynN" vs. total forebrain homogenate "total") was pooled from 3-4 forebrains, and 3 independent pairs of samples were tested in parallel on microRNA microarrays by Invitrogen. The analysis of this was performed by Smalheiser N.R. An additional 3 pairs of samples were prepared and measured for follow-up experiments.

About three-quarters (178 of 232) of the mouse microRNAs present on the microarrays were detectably expressed in the forebrain homogenate using the threshold

criterion of having average intensity values ≥2.5 X background. Of the microRNAs expressed in forebrain, 78% were detectable within the SynN fraction using the same criterion. Normalizing the intensity values to the mean intensity values of the microRNA population as a whole (i.e., the mean value was chosen for one dye channel on one chip, and the others were normalized relative to that one) had only a slight effect on the distribution of intensity values (Figure 8). However, this did improve the linearity of the assay and adjusted for possible variations among preps as well as for possible differences in the red vs. green dye channels. Thus, this was the preferred method for normalizing the microarray data.

Individual microRNAs showed a wide range of relative enrichment ratios (Figure 9). The lowest ratio was observed with miR-143, which was ~7-fold less abundant in the SynN fraction than in the total homogenate, whereas miR-200c was ~5-fold more abundant in the SynN fraction. Thirty-seven microRNAs showed an enrichment ratio of 2-fold or greater in the SynN fraction, which, in this experiment, was similar to the number of microRNAs (31) which achieved statistical significance at $p \leq 0.05$ (Table I). Numerous microRNAs still achieved significance at more stringent criteria (Table I).

The synaptic enrichment was also analyzed by quantile ranking of the microRNAs. This is a nonparametric method by which each microRNA in a sample is simply ranked in order of its average intensity value, from greatest to least, and assigned a quantile value (from 100% to 0%). Then, for each microRNA, one computes the difference between its rank value in synaptoneurosomes versus its rank value in the total forebrain homogenate. As shown in Figure 10, there was very good agreement between the findings obtained using enrichment ratios and obtained using rank differences.

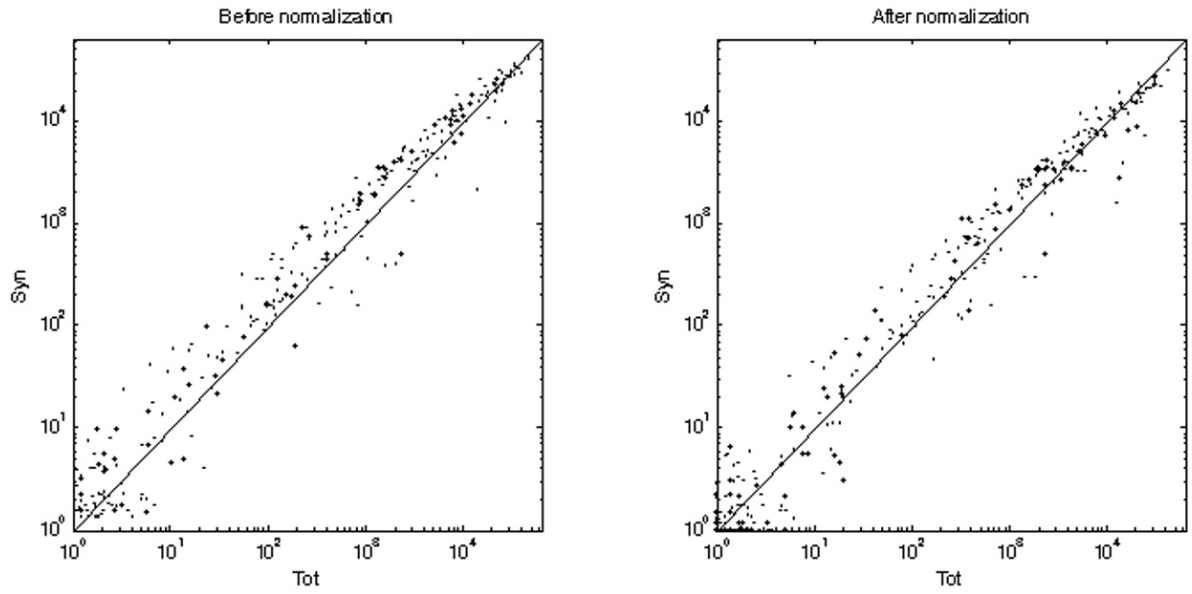

Figure 8. MicroRNA intensity values in synaptoneurosomes vs. total forebrain homogenate as measured by microarray.

Data were plotted before vs. after normalizing values to the mean value of the overall microRNA population as described in Results.

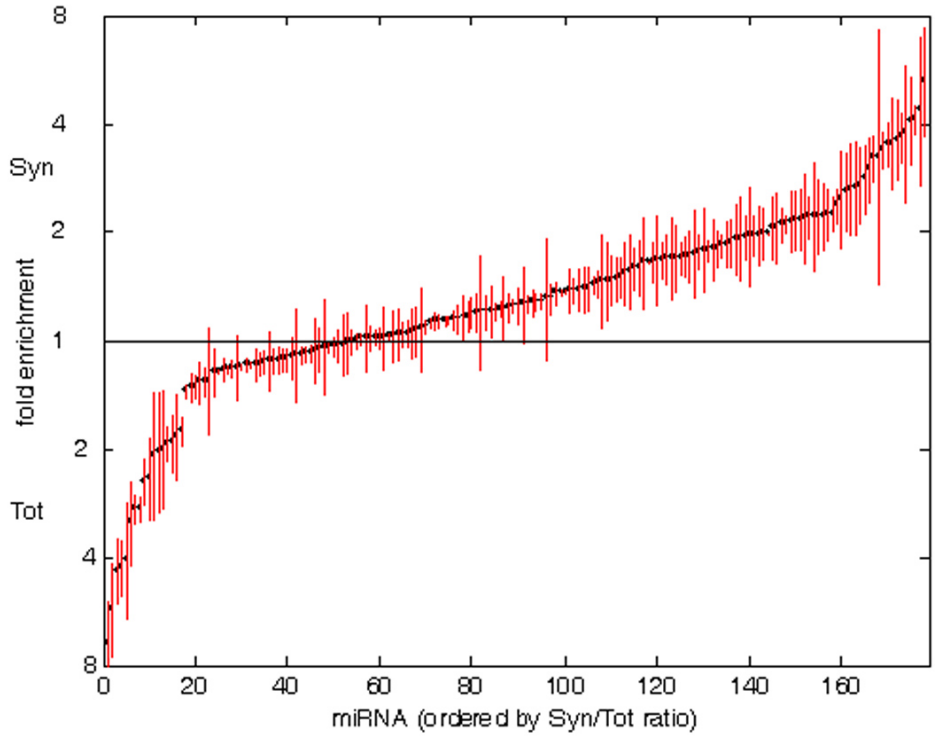

Figure 9. Enrichment ratio ± s.e.m. of forebrain microRNA intensity values (synaptoneurosomes/total homogenate) as measured by microarray.

TABLE I

NUMBER OF MICRORNAS (ENRICHED IN SYNAPTONEUROSOMES) MEASURED BY MICROARRAY THAT ACHIEVE STATISTICAL SIGNIFICANCE AT DIFFERENT STRINGENCY CRITERIA.

p-value	# observed microRNAs	# expected by chance
0.10	65	12.4
0.05	31	6.2
0.01	7	1.24
0.005	4	0.62
0.001	2	0.12

Statistics were computed using the t-test (two-sided). Note that the Bonferroni correction for multiple testing is not appropriate for these data, since different microRNAs are not expressed independently of each other; see text.

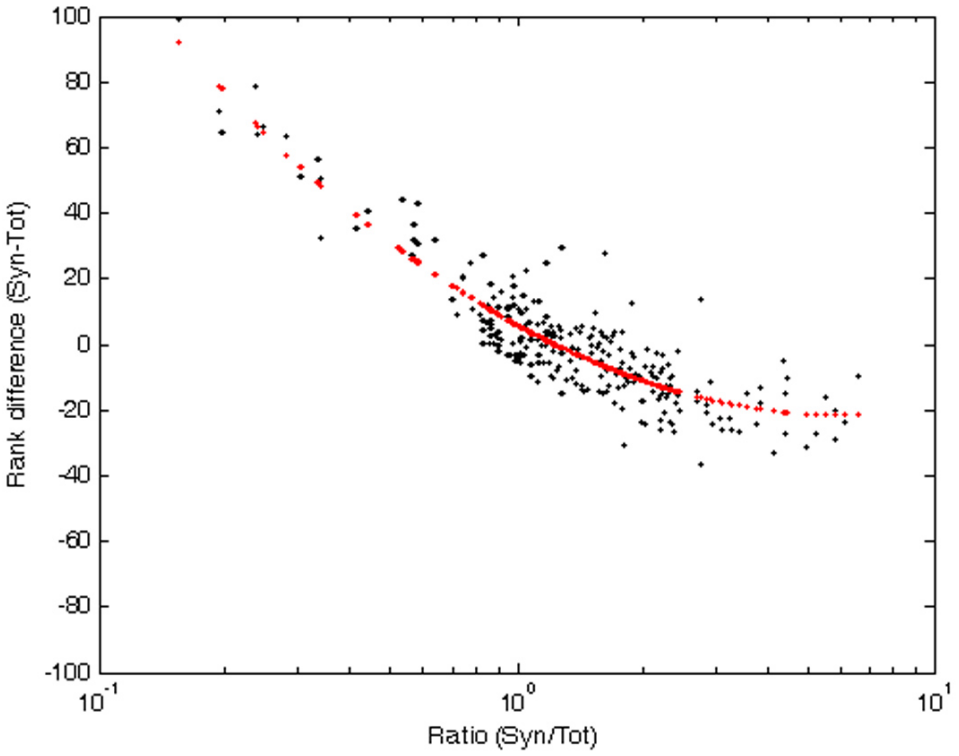

Figure 10. MicroRNA enrichment in synaptoneurosomes vs. total homogenate.

Data were computed as the enrichment ratio (X-axis) vs. computed as quantile rank differences (Y-axis). See text for details.

Quantitative real-time RT-PCR (qRT-PCR) measurements were made of selected microRNAs chosen because they covered a range of intensities and enrichment ratios (Table II). Mir-124a, an abundant microRNA which is thought to be ubiquitously expressed in neurons (but not glial cells), had an enrichment ratio of 1.04, which is similar to the value estimated by microarray (0.87). Thus, miR-124a is neither enriched nor depleted from the SynN fraction. This result is consistent with the lack of enrichment for other neuronal microRNAs measured by microarray (e.g., miR-128a, enrichment ratio = 0.85). The enrichment ratios measured by qRT-PCR generally showed close agreement with the values determined by microarray for most microRNAs (Table II), including that for miR-143 which was strongly depleted from the SynN fraction (0.11 vs. 0.15; Tables II, III). A quantitative discrepancy between qRT-PCR and microarray enrichment values was observed for miR-339, which showed a lesser magnitude of enrichment ratio by qRT-PCR (1.46, Table II) than by microarray (4.07; Table III). Similarly, miR-350 showed an enrichment ratio of 1.48 by qRT-PCR in contrast to a measured value of 3.44 by microarray (Table II, III). This result suggests that the microarray system did not maintain linearity throughout the measured range. Nevertheless, the qRT-PCR method did confirm that both miR-339 and miR-350 were significantly SynN-enriched (Table II).

As shown in Figure 11, SynN-enriched microRNAs exhibited a wide range of intensity values, and were NOT predominantly found among the least abundant microRNAs (this was checked since small changes in intensity values for microRNAs near threshold could potentially cause enrichment ratios to be artifactually inflated). This finding, together with the agreement between enrichment ratios and rank differences (Figure 10), confirms that the observed enrichment of certain microRNAs in the SynN fraction is robust.

TABLE II

ENRICHMENT RATIOS (SYNAPTONEUROSOMES/TOTAL HOMOGENATE) OF SELECTED MATURE MICRORNAS MEASURED BY REAL TIME RT-PCR.

	Mean ± s.e.m.
miR-124a	1.04 ± 0.13
miR-125b	1.08 ± 0.22
miR-134	1.70 ± 0.59
miR-143	0.11* ± 0.022
miR-339	1.46* ± 0.13
miR-99a	1.79* ± 0.22

MicroRNAs were measured in 3-6 independent preps (3 used in the microarray experiments and/or in 3 others prepared similarly). *Significantly enriched (or depleted) at a confidence level of $p<0.01$ or better.

TABLE III

MICRORNAS MOST AND LEAST ENRICHED IN SYNAPTONEUROSOMES AS MEASURED BY MICROARRAY.

Top 20

(syn/tot) Ratio	Syn Intensity	Total Intensity	miR	Expression
4.8	382	79	miR-200c	vertebrate
4.07	819	200	miR-339	rodent
4.03	315	78	miR-322	rodent
3.72	408	109	miR-466	vertebrate
3.69	255	69	miR-425	vertebrate
3.55	852	239	miR-182	vertebrate
3.44	2671	777	miR-350	rodent
3.4	247	72	miR-183	vertebrate
3.33	577	173	miR-351	rodent
3.16	124	39	miR-297	rodent
3.13	1546	494	miR-429	vertebrate
2.98	253	84	miR-213	vertebrate
2.83	702	248	miR-325	mammalian
2.68	1641	613	miR-200b	vertebrate
2.65	1371	517	miR-337	rodent
2.65	631	238	miR-323	mammalian
2.64	15076	5706	miR-146	vertebrate
2.49	944	378	miR-467	rodent
2.34	5077	2168	miR-345	mammalian
2.27	1903	840	miR-433-5p	rodent

Bottom 20

(syn/tot) Ratio	Syn Intensity	Total Intensity	miR	Expression
0.76	5489	7260	miR-218	vertebrate
0.75	655	868	miR-219	vertebrate
0.74	28233	38290	let-7b	C. elegans homolog
0.57	10211	17797	miR-125a	vertebrate
0.55	2456	4460	miR-29c	vertebrate
0.54	211	394	miR-148a	vertebrate
0.53	1454	2749	miR-101a	vertebrate
0.5	151	300	miR-377	rodent
0.49	11006	22420	miR-29b	vertebrate
0.48	96	201	miR-19b	vertebrate
0.43	420	1003	miR-34c	C. elegans homolog
0.4	157	389	miR-34b	C. elegans homolog
0.35	9101	26059	miR-126-3p	vertebrate
0.35	49	144	miR-126-5p	vertebrate
0.32	4791	15041	miR-153	vertebrate
0.25	557	2219	miR-301	vertebrate
0.24	359	1473	miR-145	vertebrate
0.23	3437	14784	miR-150	vertebrate
0.18	281	1536	miR-451	vertebrate
0.15	1960	13353	miR-143	vertebrate

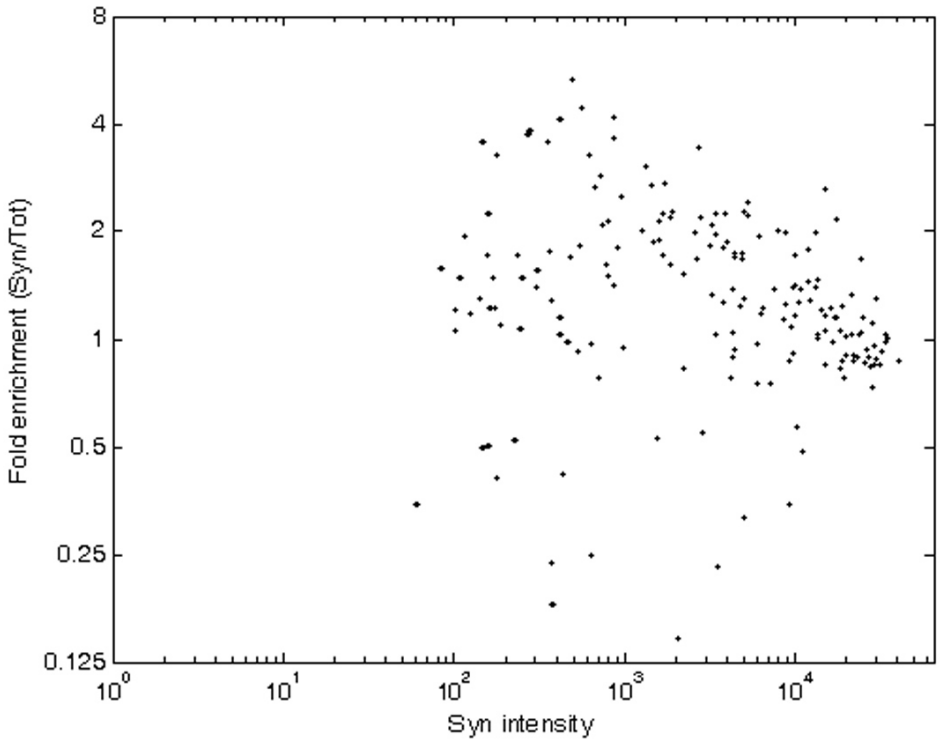

Figure 11. Relationship between the microRNA intensity values observed in synaptoneurosomes and their enrichment ratios as measured by microarray.

To analyze the biological features of SynN-enriched microRNAs, the top 20-most enriched microRNAs were compared to the bottom 20 (least-enriched) microRNAs (Table III). The top 20 include 8 microRNAs that were cloned originally from cultured cortical neurons (miR-322-352, Kim, 2003), whereas none of these were found among the bottom 20. This is consistent with the expectation that synaptoneurosomes are enriched in pinched-off dendritic spines that are derived from pyramidal neurons. Conversely, many of the bottom 20 microRNAs are expressed in many tissues and have been widely studied as being important in growth, differentiation and cancer (e.g., let-7b, miR-125a, 126, 143, 145, etc.). Several of the bottom 20 microRNAs have been reported to be expressed predominantly in astrocytes (miR-29b and 29c, Smirnova, 2005). The two sets of microRNAs differed in their evolutionary histories as well. The top 20 includes 11 microRNAs that have only been described in rodents and/or other mammalian species, which none have homologues in invertebrates. In contrast, the bottom 20 includes only 1 microRNA whose expression is restricted to mammals; most are expressed in fish and at least three have homologues in *C. elegans* (Table III). Moreover, several of the bottom 20 microRNAs (but none of the top 20) arise from multiple precursor genes (data not shown). It is likely that this reflects microRNA gene duplication and divergence over evolutionary time. In conclusion, the microRNAs that are enriched in synaptoneurosomes tend to be expressed predominantly in pyramidal neurons, and tend to be evolutionarily newer than forebrain microRNAs that are relatively depleted from the Synaptic fraction.

In many cases, two microRNAs encoded on the same chromosome at adjacent sites (presumably transcribed by the same primary transcript) showed very similar SynN enrichment ratios. For example, this was observed for 3 pairs of microRNAs within the top

20 (miR-322 and 351; miR-182 and 183; miR-429 and 200b) and 4 pairs within the bottom 20 (miR-29b and 29c; miR-34b and 34c; miR-126-5p and 126-3p; and miR-143 and 145). This underscores the consistency of the microarray results. Biologically, the phenomenon may simply reflect the fact that a primary transcript will be processed within the same cell type as the resulting mature microRNAs. Regardless, these cases are common and are important to note for data analysis, because they emphasize that the expression of any one microRNA cannot be assumed to be independent of the others.

1.3. Pre-miRNAs are expressed in synaptoneurosomes

Using qRT-PCR, the expression of selected microRNA precursors was compared in synaptoneurosomes vs. the total forebrain homogenate. The qRT-PCR products were confirmed by melting curves and by running the PCR products on agarose gel. To validate the correct sequence, selected pre-miRNAs were further tested to verify that they were cut by specific restriction enzymes, resulting in pieces of the expected size (Figure 12). Each restriction enzyme was chosen to cut the pre-miRNA in a stretch of nucleotides that reside between the amplified primer sequences.

As shown in Figure 13, microRNA precursors were readily detected within the SynN fraction, at levels that were comparable to the total homogenate. Because the primers derive from precursor sequences lying beyond the mature microRNA, this method does not amplifies mature microRNAs. On the other hand, the method detects both primary microRNA gene transcripts (pri-miRNAs) and small hairpin precursors (pre-miRNAs), as discussed further in section (4).

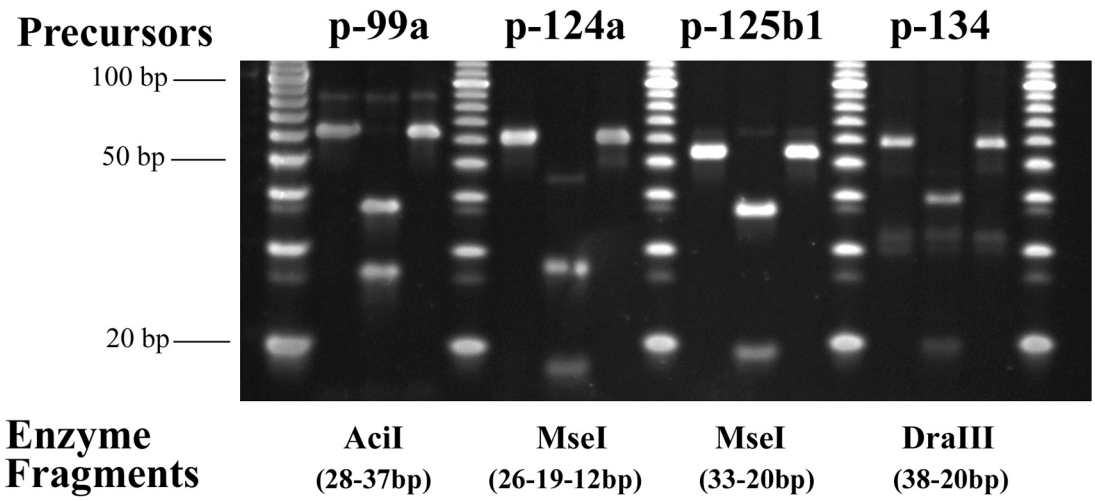

Figure 12. Restriction enzyme digestion of qRT-PCR products for 4 microRNA precursors.
PCR products were run (left lanes of each pre-miR as indicated) and gave the expected size appropriate to each microRNA precursor (pre-miR-99a = 62 bp; pre-miR-124a= 57-59 bp; pre-miR-125b1= 53 bp; pre-miR-134 = 58 bp) relative to lanes loaded with 10 bp DNA ladder (Invitrogen). Products were also incubated with restriction enzymes (middle lane) or incubated without enzymes (right lane) as indicated. Enzymes (New England Biolabs) were added to 10 μl PCR product + 1.3 μl enzyme buffer +2 μl water and incubated at 37C for 90 min, then resolved on a 15% TBE criterion gel (Bio-Rad) and stained with Syber Gold. Each restriction enzyme produced fragments of the expected sizes (as shown below the gel) appropriate to each microRNA precursor sequence.

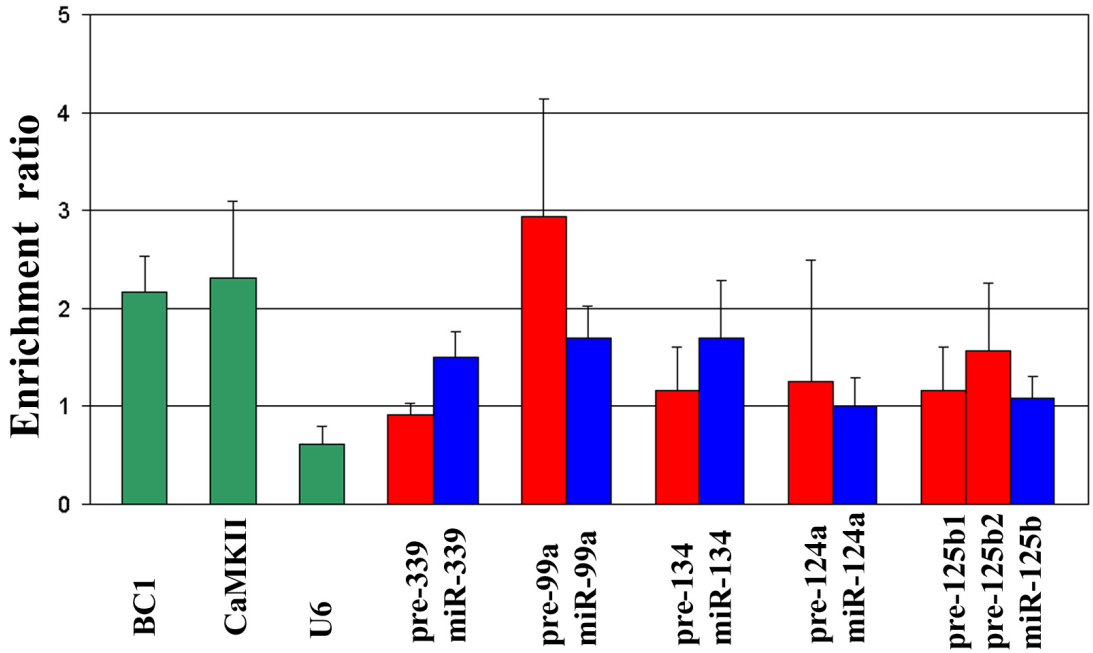

Figure 13. Enrichment ratio (synaptoneurosomes/total homogenate) of various RNAs as measured by qRT-PCR.

Data represent the average of 3 independent preps.

2. MicroRNA precursors in synaptosomes and postsynaptic densities

2.1. Synaptosomes

Synaptosomes, a well-studied synaptic fraction, are thought to consist predominantly of axon terminals with adherent postsynaptic densities. Detergent extraction of synaptosomes using Triton X-100 results in isolated postsynaptic densities (PSDs). The PSD is a protein complex that appears as an electron-dense structure underneath the postsynaptic membrane at the synaptic zone. The PSD is involved in anchoring and organizing key elements of the postsynaptic response, such as channels, neurotransmitter receptor and transduction molecules (Vinade, 2003).

Synaptosomes and isolated synaptic densities were prepared and characterized as described in previous publications (Smalheiser, 2000; Lugli, 2005; see also Figure 14). Synaptosomes and isolated postsynaptic densities are more extensively rinsed than synaptoneurosomes, and their isolation requires additional steps (e.g. sucrose gradients and detergent extraction) that should remove most contaminants. On the other hand, losses of RNA may occur because of the longer time required to prepare synaptosomes and PSDs and/or their extensive rinsing. We noted that levels of all RNAs measured, including ribosomal 18S RNA, U6, CAMK2a and BC1, as well as mature microRNAs and their precursors, were lower in Synaptosomes, relative to that observed in synaptoneurosomes. Because the components that were soluble (see below) were disproportionately lower in synaptosomes relative to synaptoneurosomes, it is likely that the losses predominantly reflect the more extensive rinsing of these preps. Nevertheless, microRNA precursors were readily detected within synaptosomes and postsynaptic densities and were amenable to study.

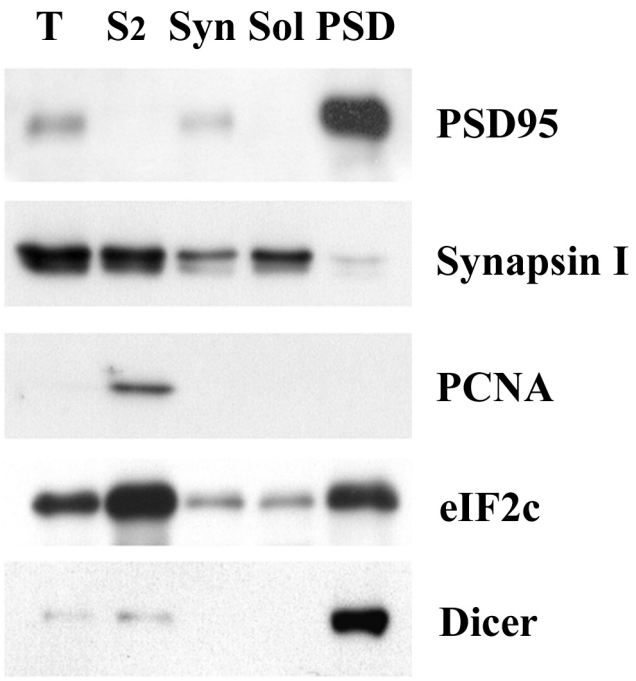

Figure 14. Distribution of synaptosomal proteins in soluble vs. PSD fractions after extraction with Triton X-100.
Total forebrain homogenate (T) was processed to obtain a soluble cytoplasmic fraction (S2) and a synaptosomal fraction (Syn) that was then lysed with 1% Triton X-100 to yield a soluble fraction (Sol) and an insoluble fractions (PSD) as described in Methods.
Equal amount of protein were loaded and blotted for different antibodies as indicated. The Dicer antibody was chicken polyclonal anti-Dicer (Lugli et al, 2005).

2.2. Pre-miRNAs are associated to the PSD fraction in synaptosomes

Synaptosomes were extracted with non-ionic detergent and measurements were made of the soluble extract vs. the insoluble residue (i.e., the PSD fraction). As shown in Figure 15, the microRNA precursors were all predominantly associated with the PSD fraction. In contrast, the mature microRNAs were predominantly detected in the Triton-soluble fraction (Figure 15). The small RNA BC1 was also almost entirely soluble. These results were also confirmed for mature miR-124a and BC1, using Northern blotting of synaptoneurosomal lysates (Figure 16).

To further verify that microRNA precursors are not simply contaminants of synaptic fractions that are co-isolated during subcellular fractionation, synaptosomes were lysed with RIPA detergent and, using an antibody against PSD-95, immunopurification was carried out under stringent conditions. PSD-95 is a protein that belongs to the membrane-associated guanylate kinase (MAGUK) family and is considered to be a marker for PSDs (Vinade, 2003). As a negative control, an antibody was employed against Synapsin I, which is associated with presynaptic vesicles in this prep. Other negative controls included omission of the primary antibody and the synaptosomal lysate. As expected, the anti-PSD95 and anti-Synapsin I antibodies brought down the respective proteins (Figure 17a). As shown in Figure 17b, anti-PSD95 brought down a striking amount of microRNA precursors (67.9-fold over baseline) and detectable, although small amounts of mature microRNAs (1.62-fold over baseline), both of which are significant at $p < 0.05$. Synapsin I antibody did not bring down significant amounts of either microRNAs or precursors (Figure 17b).

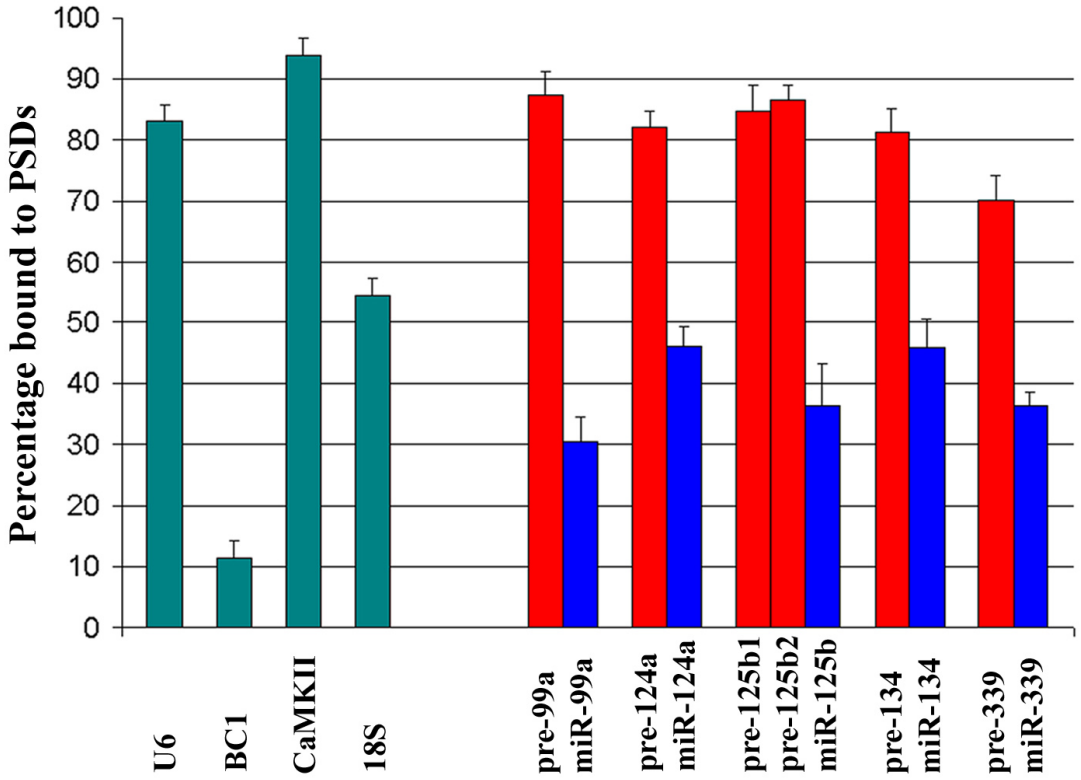

Figure 15. Distribution of synaptosomal RNAs in soluble vs. PSD fractions after extraction with Triton X-100.

Total RNA was prepared from synaptosomal fraction (Syn), that was then lysed with 1% Triton X-100 to yield soluble fraction (Sol) and insoluble fractions (PSD). qRT-PCR measurements of RNAs were performed from each fraction as described in Methods. The PSD/Syn ratio was calculated for 3 independent preps and is plotted as shown.

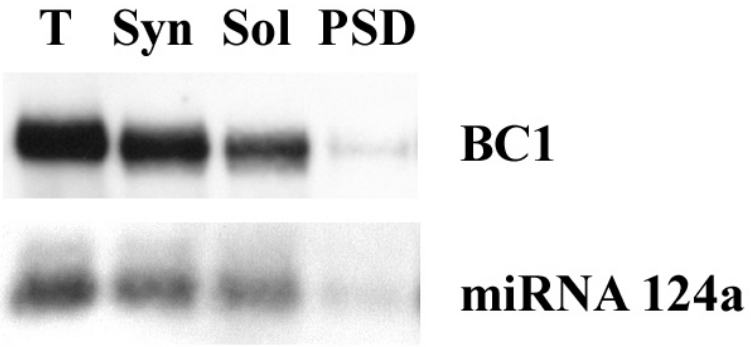

Figure 16. Within synaptoneurosomes, BC1 RNA and mature miR-124a are predominantly soluble components.
Total forebrain homogenate (T), synaptoneurosomes (Syn), and Triton-soluble (Sol) and insoluble (PSD) fractions of synaptoneurosomes were prepared. Equal amounts of total RNA were separated on agarose gels, transferred to Nylon membranes and blotted with biotinylated LNA oligonucleotide probes for BC1 and mir-124a, respectively (see Methods).

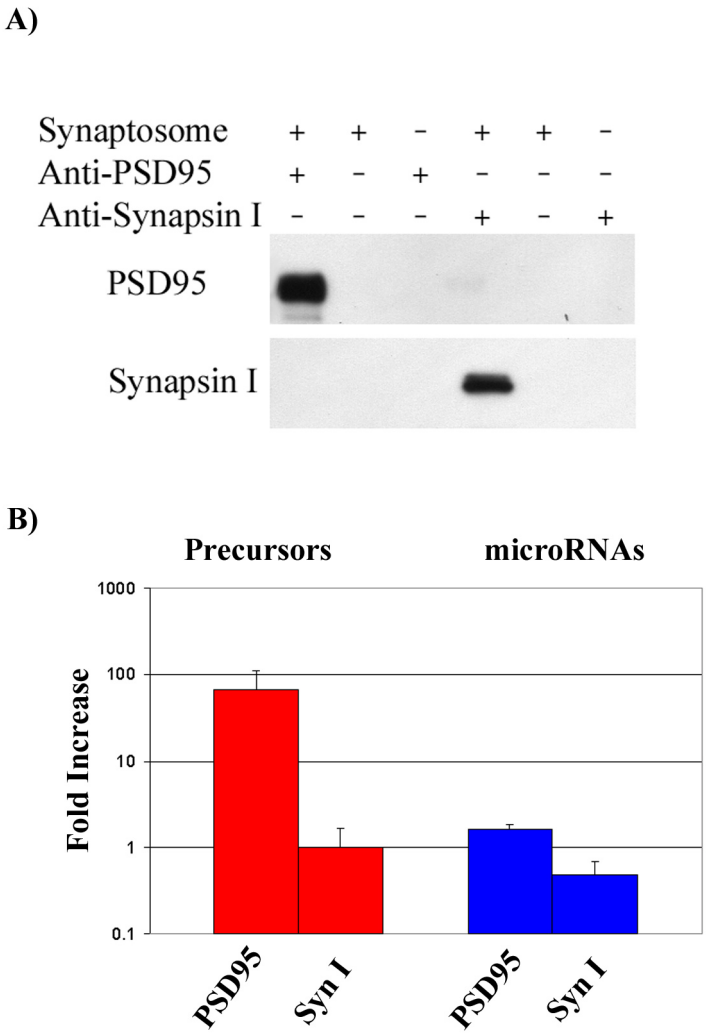

Figure 17. Co-immunoprecipitation of microRNAs and their precursors with PSD95 or Synapsin I. Synaptosomes were diluted 1:1 with RIPA buffer and incubated with anti-PSD95 or anti-Synapsin I (see Methods). Negative controls include omitting antibody, or omitting synaptosomes. **A**. Equal fractions were loaded and immunostained for PSD-95 and Synapsin I. **B.** Total RNA was isolated from immunoprecipitates and measured for mature microRNAs (99a, 124a, 125b, 134, 143, 339) and their precursors (99a, 124a1-3, 125b1, 125b2, 134, 339) by qRT-PCR. Results were computed as the ratio between the amount of each RNA brought down by each antibody and the corresponding amount brought down in the baseline group lacking specific antibody. Because results were similar for all microRNAs and for all precursors, the data were pooled and displayed as red bars (precursors) vs. blue bars (mature microRNAs).

3. Association of microRNAs and their precursors with protein complexes

Mature microRNAs are known to bind to the Argonaute homologue eIF2c as part of the RISC complex, and are also associated with FMRP (Ishizuka, 2002; Caudy, 2002). Several previous studies have also noted an association of FMRP with pre-microRNAs (Jin, 2004; Plante, 2006; Wulczyn, 2007), which is very exciting, because FMRP or its homologues may potentially help to transport pre-miRNAs to dendrites (Davidovic, (2007), who found that FMRP is a molecular adaptor between RNA granules and kinesin motors), and/or may potentially sequester pre-microRNAs from being cleaved by Dicer. To investigate the association of microRNA precursors with proteins in the brain *in vivo*, I prepared a low-speed S1 cytoplasmic fraction of forebrain homogenate and carried out immunoprecipitations using antibodies specific to a variety of microRNA pathway components, including Dicer, eIF2c, FMRP, and PACT, as well as antibodies against PSD95, Synapsin I, and MECP2. The immunoprecipitates were extracted for total RNA and measured for a series of selected mature microRNAs and microRNA precursors. The immunoprecipitations were carried out under stringent conditions, *i.e.*, in the presence of RIPA buffer. Thus, binding that is detected in RIPA is likely to be specific and strong.

As shown in Figure 18, FMRP showed a striking association with both microRNA precursors and mature microRNAs. Dicer showed a strong association with microRNA precursors as well, but no significant interaction with mature microRNAs.

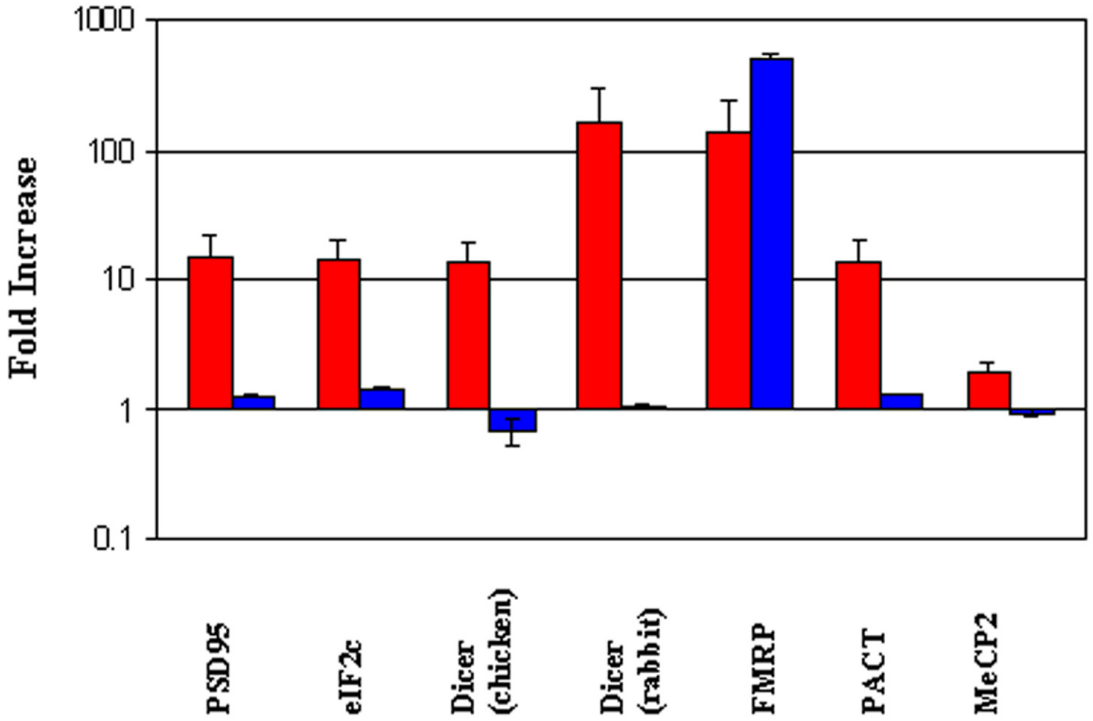

Figure 18. Co-immunoprecipitation of mature microRNAs and microRNA precursors with different proteins. S1, low speed cytoplasmic supernatant (1500xg for 10 min; final concentration 1.8 mg/ml) was diluted 1:1 with RIPA buffer; each tube had 800 µl final volume. Immunoprecipitations were performed with a variety of affinity purified antibodies (commercially available or made and characterized in Lugli (2005): a) mouse monoclonal anti-PSD95 (clone 28/86); b) rabbit polyclonal anti-eIF2c; c) chicken polyclonal anti-Dicer recognizing a region (1389–1404) located between the first and second RNAse III domains; d) rabbit polyclonal anti-Dicer recognizing the C-terminus; e) mouse monoclonal anti-FMRP (clone 7G1-1, Developmental Studies Hybridoma Bank, Iowa City, IA); f) rabbit polyclonal anti-PACT (ProteinTech Group Inc., Chicago, IL); g) rabbit polyclonal anti-MeCP2 (Upstate Biotech, Lake Placid, NY). As a negative control, rabbit polyclonal anti-Synapsin I was used (Chemicon, AB1543P). All antibodies brought down their respective proteins as expected (data not shown). Total RNA was extracted and each immunoprecipitate was measured for mature microRNAs (99a, 124a, 125b, 134, 143, 339) and their precursors by qRT-PCR. Results were computed as the ratio between the amount brought down by each antibody and the corresponding amount brought down by anti-Synapsin I. Because results were similar for all microRNAs and for all precursors, the data were pooled and displayed as red bars (precursors) vs. blue bars (mature microRNAs). Note the log scale.

4. Primary microRNA transcripts in synaptoneurosomes

Although primary microRNA transcripts (pri-miRNAs) are generally thought to be processed within the nucleus, there are some reports that pri-miRNAs can be transported intact to the cytoplasm under some conditions (Eis, 2005; Barthelson, 2007). Additionally, a noncoding RNA localized to the rat neuromuscular junction (Velleca, 1994) was identified as encoding a primary microRNA transcript (Rodriguez, 2004). Thus, pri-miRNAs could also possibly be expressed in the cytoplasm or within Synaptic compartments in the CNS.

When I started measuring the pre-miRNAs and the mature microRNAs in synaptic fractions of adult mouse forebrain, very little was known about the structure of pri-miRNA transcripts. We knew the genomic coordinates of the mature and precursor microRNAs, and we had some understanding regarding the extensive length of the pri-miRNAs of more than a few hundreds nucleotide in length (Lee, 2004). We were aware that approximately 50% of human miRNAs appeared to be expressed from introns of protein-coding transcripts (intronic) (Rodriguez, 2004). An interesting study provided strong evidence for the complete transcript structure of a small number of intergenic human miRNAs, including their transcription start site, promoter and transcription site (Saini, 2007). Still, none of these intergenic human miRNAs was the primary transcript of the microRNAs or pre-miRNAs that I was measuring as part of this study.

To investigate pri-miRNAs expression in synaptic fractions of adult mouse forebrain, I employed the same SynN preps that had been previously characterized by western blotting of PSD95 and by quantitative RT-PCR measurements of BC1 and CaMK2a to verify that these components were enriched relative to total forebrain homogenate (Figure 13 and Figure 14).

I selected a limited but diverse range of pri-miRNA transcripts to measure by qRT-PCR. I chose five sequences whose mature microRNAs were enriched in the Synaptic fraction (pri-99a, pri-134, pri-146a, pri-350), a couple of which belonged to the top-20 list of enriched microRNAs in synaptoneurosomes measured by microarray (pri-146, pri-350); some pri-miRNAs whose microRNA was part of the bottom-20 list (pri-125a, pri-126, pri-143, pri-153) and two pri-miRNAs whose microRNA showed neither enrichment nor depletion from Synaptic fractions (pri-100, pri-132). In general, pri-miRNAs are thought to be much less abundant in the cell than their microRNA. Thus, I favored the pri-miRNAs whose microRNA showed higher intensity value as measured by microarray in order to increase the chances that I could perform reliable measurement by qRT-PCR. Also, I wanted a few pri-miRNAs that are intergenic (pri-99a, pri-132, pri-134, pri-143, pri-146a) and others that are intronic to cover different pri-miRNAs processing pathways (Table IV) (as described in the introduction). Finally, I included the primary transcripts of miR-132 and miR-134, because they were shown to have some specific synaptic function (Schratt, 2006; Vo, 2005).

To rule out possible cross-amplification of pre-miRNAs, two pairs of primers for each selected pri-miRNA were designed with the use of the Primer3 online open access software. The first pair was picked from within the sequences flanking the pre-miRNA, and each 3' primer-end anneals the transcript at least 30 bases away from either end of the pre-miRNA. The only exception was the primer pair for pri-132 which I chose because I wanted to use previously validated primers in which one anneals within the pre-miRNA sequence (Wibrand, 2010). To prevent cross-amplification of the pre-miRNA sequence, the PCR products are designed to range in size from 128 base pairs (bp) to 247 (bp), which are almost double the size of the pre-miRNA. To further rule out possible cross amplification with the

TABLE IV

GENOMIC CHARACTERISTIC OF THE DIFFERENT PRI-MIRNAS

PRI-99a	Intergenic	Overlapping transcript antisense (Intron) of a predicted protein
PRI-100	Intronic	Overlapping transcript sense (Intron) of a predicted protein
PRI-125a	Intronic	Overlapping transcripts sense (exon) of a non coding RNA
PRI-126	Intronic	Overlapping transcripts sense (Intron) of EGFL-7
PRI-132	Intergenic	
PRI-134	Intergenic	
PRI-143	Intergenic	
PRI-146a	Intergenic	
PRI-153	Intronic	Overlapping transcript sense (Intron) of ptprn-2
PRI-350	Intronic	Overlapping transcript sense (Intron) of centrosomal protein 170 Gene

pre-miRNAs, the second pair of primers polymerizes a sequence of the pri-miRNA at least 50 bases upstream of the pre-miRNA. The PCR products range in size from 90 bp to 201 bp. I chose to PCR the upstream genomic location with this set of primers to confirm also that the reverse transcription reaction would reverse transcribe a sequence not shorter than 300 nucleotide. This was accomplished using a single short specific reverse primer for each pri-miRNA located at least 50 nucleotides downstream of the pre-miRNA (Table V).

The primer pairs were tested first in total brain RNA to evaluate their specificity. As negative controls, reactions omitting the RNA and the reverse transcriptase were also included. And indeed no sequence was amplified. This confirms that there was no genomic DNA contamination present and no primer dimers were formed. The products were run in an agarose gel to confirm their size (Figure 19), and their melting curves were recorded as specific characteristic of the PCR products (Table VI). I also tested the quantitative RT-PCR in high (1 μg) and low (0.25 μg) RNA input to make sure that they were in a linear and reliable range for future measurements. Reliability was assessed by the Cycle threshold (Ct) values and their standard deviation (Table VI). Since both high and low range were linear and their standard deviation was less than 1, I decided to use 0.5 μg of RNA for the future measurements.

TABLE V

LIST OF PRIMERS EMPLOYED TO MEASURE THE PRI-MIRNAS FLANKING THE HAIRPIN AND UPSTREAM THE HAIRPIN

	Short -RT	Forward Primer	Reverse Primer
PRI-99a fla.	CTGGAGTGTGAG	TTCAGAGCAAATGCTACGTTAGT	CTGGAGTGTGAGCAGGAGTG
PRI-100 fla.	GAGGGCAGGAGA	TTTGTTGGACTAATGGCTTTAACA	GAGGGCAGGAGAAGGTGTACT
PRI-125a fla.	GGCTCCAGCTAG	ACCTCTGGGGAAAAGGGTTT	GGCTCCAGCTAGAGGAAGGT
PRI-126 fla.	TGCCAAAGCACA	AGTGAAAGAGCCCCACACTG	TGCCAAAGCACACAGCTAAC
PRI-132 fla.	GCTCTGTATCTGC	AACCGTGGCTTTCGATTGTTA	GCTCTGTATCTGCCCAAACC
PRI-134 fla.	CACAGCCATCAA	GCCCCCAAGTATCAGCTTAC	CACAGCCATCAAGTCCATTG
PRI-143 fla.	GAGCCCTCTGG	GGATAGGAGGCAGACCACTG	GCTATCCCATGCCAACACTT
PRI-146a fla.	GGCCTTCAGAGT	TTTACAGGGCTGGCAGGAT	GGCCTTCAGAGTTTGTTCCA
PRI-153 fla.	CGAACAGCAAGC	GCTCACTGTCAAACCGACAA	CGAACAGCAAGCAAAGTCAG
PRI-350 fla.	CCTCAGGTTAGC	TGGACTTTGAGCAACTGTGAA	CCTCAGGTTAGCTTGGCTGT
PRI-99a up		GGAAGGAAGGATGGATTTGA	CTAACGTAGCATTTGCTCTGAA
PRI-100 up		TGAAGCTCACTTCATCAAGCA	TGTTAAAGCCATTAGTCCAACAAA
PRI-125a up		GAGCTGGGGTGTCTTCTCTG	CAGGAGATGCCTCAAAAAGC
PRI-126 up		GGGTAGTCCTTGGGTTGTGA	CAATGCCTTCCAGAAACCTC
PRI-132 up		TGGCAAGAGGTGTGCTCAGAAA	GATGTTCAGACACTCCGCGGAT
PRI-134 up		AAGGATTTCCTGGACATGATGG	AGGTGGATCAGATGCTCAGG
PRI-143 up		TGCTGCGTGCATAAAGAGAC	GAGCCCTCTGGGACTGAAAT
PRI-146a up		TCTGTCATCACGGACCTGAA	CACATCAATCCAACATGACTCC
PRI-153 up		GTGAGGGCTTGGCTCTACAA	AGGGTTTGTCGGTTTGACAG
PRI-350 up		GCCAAGCTAACCTGAGGGATA	ACC CAA GGG GAA AAG TTG AG

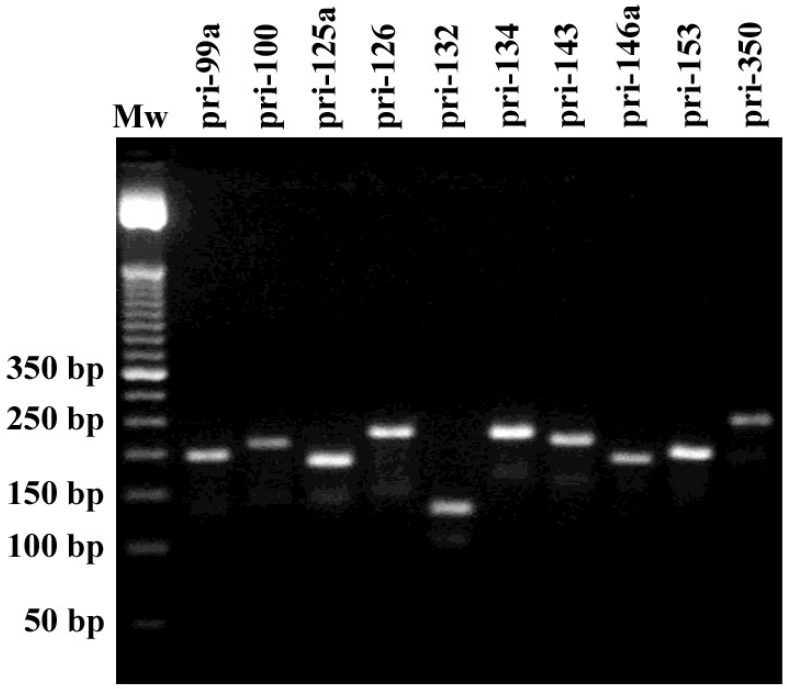

Figure 19. Agarose gel of the qRT-PCR products of the Pri-miRNAs flanking the hairpin.

PCR products (see top of the gel) were run on a 2.5% agarose gel. All the amplified products gave the expected size relative to the 50bp DNA ladder (Mw) (Invitrogen).

TABLE VI

RNA TITRATION, MELTING CURVE AND SIZE
OF THE PCR PRODUCTS OF THE PRI-MIRNAS

miRNA enrichment	Name	1 µg	St. Dev.	0.25 µg	St. Dev.	No RNA	No RT 1 µg	TM	Peaks Denat.	Size bp
top	**PRI-99a fla.**	26.3	0.04	28.18	0.2	no ct	no ct	82.83	1	194
	PRI-100 fla.	27.33	0.14	29.15	0.06	no ct	no ct	82.7	1	209
bottom	**PRI-125a fla.**	25.45	0.01	27.5	0.09	no ct	no ct	85.85/86.35	1	185
bottom	**PRI-126 fla.**	27.63	0.13	29.12	0.32	no ct	no ct	86.33	1	225
	PRI-132 fla	30.68	0.15	31.56	0.07	no ct	no ct	86.8	1	128
top	**PRI-134 fla.**	24.17	0.02	25.71	0	no ct	no ct	84.20/84.78	2	224
bottom	**PRI-143 fla.**	31.97	0.39	33.76	0.03	no ct	no ct	87.85	1	211
top	**PRI-146a fla.**	30.23	0.1	32.23	0.12	no ct	no ct	82.22	1	188
bottom	**PRI-153 fla.**	25.91	0.13	27.73	0.03	no ct	no ct	83.35	1	198
top	**PRI-350 fla.**	27.11	0.01	28.93	0.1	no ct	no ct	80.25	2	247

miRNA enrichment	Name	1 µg	St. Dev.	0.25 µg	St. Dev.	No RNA	No RT 1 µg	TM	Peaks Denat.	Size bp
top	**PRI-99a up**	29.31	0.28	30.75	0.16	no ct	no ct	75.85	1	198
	PRI-100 up	28.1	1.06	29.13	0.03	no ct	no ct	77.85	1	148
bottom	**PRI-125a up**	24.63	0.06	25.56	0	no ct	no ct	79.35	1	196
bottom	**PRI-126 up**	27.28	0.03	28.44	0.03	no ct	no ct	86.35	1	161
	PRI-132 up	24.39	0.03	26.03	0.02	no ct	no ct	83.85	1	90
top	**PRI-134 up**	23.94	0.04	25.56	0.01	no ct	no ct	83.33	1	150
bottom	**PRI-143 up**	28.2	0.01	30.34	0.03	no ct	no ct	79.85/85.35	2	201
top	**PRI-146a up**	30.3	0.06	31.71	0.25	no ct	no ct	82.85	1	141
bottom	**PRI-153 up**	27.21	0.03	28.61	0.1	no ct	no ct	83.35	1	152
top	**PRI-350 up**	26.94	0.4	28.48	0.05	no ct	no ct	77.83	1	166

Using quantitative RT-PCR, the expression of the selected pri-miRNAs was assessed and compared using the same synaptoneurosomes and total forebrain homogenate previously used in the microarray study. I had to perform a new RT reaction that would include the reverse primers for the pri-miRNAs, so I decided to include other short specific primers to measure other RNAs in order to further characterize this preps. Therefore, I used microtubule-associated protein 2 (Map2) mRNA (Tucker, 1989) as another marker for relative Synaptic enrichment. To further confirm the relative small contamination of cytosolic and nuclear RNAs, I included two other controls. I measured a prominent cytoplasmic expressed mRNA, glyceraldehyde-3-phosphate dehydrogenase (GAPDH) which is also absent from the nuclei and nucleoli (Schad, 2003), and two small nucleolar RNAs, which are thought to be retained in the nucleolus within the nucleus, U40 (Nicoloso, 1996) and MBII-52, also known as snorD115 (Vitali, 2009).

As shown in Figure 20, pri-miRNAs were readily detected and enriched 2-4 fold in the SynN fraction when compared to the total homogenate. Both pairs of primers for each pri-miRNA report similar enrichment ratios. This result confirms that I am actually measuring the primary miRNA transcript or at least a fragment much longer than the pre-miRNA. The positive controls, CaMK2a and MAP2 mRNAs, as well as BC1, were significantly enriched in the SynN fraction as compared to the negative controls, GAPDH mRNA, U6, MBII-52, and U40, which were all depleted. This result confirms the Synaptic relative enrichment of the pri-miRNAs measured in these preps.

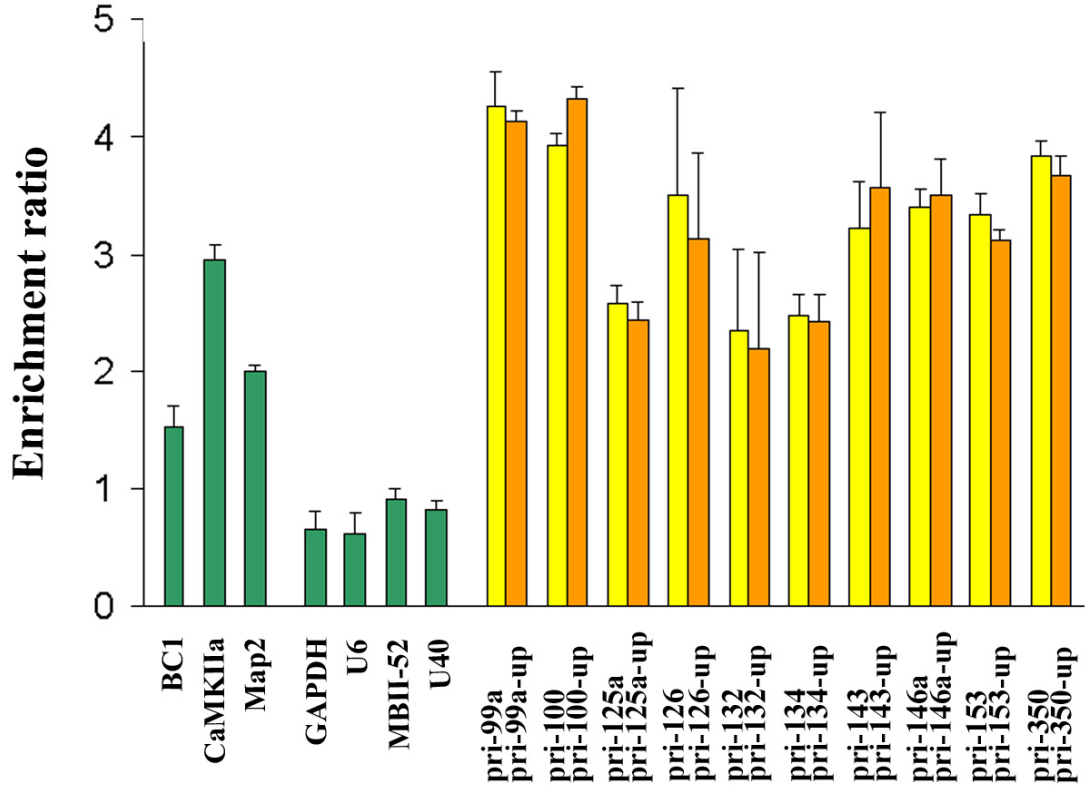

Figure 20. Enrichment ratio (synaptoneurosomes/total homogenate) of various RNAs as measured by qRT-PCR.

Green bars are the controls. Yellow and orange bars correspond to pri-miRNA PCR products. Yellow are the PCR products flanking the hairpin and orange are the PCR products upstream the hairpin.

Data represent the average of 3 independent preps.

5. Pri-miRNAs are present in synaptosomes

I also wanted to investigate if the pri-miRNAs are located in the synaptosomal fraction, but discover especially if they are bound to the PSD more than the triton-x soluble fraction. The presence of pri-miRNAs in the PSD fraction could open a whole new scenario in synaptic microRNA regulation, and could also raise many more questions similar to whether:

1. The previously identified pre-miRNAs may arise from locally anchored pri-miRNAs;
2. The pre-miRNAs, I previously measured in synaptic fractions, were actually pri-miRNAs, or there is pool of unprocessed pri-miRNAs and pre-miRNAs that co-exists;
3. Some pri-miRNAs are transported down the dendrites and "held" stably in association with the PSDs;
4. Locally expressed Dicer is able to process the pri-miRNAs in functionally mature miRNAs upon synaptic stimulation that elicits a rise of calcium beyond a certain threshold, causing activation of Calpain, which cleaves Dicer, activates its RNase III activity, and releases it from PSDs;
5. Drosha and DGCR8 are also expressed at PSDs, to perform the processing of at least the intergenic pri-miRNAs into the pre-miRNAs, which they would then be processed by Dicer.
6. Drosha and/or DGCR8, if present, may be in an inactive state until some stimuli trigger their catalytic activity.

To address these questions I decided to focus on intergenic pri-miRNAs, which require Drosha and DGCR8 processing. Because they do not arise from spliced introns of mRNA precursors they are less likely to be just a by-product of mRNA-splicing present in this fraction.

The synaptosomes were characterized as I explained previously (see section 2). As shown in Figure 21, the measured pri-99a, pri-132 and pri-134, are still enriched in this fraction. The positive control CaMK2a mRNA was confirmed to be enriched and the negative controls, the two nucleolar RNAs, MBII-52 and U40, were still depleted. Again both sets of primer pairs for each pri-miRNA measured showed a very close enrichment ratio. These pri-miRNAs showed also to be predominantly associated with the PSD fraction (Figure 22), whereas BC1 was still almost entirely detected in the soluble fraction. The controls, CaMK2a, BC1, and 18S, are in close agreement with what I previously reported for the other synaptosomal preps (Figure 15).

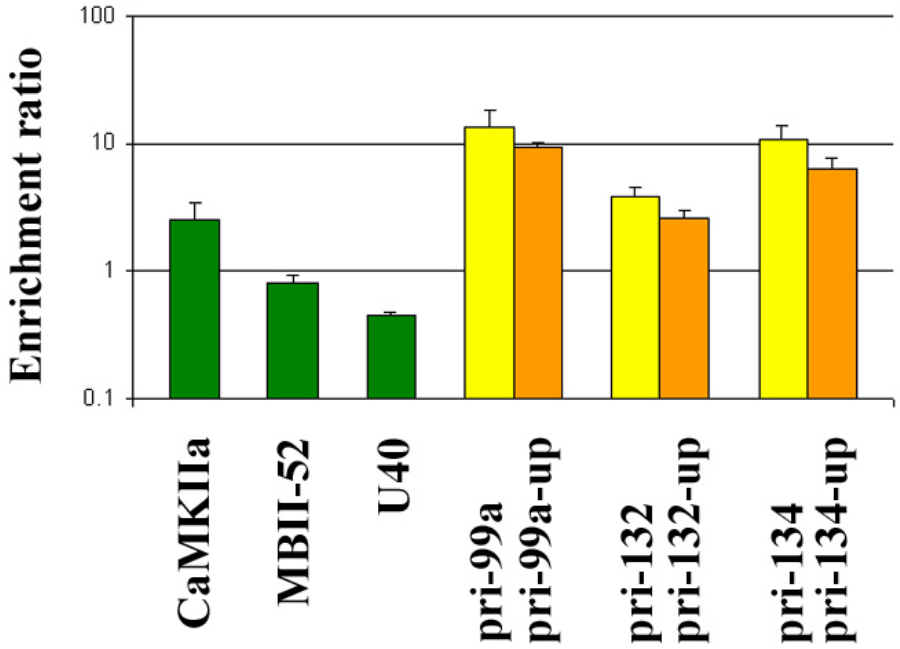

Figure 21. Enrichment ratio (synaptosome/total homogenate) of intergenic pri-miRNAs measured by qRT-PCR.
Green bars are the controls. Yellow and orange bars correspond to pri-miRNA PCR products. Yellow are the PCR products flanking the hairpin and orange are the PCR products upstream the hairpin.
Data represent the average of 3 independent preps. Note the log scale.

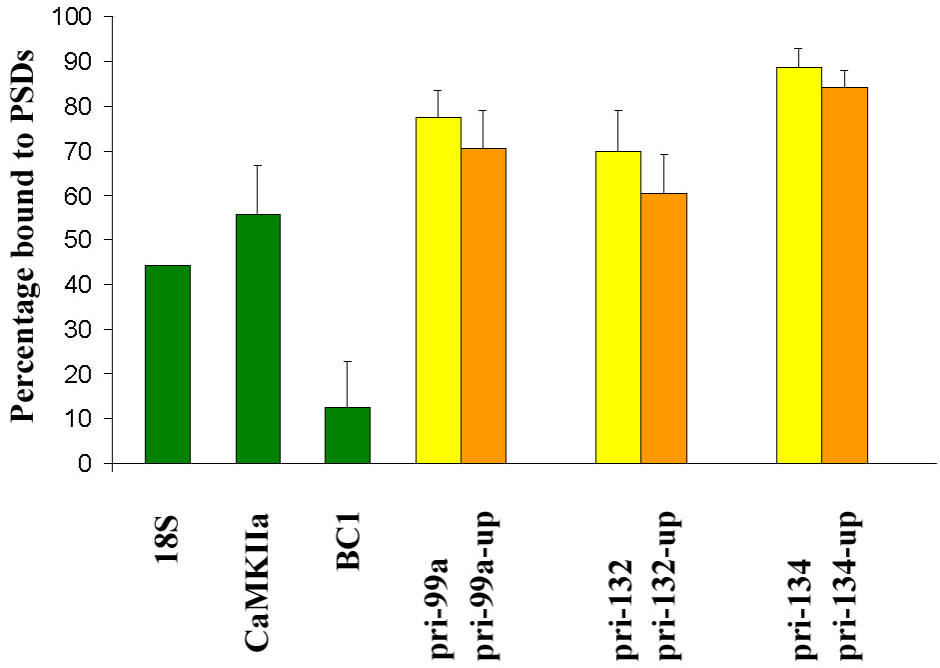

Figure 22. Distribution of synaptosomal pri-miRNAs and control RNAs in soluble vs. PSD fractions after extraction with Triton X-100.
Total RNA was prepared from synaptosomal fraction (Syn) that was then lysed with 1% Triton X-100 to yield soluble fraction (Sol) and insoluble fractions (PSD). qRT-PCR measurements of RNAs were performed from each fraction as described in Methods. Green bars are the controls. Yellow and orange bars correspond to pri-miRNA PCR products. Yellow are the PCR products flanking the hairpin and orange are the PCR products upstream the hairpin.
The PSD/Syn ratio was calculated for 3 independent preps and is plotted as shown.

6. Drosha and DGCR8 are present in the PSD fraction

The presence of these intergenic pri-miRNAs, or at least transcripts longer than pre-miRNAs, in PSDs fractions, opened to the possibility that also Drosha and/or DGCR8 could be localized in synaptic fractions.

6.1. Characterization of the anti-Drosha antibody

We decided to rise and to affinity purify an antibody against the C-terminal peptide sequence of mouse Drosha protein (1354-1373). We opted to raise the antibody in chicken, because we already had other rabbit antibodies, such as anti-Dicer and anti-eIF2c, and we wanted to be able to have the option to perform eventually multi-labeling in immunohistochemistry (IHC) staining.

In western blots of high speed supernatant (S2), and high speed pellet (P2) (preparation explained in method section), chicken anti-Drosha recognized several bands including the predicted 160 kDa band (Figure 23 a, d) (Fortin, 2002). This antibody was able to immunoprecipitate (IP) the same 160 kDa band, and probably a few other fragments, when immunoprecipitation was carried out in the two brain fractions (Figure 23 b, e). Since Drosha and DGCR8 act symbiotically and are tightly associated, I used a commercially available anti-DGCR8 antibody raised in rabbit which was still able to co-IP mainly the full length of Drosha (160 kDa) fragment in S2 fraction, plus other immunopositive bands are seen in P2 fraction (Figure 23 c,g). As positive control anti-DGCR8 antibody did also immunoprecipitated DGCR8 protein from the same fractions (Figure 24, c, f). To further support that the 160kDa band recognized by this antibody is Drosha, I knocked-down mouse Drosha mRNA in mouse neuroblastoma cells (N2a) with a pre-designed siRNA.

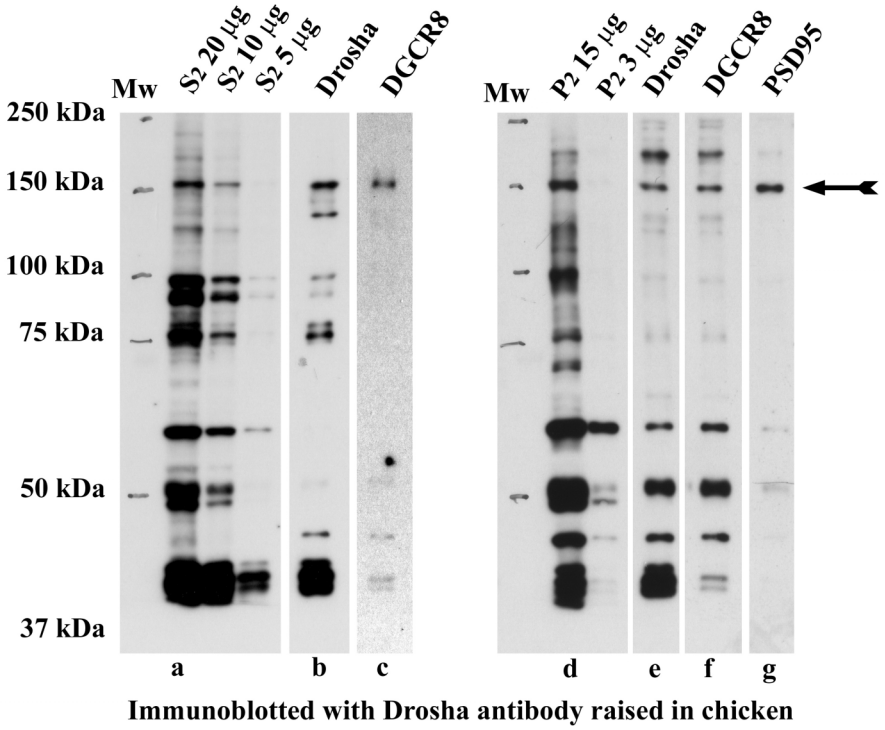

Figure 23. Adult mouse brain fractions immunoblotted with anti-Drosha antibody raised in chicken.

Cytosolic fraction (20,000g x 20min) (S2) and high speed pellet (20,000g x 20min) (P2) are loaded at different protein concentrations and immunoblotted with chicken anti-Drosha antibody (a, d). S2 and P2 fractions were immunoprecipitated using chicken anti-Drosha antibody (b, e) and rabbit anti-DGCR8 (c, f) antibody. In P2 fraction mouse anti-PSD95 antibody (g) is also used. Equal fractions of the co-immunoprecipitated samples were loaded in 7.5% Tris-HCl acrylamide gel, and immunoblotted with chicken anti-Drosha antibody (1:2,500) followed by rabbit anti-chicken IgY-peroxidase (1:50 000). The arrow on the right indicates the Drosha 160kDa immunoreactive band. On the top of the gel the different concentrations of S2 and P2 fractions are indicated, as well as the antibodies used for co-immunoprecipitation.

On the left of the blots are indicated the molecular mass standards (MW) of 250, 150, 75, 50 and 37kDa as they appear in the blots, which were reported on the films.

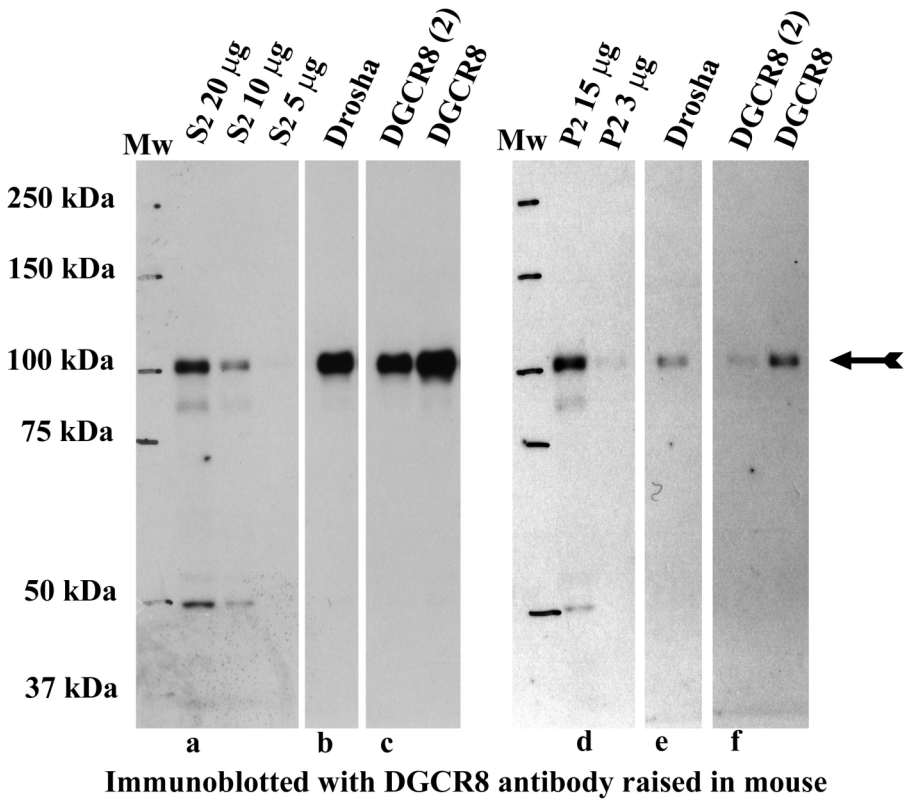

Figure 24. Adult mouse brain fractions immunoblotted with anti-DGCR8 antibody raised in mouse.

Cytosolic fraction (20,000g x 20min) (S2) and high speed pellet (20,000g x 20min) (P2) are loaded at different protein concentrations and immunoblotted with mouse anti-DGCR8 antibody (a, d). S2 and P2 fractions were immunoprecipitated using chicken anti-Drosha antibody (b, e) and two rabbit anti-DGCR8 antibodies (c, f). Equal fractions of the co-immunoprecipitated samples were loaded in 7.5% Tris-HCl acrylamide gel, and immunoblotted with mouse anti-DGCR8 antibody (1:5,000) followed by sheep anti-mouse IgG-peroxidase (1:30,000). The arrow on the right indicates the DGCR8 ~110kDa immunoreactive band. On the left are indicated the molecular mass standards (MW) of 250, 150, 75, 50 and 37kDa as they appear in the blots that were reported on the films.
A second band that migrates at ~50kDa can be noticed both in the S2 (a) and in the P2 (d) fractions and it most likely corresponds to mouse IgG present in the mouse brain extract that reacts with the anti-mouse secondary antibody (seen also when omitting the primary antibody). On the top of the gel the different concentrations of S2 and P2 fractions are indicated, as well as the antibodies used for co-immunoprecipitation.

As negative control, I also employed a siRNA, which has limited sequence similarity to known genes in mouse, rat and human, and it has been functionally proven to have minimal effects on cell proliferation and viability. As results, the Drosha-immunoreactive 160 kDa protein band was specifically decreased in abundance (Figure 25), in contrast Dicer full length immunoreactive band did not change significantly, and DGCR8 showed a markedly increase in intensity. Knock down of Drosha caused a significant increase in DGCR8 mRNA transcription and protein translation. This is in accordance with the report from Trboulet (2009) and Han (2009) where knockdown of Drosha leads to an increase in DGCR8 mRNA and protein levels in cells, because they regulate each other posttranscriptionally. This evidence confirms the effective knock down of endogenous Drosha in N2a cells. In addition, it strongly supports the appurtenance to Drosha of the 160 kDa immunoreactive band.

Meanwhile, another anti-Drosha antibody raised in goat and affinity isolated became commercially available. This antibody reacts with a different peptide (810-821) of Drosha, located between the RS and the first catalytic domains. Full length Drosha is recognized both in S2 and P2 fraction of mouse forebrain by this antibody (Figure 26, a, b). In addition, it also immunoreacts with the co-IP from anti-Drosha chicken antibody and anti-DGCR8 rabbit antibody (Figure 26 b, c, e, f). Thus, I concluded that the C-terminal Drosha chicken antibody does recognize Drosha in mouse brain, and it is suitable for co-IP of the microprocessor complex (Drosha and DGCR8).

Figure 25. Down-regulation of Drosha using siRNA in N2a cells causes a loss of Drosha-immunoreactive band as detected with chicken anti-Drosha antibody.
N2a cells were transfected with siRNAs at 50nM concentration and three days later S2 fractions were collected and equal protein concentrations were loaded in a 4-15% SDS-PAGE followed by immunoblotting with different antibodies as show on the right.
The top immunoblot shows that full-length Drosha (160 kDa) is almost undetectable in cells transfected with Drosha siRNA.
To confirm equal amount of protein loaded, the blot was re-blotted with anti-Dicer antibody (middle blot). Immunoblot with anti-DGCR8 antibody (bottom blot) shows a strong increase in DGCR8 immunoreactive band, confirming the successful knock-down of endogenous Drosha.

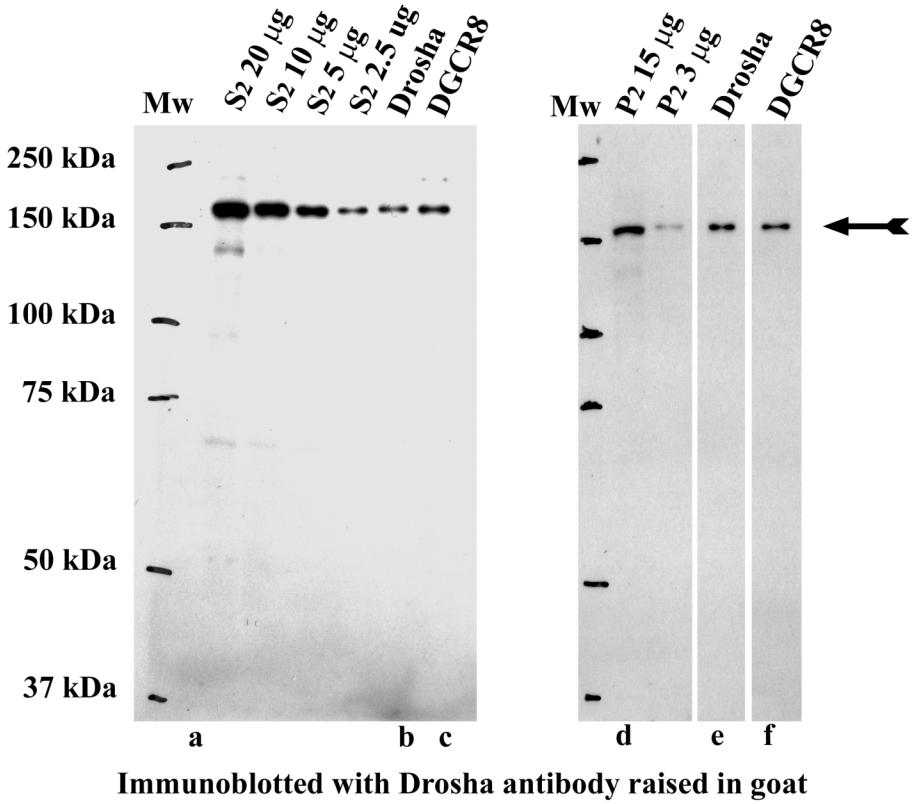

Figure 26. Adult mouse brain fractions immunoblotted with anti-Drosha antibody raised in goat.

Cytosolic fraction (20,000g x 20min) (S2) and high speed pellet (20,000g x 20min) (P2) are loaded at different protein concentrations and immunoblotted with goat anti-Drosha antibody (a, d). S2 and P2 fractions were immunoprecipitated using chicken anti-Drosha antibody (b, e) and rabbit anti-DGCR8 (c, f) antibody. Equal fractions of the co-immunoprecipitated samples were loaded in 7.5% Tris-HCl acrylamide gel, and immunoblotted with goat anti-Drosha antibody (1:2,000) followed by mouse anti-goat IgG-peroxidase (1:10 000). The arrow on the right indicates the Drosha 160kDa immunoreactive band. On the top of the gel the different concentrations of S2 and P2 fractions are indicated, as well as the antibodies used for co-immunoprecipitation.

On the left of the blots are indicated the molecular mass standards (MW) of 250, 150, 75, 50 and 37kDa as they appear in the blots, which were reported on the films.

6.2. Characterization of the anti-DGCR8 antibody

At the same time I confirmed that the anti-DGCR8 (C-terminal 701-714 aa) affinity purified rabbit polyclonal antibody recognizes full length DGCR8 protein both in S2 and in P2 fractions of mouse brain (Figure 24 a, d). The same immunopositive band is seen in the co-IP fractions from chicken anti-Drosha antibody which is cross-blotted with a DGCR8 mouse monoclonal antibody (Figure 24 b, e). Full length DGCR8 was also co-immunoprecipitated with another rabbit polyclonal antibody raised against the C-terminal half of human DGCR8 (423-773 aa) (Figure 24 c, f). This last antibody was also used to blot the Drosha Knock-down blot (Figure 25), and it has already been validated to immunoreact to DGCR8 protein in mouse tissue (Triboulet, 2009). To further support the specificity of these anti-DGCR8 antibodies, anti-Drosha chicken antibody is able to co-IP full length DGCR8 (Figure 24 b, e).

6.3. Drosha and DGCR8 are expressed in the PSD fraction of adult mouse forebrain

Subcellular fractionation of adult mouse forebrain showed that Drosha and DGCR8 are present in purified postsynaptic densities (PSDs) (Figure 27). Synaptosomes were prepared as previously described (see section 2). The PSD95 immunoreactive band is clearly enriched in the PSD fraction, absent in the S2 and in the synaptosomal soluble fraction. In addition Synapsin-I becomes soluble after treatment with Triton X-100 detergent, and this results are both in agreement with Figure 14. As additional positive postsynaptic marker, I immunoblotted these fractions for spinophilin (Figure 27), which is highly enriched in dendritic spines (Allen, 1997, Feng, 2000).

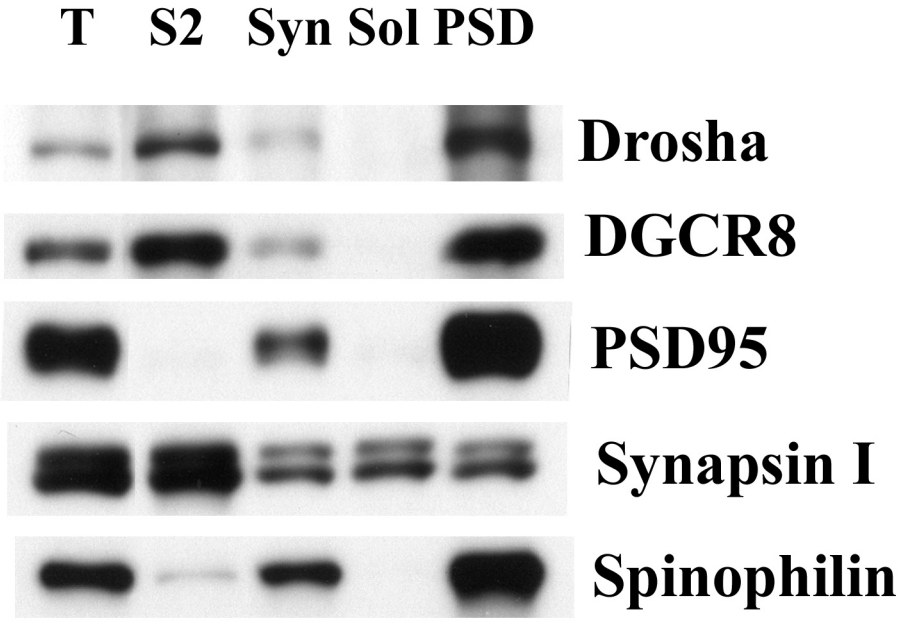

Figure 27. Expression of Drosha and DGCR8 in brain subcellular fractions.
Total forebrain homogenate (T) was processed to obtain a soluble cytoplasmic fraction (S2) and a synaptosomal fraction (Syn) that was then lysed with 1% Triton X-100 to yield a soluble fraction (Sol) and an insoluble fractions (PSD) as described in Methods.
Equal amounts of proteins (20 μg) were separated by SDS-PAGE under reducing conditions and immunoblotted with different antibodies as see on the left side of the blots. Anti-Drosha and anti-DGCR8 antibodies show to be immunopositive in PSDs, where PSD95 and Spinophilin are highly enriched.

6.4. Co-immunoprecipitation of Drosha and DGCR8 in synaptosomes

To rule out Drosha and DGCR8 as simple contaminants of Synaptic fractions that are co-isolated during subcellular fractionation, I employed an affinity-based strategy to additionally purify the triton-derived PSD fraction (Vinade, 2003). Moreover, the use of synaptosomes minimizes the contribution from extrasynaptic-intracellular PSD95 pools, and it is a PSD-enriched fraction from which such non-synaptic complexes have been largely eliminated (Dosemecy, 2007). Nevertheless, protein complexes could still be part of the main PSD complex and not physically anchored to PSD95 protein. Other similar PSD scaffolding proteins are PSD-93, PSD-92, SAP-97 and SAP-102 and they all belong to the larger MAGUK family, characterized by the presence of one to seven PDZ domains followed by an SH3 and a guanylate kinase-like domain.

To address this possible scenario, I lysed synaptosomes with either Triton X-100 detergent or RIPA buffer and immunopurification was carried out using mouse monoclonal anti-PSD95 antibody (Vinade, 2003) and mouse monoclonal anti-MAGUK antibody (Lugli, 2008). As additional positive controls, the two previously characterized antibodies, anti-Drosha antibody raised in chicken and anti-DGCR8 polyclonal antibody raised in rabbit were also used. As negative controls, to rule out co-immunoprecipitation due to non-specific binding to IgG antibodies of a specific species, two irrelevant antibodies were employed: a mouse monoclonal antibody (IgG ms) of the same IgG type of anti-PSD95 and anti-MAGUK antibodies, and a rabbit polyclonal antibody (IgG rbt), to counterbalance rabbit anti-DGCR8 antibody. The two negative control antibodies are irrelevant because the mouse monoclonal antibody is against Bromodeoxyuridine (BrdU) which is not present endogenously and the

rabbit polyclonal antibody is against Synapsin-I, which is associated with presynaptic vesicles, and I had previously shown to not co-IP with PSD95 (Figure 17a).

All antibodies were cross-linked to magnetic Dynabeads to avoid non-specific co-sedimentation of particulate contaminants (Vinade, 2003) during the procedure. The efficiency of the cross-linking to the beads was assessed by measuring the optical density (OD) of the antibody solutions before and after the coupling reaction, which was at least 90%, and by the ability of the antibodies to bring down the respective protein.

The anti-PSD95, anti-MAGUK, anti-Drosha and anti-DGCR8 antibodies did, as expected, bring down the respective protein in both detergent conditions (Figure 28). On the contrary, anti-BrdU and anti-Synapsin I did not co-precipitate any of them. As a further control, it is important to note that Drosha and DGCR8 co-immunoprecipitated the respective partner (Figure 28), as seen also previously (Figure 24 and Figure 26). Most importantly, the affinity PSD purified fraction was also immunopositive for Drosha and DGCR8, and vice versa, confirming that Drosha and DGCR8 are anchored to PSDs. Even though the band intensity for Drosha and DGCR8, affinity purified by the respective antibodies, does not seem to change between the two employed detergents, it is clearly more prominent after co-purification with anti-PSD95 and anti-MAGUK antibodies. There are many possible reasons for this outcome. The most likely one is that the RIPA buffer removes from the PSDs several peripheral attached proteins, allowing the antibody to reach epitopes that are now more available and that were before masked by other proteins. Moreover, the marked decrease of immunostaining of spinophilin in the RIPA co-IP compared to the Triton X-100 co-IP, suggests that loosely attached proteins and contaminants are actually more likely solubilized and detached by the PSD fraction (Fig 28).

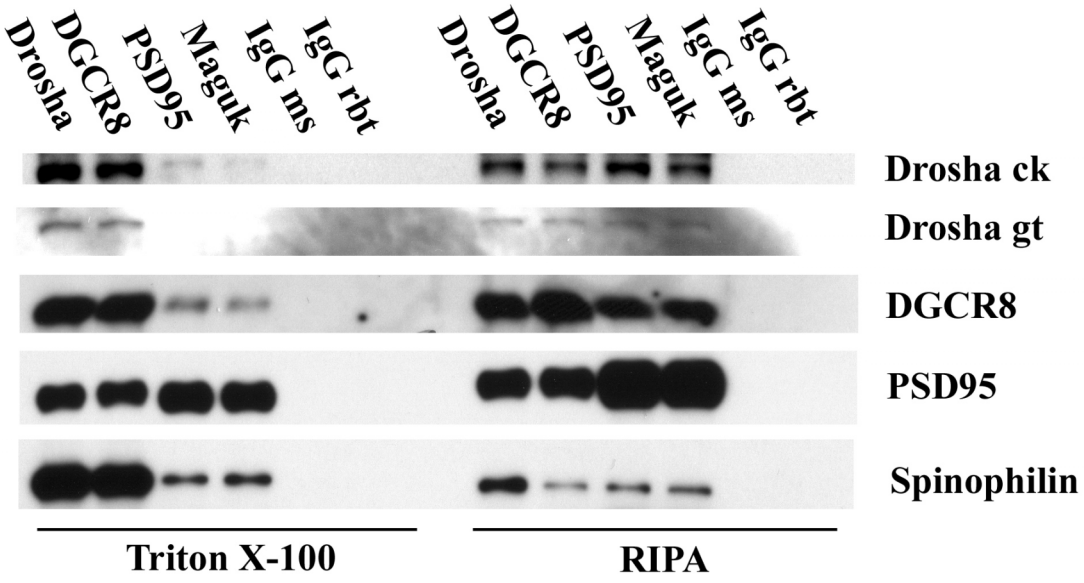

Figure 28. Co-immunoprecipitation of Drosha and DGCR8 with PSD95.
Synaptosomes were diluted 1:1 with either homogenization buffer supplemented with Triton X-100 or RIPA buffer (as indicated at the bottom of the immunoblot), and incubated with different antibodies (see top of the blot). Equal fractions were loaded in SDS-PAGE gel and immunostained for a series of antibodies, as indicated on the right side. Anti-PSD95 and anti-MAGUK antibodies immunoprecipitated Drosha and DGCR8 from lysed Synaptosomes. Co-immunoprecipitation was confirmed by cross-immunoblotting with both anti-Drosha antibodies (raised in chicken and goat) and DGCR8 antibody. Negative controls include anti-IgG mouse and anti-IgG rabbit to counterbalance the species of the other antibodies.

Another explanation is that the antibody has more affinity to the protein in a slightly denatured conformation. It is important to note that RIPA buffer contains a small percentage of the anionic surfactant sodium dodecyl sulfate (SDS), which in addition to disrupting the non-covalent bonds in the proteins, could also denature them and cause the molecules to lose their native conformation.

6.5. Drosha co-localizes with PSD95 in adult mouse hippocampus

As final evidence of Drosha co-localization with PSD95 in postsynaptic densities, Michael Demars performed immunohistochemistry (IHC) of the adult mouse hippocampus. Samples were prepared as described in the method section. As positive control for PSD localization, we used anti-PSD95 antibody and as negative control we employed anti-NeuN antibody, a neuronal specific nuclear protein marker (Mullen, 1992). Additional negative control constituted the omission of the primary antibodies, which did not give any detectable signal at the set values for the detector gain of the confocal laser microscopy.

As seen in Figure 29, the positive control, anti-PSD95 antibody, shows labeling in the dendritic projection, the negative control, anti-NeuN, clearly shows a strong localization in the nuclei but not in the dendrites. Anti-Drosha antibody labels nuclei and dendritic projections. The overlaid picture shows co-localization of Drosha with NeuN and with PSD95. The 100x enlargement picture (Figure 30), of a section of the CA1 area of the hippocampus, better elucidates and shows the labeling pattern of the different antibodies. Still, we can see co-localization of PSD95 and Drosha in the apical dendrites of the CA1 pyramidal neurons, and no PSD95 staining in the nuclei. A closer look at the apical dendrites of this section (Figure 31) shows no staining of NeuN. On the other hand, it is evident the

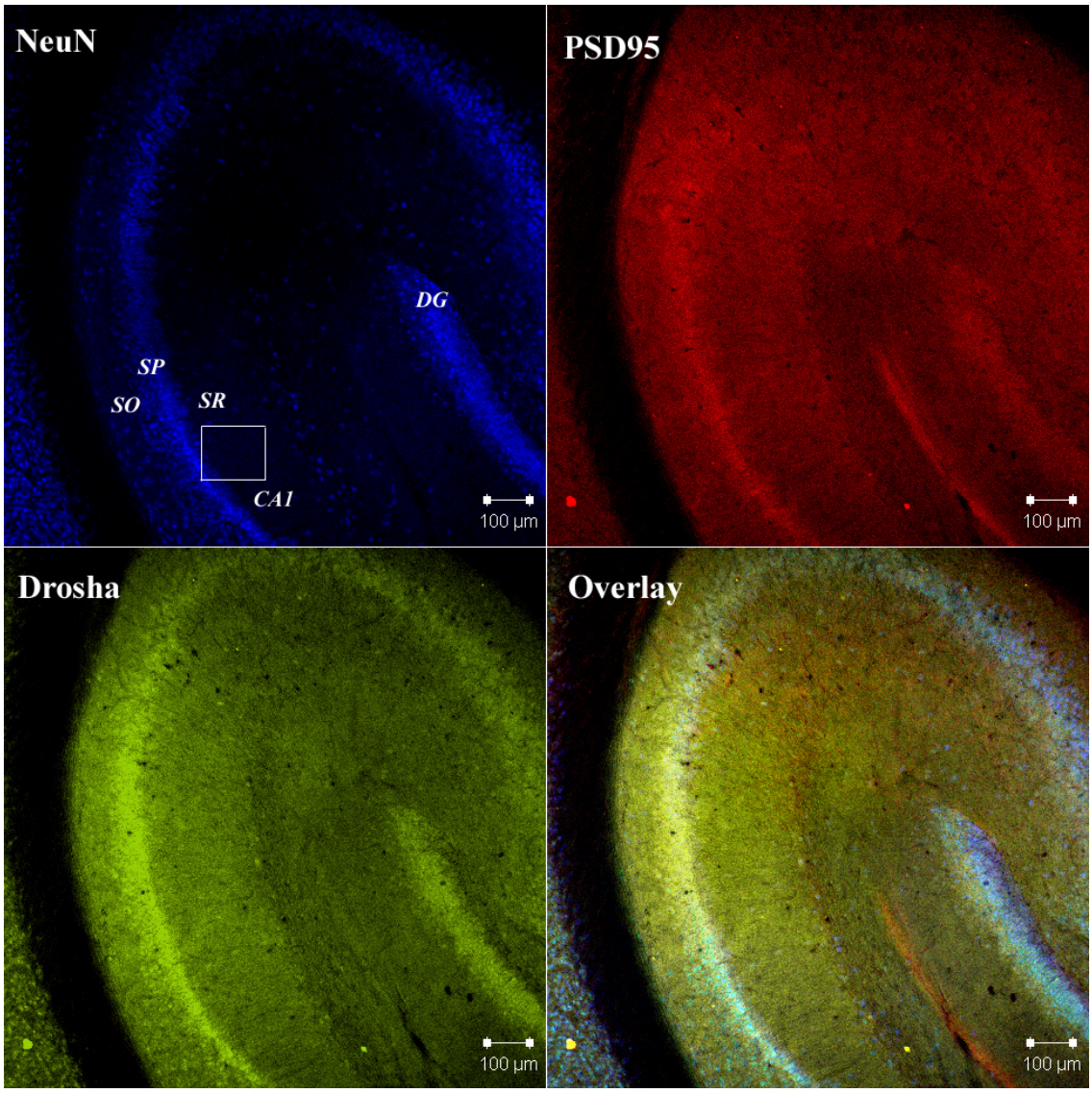

Figure 29. Immunolocalization of Drosha (green) in adult mouse hippocampus
Free floating section of adult mouse brain immunostained with goat anti-Drosha antibody. Tissue was counterstained with anti-NeuN antibody (blue) to label cell nuclei and anti-PSD95 (red) to reveal postsynaptic densities. On the bottom right of the panel the overlay of the three antibodies.
The square indicates part of the hippocampal area CA1 seen in the following figures in higher magnification. SO, stratum oriens; SP, stratum pyramidale; SR, stratum radiatum; DG, Dentate gyrus. Scale bars is 100 µm.

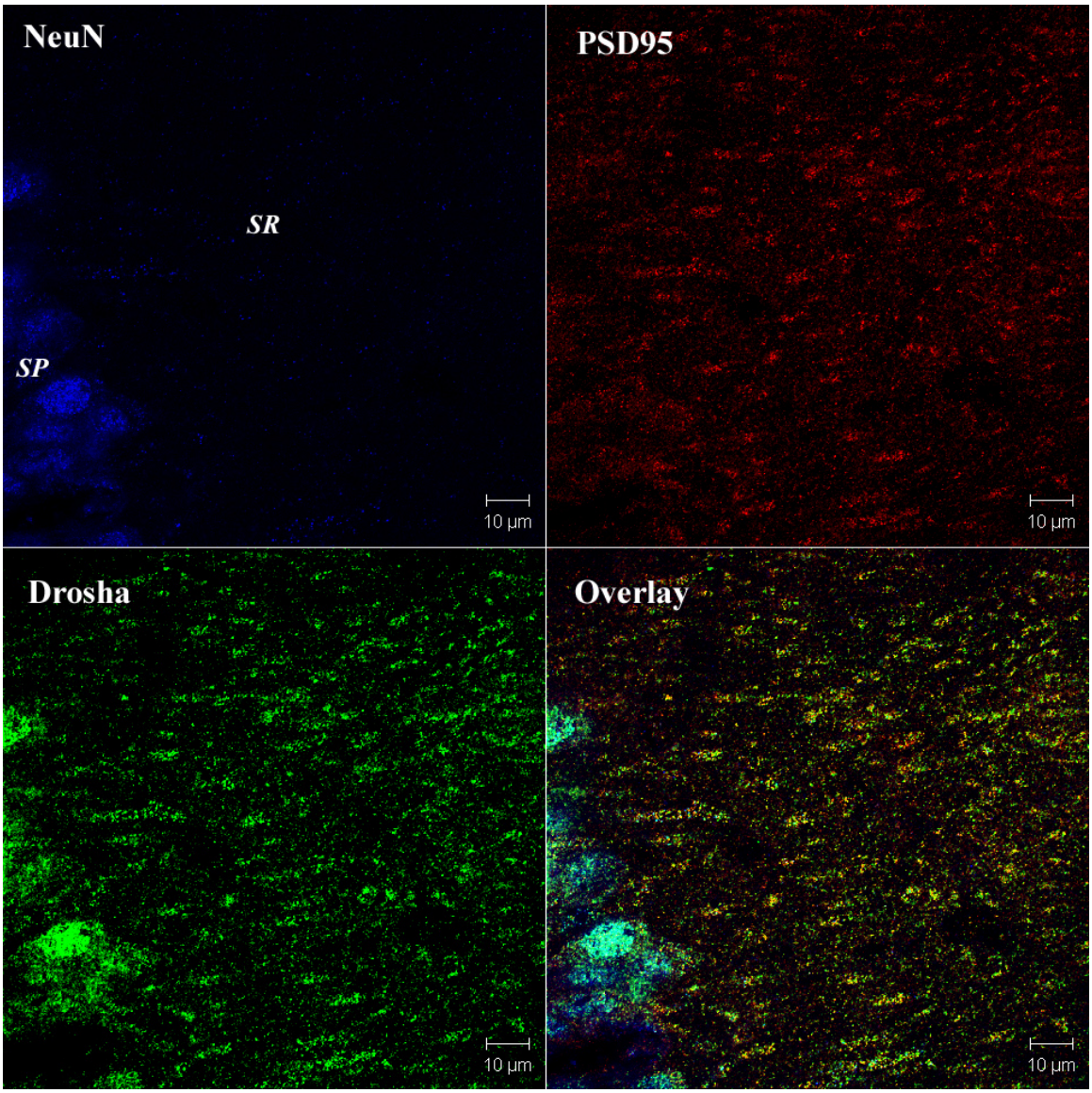

Figure 30. Co-localization of Drosha and PSD95 in CA1 area of adult mouse hippocampus

Magnification of the CA1 hippocampal area (from fig.29). Anti-PSD-95 (red) antibody reveals postsynaptic puncta in the stratum radiatum that are also immunopositive for Drosha (green), that turn yellow in the overlay image. We can also better notice the positive labeling of Drosha in the nuclei, which are not stain by anti-PSD95 antibody. NeuN is clearly in the SP and not detected in the SR.

SP, stratum pyramidale; SR, stratum radiatum. Scale bar is 10 µm.

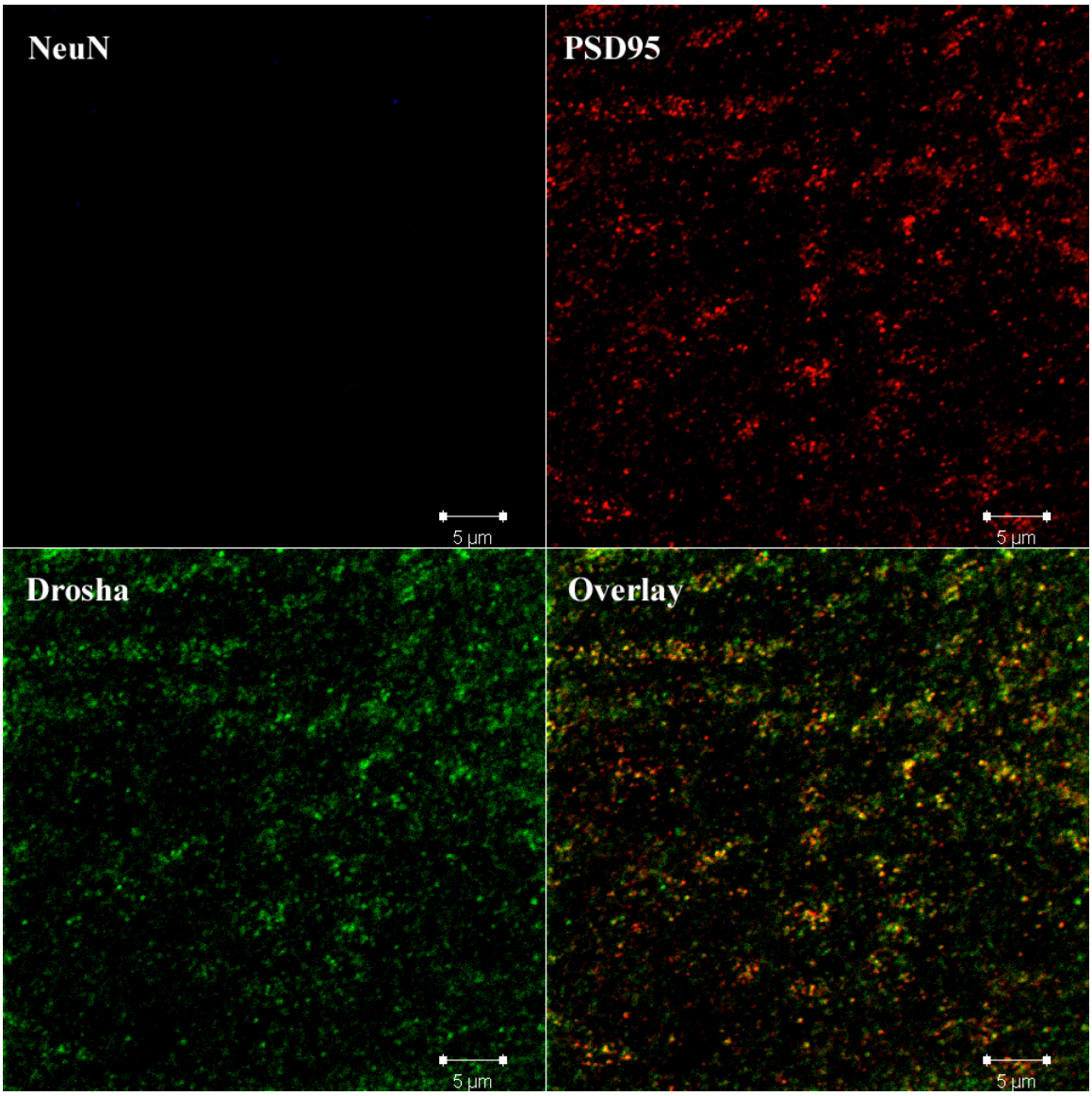

Figure 31. Drosha and PSD95 co-localize in stratum radiatum of CA1 area of adult mouse hippocampus

Magnification of the SR in the CA1 hippocampal area (see figure 30). Anti-PSD-95 (red) antibody reveals postsynaptic puncta in the stratum radiatum that are also immunopositive for Drosha (green), that turn yellow in the overlay image. NeuN is not detected in the SR. SR, stratum radiatum. Scale bar is 5 µm.

immunostaining of Drosha in many PSD95 positive punctuates. To rule out overlay staining due by single plane detection, we obtained images of this plane at different depth (z-stacks). Figure 32 shows the orthogonal view of a z-stack picture.

7. Dicer is able to process a primary-like RNA structure

The presence of Drosha, DGCR8 and pri-miRNAs in PSDs suggests that in adult neurons we are facing a more complex scenario of the microRNA pathway (see section 5). The co-existence of un-processed intergenic pri-miRNAs strongly supports the subcellular localization of Drosha and DGCR8, and vice versa. But I still have no evidence that the RNase III catalytic activity of Drosha and DGCR8 can be activated at PSDs, nor any evidence that they get activated there. Maybe they are just chaperones preventing the pre-miRNA from being processed pending further cellular signal. And if they are not somehow active or activated, why are pre-miRNAs at PSDs? Is it possible that Dicer liberated from the PSD and activated by Calpain is also able to process pri-miRNAs into mature microRNAs?

I had already confirmed in my previous study (Lugli, 2005) that recombinant Dicer is able to process long dsRNA into 22 nt fragments in a Mg-dependent manner, and that its RNase III activity is stimulated by Calpain. Thus, to address this question, I prepared a synthetic pri-miRNAs, as suggested in other studies (Lee, 2003; Fokuda, 2007), to possess all the structural characteristics to be processed by Drosha and DGCR8. The sequence is homologous to mouse pri-122, it is intergenic, it is 180 nt long and it flanks the hairpin at least 50 nucleotides on each side. Lee (2004) reported that exogenous pri-miRNAs with at least 25 nt. spanning from each end of the pre-miRNA are sufficient for Drosha processing.

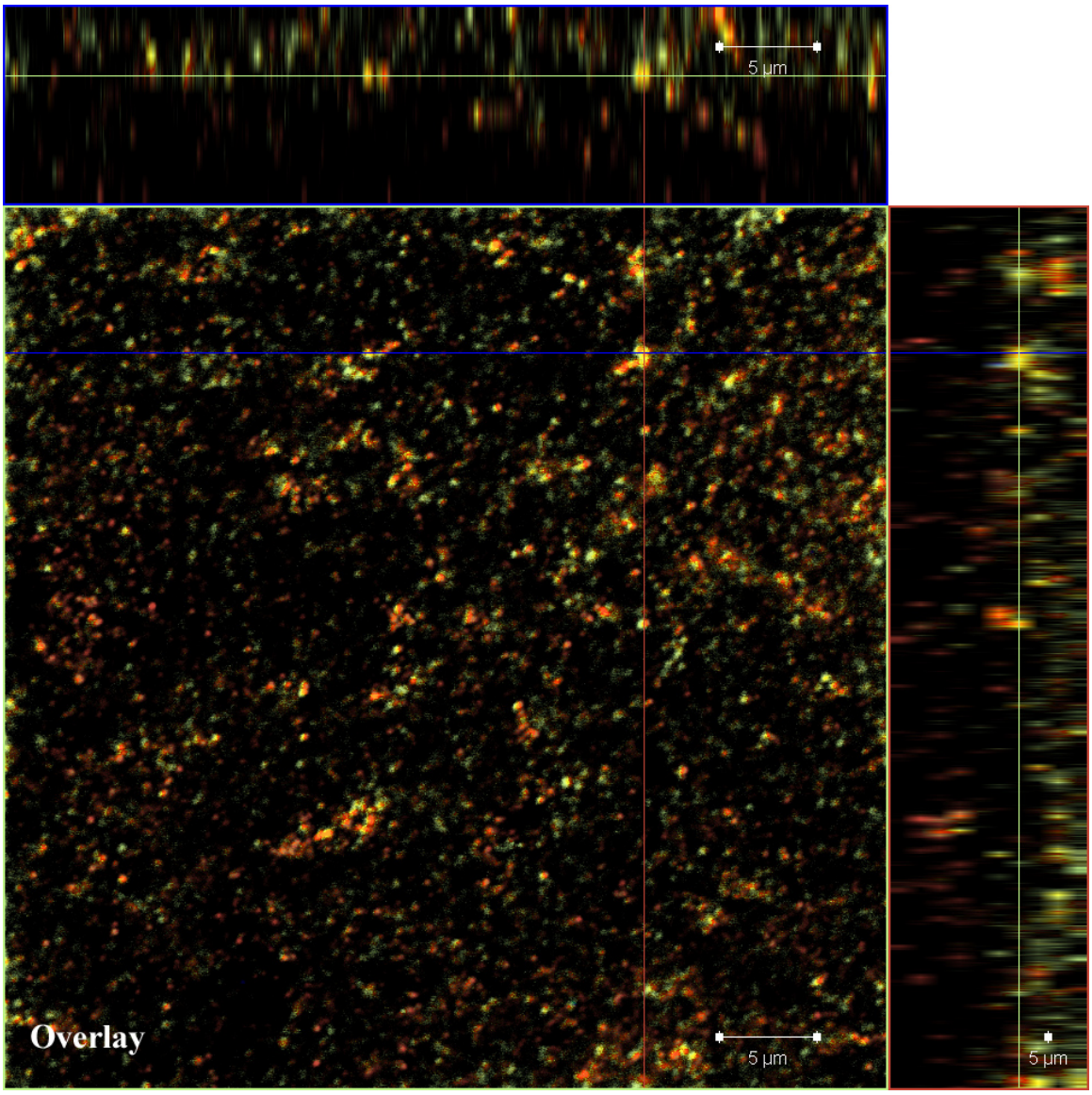

Figure 32. Orthogonal view of the co-localization of Drosha and PSD95 in the stratum radiatum

Orthogonal view of a z-stack image from the magnification of the stratum radiatum. Some of the PSD95 (red) positive postsynaptic puncta co-localize with Drosha (green). Co-localization is seen in the other two planes of this z-stack image as yellow puncta. Scale bar is 5 µm.

After gel size purifying pri-122 RNA, I confirmed the correct size by agarose gel (Figure 33) and also in a denaturing polyacrylamide gel. I performed an RNase III assay with re-Dicer and pri-122 RNA as substrate. As negative control, I included a group where Mg was omitted and as positive controls the substrate (pri-122) was incubated just with Dicer in the presence of Mg. As further negative control the pri-122 RNA was incubated without Dicer in the same conditions and for the same period of time.

As seen in Figure 34 Dicer processed the pri-122 RNA in an Mg-dependent manner over the time of incubation (up to 90 min). No fragments of the expected size were observed in the Mg-omitted group, or in the pri-122 group incubated by itself. This result supports the possibility that Dicer could still be the RNase III enzyme responsible for pri-miRNA processing at PSDs.

8. Drosha and DGCR8 are associated to Kinesin heavy chain in vivo.

Synaptic localization of Drosha, DGCR8 and pri-miRNAs requires most certainly that a motor protein transports them. Kinesin proteins (KIF) are the molecular motor that transports cargos along microtubules, both to axons and dendrites. Kinesin were originally identified by Brady et al. (1985), as composed of two heavy chains (KHC or KIF5) and two light chains (KLC). KIF5 are highly enriched in the brain and in neurons (Kanai, 2000). Evidence of KIF5 association with RNA-transporting granules in neurons was reported by Kanai (2004). Recently, Dictenberg (2008) reported that FMRP associates also to KIF5, and functions in the rapid, activity-regulated transport of mRNAs to dendrites, important for synaptogenesis and plasticity.

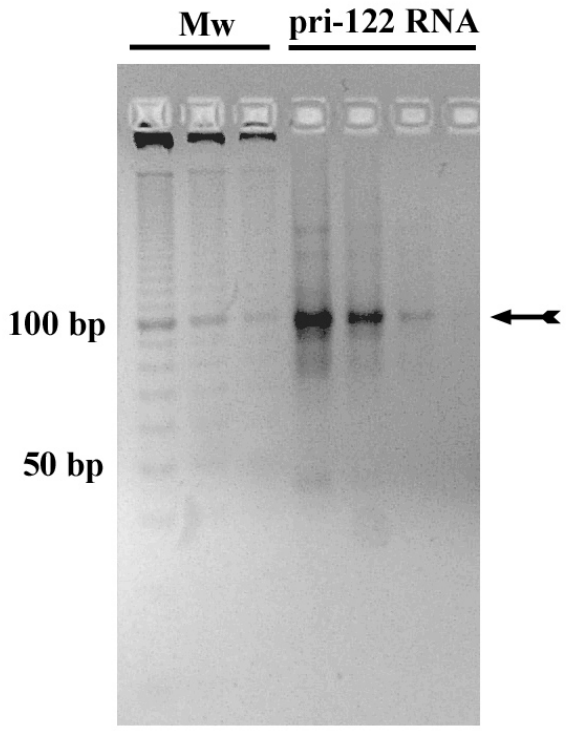

Figure 33. Agarose gel confirming the correct size and purity of the in vitro transcribed pri-122 RNA
The in vitro transcribed pri-122 RNA (180 nt) was gel purified and loaded (200, 100, 20, 4 ng/lane) in a 6% non-denaturing agarose gel. The 10bp DNA molecular marker on the left was also loaded at different concentrations per lane (500, 250, 100 ng/lane). The arrow on the right points to the pri-122 that, forming the hairpin, runs at a molecular weight of just less than 100 bp.

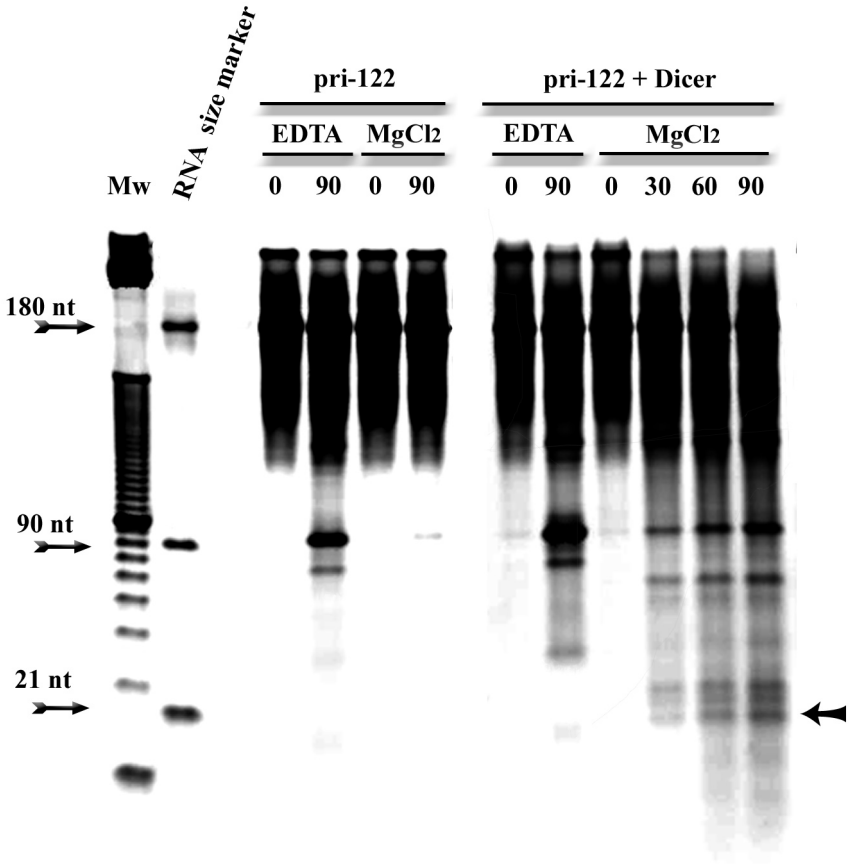

Figure 34. Processing of synthetic pri-122 intergenic hairpin RNA by recombinant Dicer.

Pri-122 hairpin RNA (180 nt top left arrow) was incubated with recombinant Dicer for up to 90 min. As negative controls, some sampled lacked Dicer or lacked $MgCl_2$. A series of small RNAs were formed in a time- and Mg-dependent manner (arrows on the bottom right). Because the DNA ladder (10 bp Mw, on the left) does not allow a direct calibration of RNA sizes, I loaded, next to the DNA ladder, three synthetic RNA sequences that are 180 nt long (pri-122 RNA), 90 nt long and 21 nt long. Samples are run in a 15% non-denaturing gel and visualize by Ethidium bromide.

To investigate the association of Drosha and DGCR8 with KIF5 motor proteins in the brain *in vivo*, I simply cross-blotted for KHC and KLC the Drosha and DGCR8 immunoprecipitates from S2 fraction (described in section 6.1 and 6.2). I used the anti-KHC and anti-KLC antibodies that have been extensively characterized by DeBoer (2008).

As seen in Figure 35, both KHC and KLC recognize the correct size protein in S2 fraction. KHC is co-isolated with Drosha and DGCR8 both in Triton and RIPA conditions, suggesting a strong and specific association (Figure 35 KHC b, c, d, e). On the contrary, KLC did not co-IP in either of these two conditions (Figure 35 KLC b, c, d, e). As positive control, anti-Drosha antibody pulled down DGCR8 and vice versa from the same fraction (Figure 24 and Figure 26). As negative control, anti-BrdU antibody did not bring down KHC nor KLC (Figure 35).

We can also observe a second higher molecular weight KHC immunoreactive band in the immunoprecipitates with DGCR8 and in the S2 fraction blotted with KHC antibody (Figure 35 KHC c, e), which is probably KIF5A. There are three known KIF5 isoforms present in the brain, KIF5A, KIF5B and KIF5C. The precise significance of the heterogeneity of KIF5s subunits from brain is unknown, but it may likely reflect functional differences (Brady, 1995). The KHC antibody recognizes all three isoforms and KIF5A has a slightly lower mobility compared to the other two kinesin isoforms, making it distinguishable (DeBoer, 2008). A specific anti-KIF5A antibody should be used to confirm the identity of the second immunopositive band in DGCR8 co-immunoprecipitate.

It should be noted that Leopold (1992) detected kinesin in purified organelle fractions, including synaptic vesicles, mitochondria, and coated vesicles, using EM microscopy. However, nuclear fractions did not contain detectable levels of kinesin.

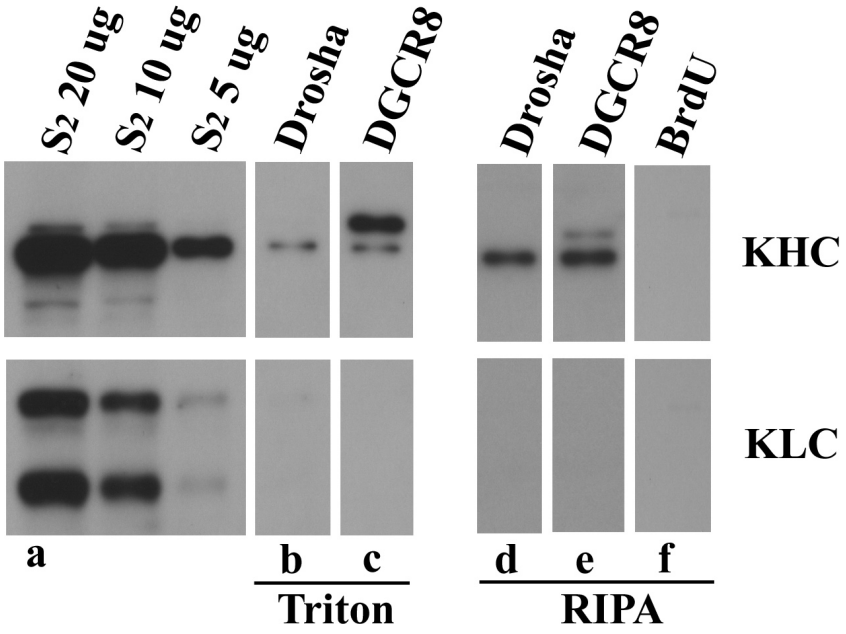

Figure 35. Drosha and DGCR8 interact with KIF5 in mouse forebrain in vivo. Immunoprecipitation was performed with anti-Drosha, anti-DGCR8 and anti-BrdU antibodies from S2 fraction of mouse forebrain, in the presence of Triton X-100 or RIPA buffer. Equal fractions were loaded in the gel and immunoblotted for kinesin heavy chain (KHC) and kinesin light chains (KLC). Three different amount of S2 fraction (a) were also loaded as positive controls. Drosha (b, d) and DGCR8 (c, e) co-immunoprecipitated KHC in both detergent conditions, and almost undetectable KLC. As negative control, anti-BrdU is immunonegative for KHC and KLC. We can also see in the co-IP with anti-DGCR8 antibody (c, e) another other immunopositive band, presumably KIF5A isoform.

Moreover, it seems that cargos binding to KLC tend to be transported mainly to axons, whereas binding to KHC is used for directing cargos to dendrites (Setou, 2002).

This result strongly indicates that immunoprecipitated Drosha and DGCR8 are associated with Kinesin in the cytoplasm, and that they are not just contaminants from nuclear leakage.

Further studies are required to address a physical and functional transport of pri-miRNAs by Drosha and DGCR8 in neurons.

IV. DISCUSSION

The present work demonstrates that most of the microRNAs expressed within the adult mouse forebrain are readily detectable within synaptic fractions, at levels that are comparable to those seen within the total forebrain homogenate. In fact, 37 microRNAs were enriched 2-fold or greater in synaptoneurosomes (SynN) as measured by microarray (Figure 9), and the enrichment was confirmed for selected microRNAs by real time qRT-PCR (Table II). The magnitude of SynN microRNA enrichment estimated by microarray (2-5 fold) was comparable to the enrichment observed with two known synaptic RNAs, BC1 and CAM kinase II alpha mRNA (Figure 13). The forebrain microRNAs that were enriched in synaptoneurosomes were biologically quite distinct from microRNAs that were relatively depleted from this fraction, both in their tissue expression patterns (many were expressed predominantly in pyramidal neurons) and in their evolutionary histories (SynN-enriched microRNAs tended to be evolutionarily new, often mammalian-specific or rodent-specific). These findings strongly suggest that a broad, diverse, yet biologically coherent population of microRNAs is expressed within dendrites and within dendritic spines, where they may be expected to contribute to the regulation of local protein synthesis.

MicroRNA precursors were also readily detected in synaptoneurosomes at levels similar to or greater than that found in the total forebrain homogenate (Figure 13). Within synaptosomes, the microRNA precursors were predominantly associated with postsynaptic densities (Figure 15). This was further confirmed by co-immunoprecipitation with PSD95 protein (Figure 17). The qRT-PCR method used here did not distinguish between primary microRNA gene transcripts (pri-miRNAs) and small hairpin precursors (pre-miRNAs). At

the same time it does not preclude the co-existence of either one of the two miRNA-precursors forms.

It was a great surprise to discover that primary microRNAs were reliably detected in synaptoneurosomes and at a greater level than that found in the total forebrain homogenate (Figure 20). Within synaptosomes, the intergenic primary microRNAs were also predominantly associated with postsynaptic densities (Figure 22). This was further confirmed, in a preliminary study, by co-immunoprecipitation with anti-PSD95 and anti-MAGUK antibodies in synaptosomal fraction of mouse forebrain (data not shown).

I therefore conclude that microRNA precursor forms (and not merely mature microRNAs) are prominent synaptic components.

The presence of intergenic primary microRNAs in postsynaptic densities strongly supports the requirements for Drosha and DGCR8 co-localization. An antibody against C-terminal of Drosha antibody has been raised and characterized, and verified suitable for immunoprecipitation studies (Figure 26). Subcellular fractionation of adult mouse forebrain revealed evident expression of Drosha and DGCR8 in postsynaptic densities (Figure 27). This finding was further confirmed by PSD95-affinity purification and by HIC for Drosha protein (Figure 28).

However, there is still no evidence that Drosha and DGCR8 present at PSDs have RNase III activity. As a matter of fact, Drosha and DGCR8 could have other functions:

- They may only be chaperones to transport pri-miRNAs to their destination, given that Drosha and DGCR8 are tightly associated to KHC (Figure 35);

- They may prevent the promiscuous processing of pri-miRNAs by Dicer in the cytosol, until they reach destination and release the pri-miRNA to Dicer to process them into mature microRNA (Figure 34).

But if Drosha and DGCR8 are present in an inactive state, and they could be enzymatically activated what would their trigger be? Are they activated by phosphorylation or a protease? Could Calpain be the Calcium-dependent protease responsible to active Drosha and DGCR8, similarly to Dicer at PSDs? Is there an inhibitor protein present at PSDs that prevents them to exhibit RNase III activity?

Clearly, further studies are required to address the many questions about Drosha and DGCR8 at PSDs. Nonetheless, I would like to propose a model based on these new findings, assuming that Drosha and DGCR8 are enzymatically active at PSDs. Drosha and DGCR8 are exported from the nucleus in association with intergenic pri-miRNAs. They are transported in an inactive state to PSDs, and anchored to scaffolding proteins. A stimulus triggers their activation and they locally process the pri-miRNAs. Newly formed pre-miRNAs are handed to Dicer and cleaved to form mature microRNAs. Through RISC, the microRNAs would bind to locally available mRNAs, and regulate synaptic plasticity.

The evident association of Drosha and DGCR8 to KIF5 protein (Figure 35) supports the suggestion that pri-miRNAs could be actively transported to PSDs. Many RNA-containing granules have been associated to KIF5 and actively transported to dendrites (Kanai, 2004; Dictenberg, 2008). Wibrand (2010) reported a striking mGluR-dependent up-regulation of pri-132/212 in dentate gyrus of adult rats. It is not clear at the moment if the transport of pri-miRNAs is selective or not, or if it can be stimulated by synaptic activity.

One of the most important pieces of this puzzle still missing is the evidence of synaptic conversion of microRNA precursors (pri-miRNAs or pre-miRNAs) upon synaptic activation to mature and active microRNAs. Park (2008) showed that chemical LTP in hippocampal slices caused the up-regulation of nearly all detectable microRNAs after 15 min. A recent study provided the first evidence that microRNA expression is specifically altered during an in vivo learning paradigm in mammals. A rapid up-regulation of 28 microRNAs occurred in the mouse hippocampus during a hippocampal-dependent learning paradigm (Smalheiser, 2010). Yet, not direct evidence has been shown to occur locally at synapses.

The finding of a possible immunopositive band for KIF5A in the DGCR8 immunoprecipitates (Figure 35) suggests that DGCR8 could also be either present in two different complexes in the mouse brain, or associated to two different KIF5s in different brain region, or type of neurons. KIF5s have considerable differences in brain distribution (Cay, 2001; Kanai, 2000). And there is strong evidence supporting the existence of KIF5 holoenzyme as homodimers in the brain (DeBoer, 2008). Nevertheless, both Drosha and DGCR8 are associated to the motor protein KIF5.

The findings reported here support earlier proposals that pathways related to RNA interference regulate long-term gene expression in the mature brain (Smalheiser, 2001; Schratt, 2006; Fiore, 2009). They also extend the observations that the RNase III enzyme Dicer is expressed within dendritic spines and is enriched in postsynaptic densities, in a form that is enzymatically inactive (Lugli, 2005; see also Figure 14). It is unlikely that Dicer bound, to PSDs, lacks a necessary co-factor needed for processing, since the RNase III enzymatic assay (Lugli, 2005) employed exogenous dsRNA, which does not require any co-

factors. Moreover, re-Dicer has been shown to exhibit catalytic activity also toward a primary-like microRNA structure (Figure 34).

The present findings also support the suggestion that the fragile X mental retardation protein (FMRP) may be involved in the processing arm of the microRNA pathway (associated with transport and/or processing of pre-miRNAs) as well as the effector arm (associated with mature microRNAs, RISC and target mRNAs). MicroRNA precursors were strongly associated with both Dicer and FMRP in cytoplasmic extracts, and Dicer interacted with FMRP, as shown by co-immunoprecipitation with specific antibodies under stringent conditions (Figure 18). Thus, it is likely that pre-miRNAs, Dicer and FMRP are part of a single complex in vivo

Finally, how might the microRNA machinery described here contribute to the regulation of protein translation near and within dendritic spines, a subject that has been intensively studied by neurobiologists because it is a fundamental mechanism of synaptic plasticity? Certainly, localized protein synthesis occurs within dendritic spines: mRNAs and translational regulatory components have been detected in close proximity to postsynaptic densities (Asaki, 2003; Suzuki, 2007), and intense stimuli that elicit LTP have been shown to cause some polyribosomes to move into dendritic spines where they are situated very close to active synapses (Ostroff, 2002; Bourne, 2007). Such conditions are also associated with localized increases of calcium and activation of Calpain.

I propose that synaptic stimulation may lead to local processing of microRNA precursors by Dicer (with or without the help of Drosha and DGCR8) acting near the postsynaptic density. This results in the loading of RISC with mature microRNAs that bind

to any available target mRNAs that are found restricted in the activated synapse. A very elegant fine tuned mechanism of posttranslational regulation active at subcellular resolution.

V. MATERIAL AND METHODS

1. Subcellular fractionation. Two month old male C57Bl/6 mice were employed in the present study. Each prep consisted of a pool of 3-4 forebrains (including cortex and hippocampus). Synaptoneurosomes, synaptosomes and isolated postsynaptic densities (PSDs) were prepared using standard methods (modified to preserve RNA integrity) and each prep was characterized to ensure that it had the expected enrichment of specific protein and RNA components, as previously described (Smalheiser, 2000; Lugli, 2005). Forebrain was rapidly dissected, placed in RNAlater (Ambion) for the time of the dissection of 3-4 mice and each pool was immediately homogenized using a Douce pestle in ice-cold HB buffer containing a cocktail of protease and RNase inhibitors (50 mM Hepes, pH 7.5, 125 mM NaCl, 100 mM sucrose, 2mM K acetate, 10 mM EDTA, 2 mM PMSF, 10 mM N-ethylmaleimide, 10 μg/ml leupeptin, 1 μg/ml pepstatin A, 2 μg/ml aprotinin, 160 U/ml Superase-In (Ambion), 160 U/ml RNase-OUT (Invitrogen)). Synaptoneurosomes were prepared as in Lugli et al. (2005), except that the synaptoneurosomes were quickly pelleted and rinsed twice in 10-20 x volume of homogenization buffer containing all inhibitors prior to extracting RNA. Synaptosomes were prepared as in Smalheiser (2000) but sucrose was treated with RNAsecure (Ambion) as per the manufacturer's instructions before making the sucrose gradient, and the sucrose solution was supplemented with RNase-OUT (Invitrogen) 320 U/ml.

2. RNA isolation. Total RNA was isolated with Trizol reagent (Invitrogen) according to manufacturer's directions with a few modifications to maximize yield of small RNAs. Glycoblue 20ug (Ambion) was added to the RNA precipitation step which was allowed to proceed overnight at -20C. The RNA pellet was spun down at 20,000g for 25 min at 4C; rinsed with 80% ethanol in DEPC-treated water (Invitrogen); resuspended and treated with RNAsecure (Ambion); and treated with DNase I using DNA-free (Ambion). Each prep was characterized for purity by OD 260/280 ratio and for integrity by running on agarose gels.

3. Northern blotting. Synaptoneurosomes were lysed with 1% Nonidet P-40, and the pellet was spun-down at 20,000g for 20 min and rinsed twice with HB buffer prior to preparing total RNA. The RNA was heated (100C, 3 min) in loading buffer type II (Ambion) and loaded (3.8 μg RNA for miR-124a, 0.5 μg RNA for BC1) in a 10 % TBE UREA criterion gel (Bio-RAD). The gel ran in 1X TBE buffer at 120 V for 1 hr and the RNA was transferred in 0.5X TBE buffer to Hybond-N+ (Amersham) for 30 min at 20 V. Membranes were UV-cross-linked for 2 min and baked at 80C for 45 min, incubated in ULTRAhyb hybridization buffer (Ambion) for 45 min at 68C on a shaker, then biotin-linked oligonucleotide probes were added (BC1 probe at 0.1 nM and miR-124a at 0.3 nM) with incubation overnight at 42C on a shaker. Membranes were rinsed and signals were detected using the BrightStar BioDetect kit (Ambion) with 1 min exposure to Hyperfilm ECL (Amersham). Probe sequences were as follows: BC1: aaaggttgtgtgtgccagttaccttgtttt; miR-124a: tgGcaTtcAccGcgTgcCttAa (lower case is DNA, upper case is Locked Nucleic Acid;

probes were modified with biotin at both 5' and 3' ends; probes were prepared by IDTDNA, Inc., Coralville, IA).

4. Primers for qRT-PCR measurements.

List of primers in TABLE V and TABLE VII. The TaqMan miRNA specific assay kit from Applied Biosystems used to measure mature microRNAs employs a set of proprietary looped primers whose sequences are not publicly available.

5. Housekeeping and synaptic RNAs (BC1, GAPDH, CAMK2A, ribosomal 18S RNA and U6). Total RNA (0.5 μg) was reverse transcribed with short gene specific primers with T_m around 38-42C using Superscript II (Invitrogen) as per the manufacturer's protocol with a few modifications. Denaturation was performed at 80-90C for 5 min, followed by 5 min at 33C, 30 min at 36C and 30 min at 42C. Real-time quantitative PCR was performed on a Stratagene MX 3005P real-time PCR Instrument. Each sample was run in duplicate or triplicate. All products were confirmed and distinguished from primer dimers by examining melting curves and by running the PCR product on 3.5% agarose gels. As negative controls, parallel samples lacked reverse transcriptase, or lacked added RNA sample. The PCR mix, 20 μl, contained 10 μl of SYBER GREEN PCR master mix (Applied Biosystem), 0.4 μM of each pair of primers, and 5 μl of dilute cDNA (1:50). PCR was performed for 20s at 95C, 25s at 58C and 25s at 72C for 40 cycles followed by the thermal denaturation protocol.

TABLE VII

LIST OF PRIMERS EMPLOYED TO MEASURE CONTROL RNAS
AND THE MICRORNA PRECURSORS

Controls		Short RT		Forward		Reverse
BC1		AAAGGTTGTGTGTG		CTCAGTGGTAGAGCGCTTG		GGTTGTGTGTGCCAGTTACCTTG
CaMKIIa		GTATGCCGCCT		GAACTTCTCCGGAGGGAAG		TGCATCCAGGTACTGAGTG
Map2		GCCAAGAGCTCA		ATCATCACACAGTCCCCAAG		GCCAAGAGCTCATGCCTAA
GAPDH		CATACCAGGAAATGA		ATGACATCAAGAAGGTGGTG		CATACCAGGAAATGAGCTTG
18S		CCATCCAATCGG		GTAACCCGTTGAACCCCATT		CCATCCAATCGGTAGTAGCG
U6		TATGGAACGCTTC		CTCGCTTCGGCAGCACA		AACGCTTCACGAATTTGCGT
MBII-52		GGCCTCAGCG		GGGTCAATGATGACAACCCAA		GGCCTCAGCGTAATCCTATTG
U40		ATGACAAGTCCTTG		AGGGTGATGAAAACGTATCCT		ATGACAAGTCCTTGCATTGG
Precursors						
pre-99a		ACAGACCCATAGAA		TAAACCCGTAGATCCGATCTTG		ACAGACCCATAGAAACGAGCTTGC
pre-124a		CTCTTGGCATTCAC		TCCGTGTTCACAGCGGAC		CATTCACCGCGTGCCTTA
pre-125b1		AGCTCCCAAGAG		GTCCCTGAGACCCTAACTTG		AGCCTAACCCGTGGATTT
pre-125b2		AGGTCCCAAGAG		GTCCCTGAGACCCTAACTTG		CAAGAACCTGACTTGTGATGTTAC
pre-134		GGTTGGTGACTAG		GTGACTGGTTGACCAGAGGG		GGTGACTAGGTGGCCCACA
pre-339		TCTGTCGTCGAG		TCCCTGTCCTCCAGGAGCT		TCTGTCGTCGAGGCGCT

6. MicroRNA precursors. RNA (1 μg) was employed for each reaction. Specific primer pairs specific to each precursor were employed, following the protocol described in Jiang (2005), employing mouse sequences. The PCR mix was as described above, and PCR was performed for 20s at 95C, and 50s at 60C for 50 cycles followed by the thermal denaturation protocol. In our hands, microRNA precursors were more "finicky" to measure using RT-PCR than other types of RNAs, and for some pre-miRNAs (especially those forming relatively tight hairpins) it was necessary to modify the Schmittgen protocols by changing the primer sequences or by raising the denaturation temperature. (We were never able to analyze pre-miR-143 successfully, presumably because it forms a very tight hairpin structure.) Besides confirming PCR products by melting curves and by running the PCR products on agarose gels, selected pre-miRNAs were also tested to verify that they were cut by specific restriction enzymes giving pieces of the expected sizes.

7. Primary microRNA transcripts. (including all the control measure in the same preps) Total RNA was isolated the samples with TRIzol reagent (Invitrogen). RNA yield was determined with A_{260}/A_{280} ratio using NanoDrop®ND-1000 (NanoDrop Technologies) and integrity was checked on a 1% agarose gel. 0.5ug of total RNA was reverse transcribed using, 1.5 μl of a 10μM mix solution of each short specific RT primer, 10mM dNTP mix, 0.1M DTT, 40units RNaseOUT and 200units SuperScript™ III. Denaturation was performed at 90 C for 5 min. RT reaction was carried out by 5 min at 38C, 30 min at 42 C, 30 min at 55 C, in a final reaction volume of 20 μl. Realtime PCR reaction was carried out in a final volume of 20μl, containing 5ul of cDNA diluted 1:10, 20uM each of specific primers, and 1X SYBR green PCR Master Mix (Applied Biosystems). All experiments are performed in

duplicate and include a non-RT and no template control. Reactions were run on Mx3005p (Strategene) with cycling conditions: 95°C for 10 min, 40 cycles 95C for 15sec and 56C for 25sec, 72C for 20sec and followed by a melting curve cycle; 95°C for 1 min, 55C for 30sec, 95C for 30sec. Primer specificity was verified by a single peak in the melting curve analysis and a single band of the right size on gel electrophoresis for all genes analyzed.

8. Mature microRNAs. Reverse transcription was performed in 20 ng of total RNA using specific TaqMan® MicroRNA Reverse Transcription and Assay kits (Applied Biosystems) following the manufacturer's protocol. MicroRNA specific PCR employed the TaqMan miRNA specific assay kit from Applied Biosystems. This recognizes dimeric PCR product in a sequence-specific manner and thus does not detect primer dimers. The looped primers are designed to avoid detecting pre-miRNAs. Although it is conceivable that some pre-miRNAs are recognized under some conditions (i.e., when the mature microRNA derives from the extreme end of the pre-miRNA), this would not have a practical effect on measuring mature microRNA levels because the steady-state levels of mature microRNAs are typically 20-50 times higher than that of the corresponding pre-miRNAs (e.g., Jiang, 2005; Schmittgen, 2008).

9. MicroRNA microarrays. Each microarray measured a single paired prep (total forebrain homogenate vs. synaptoneurosome fraction, SynN). Total RNA (10 micrograms) was size-selected and labeled with Alexa dye A3 (total homogenate) or A5 (SynN) by Invitrogen staff. The labeled RNA was mixed together and hybridized to a NCODE multi-species microRNA chip (Invitrogen version 1.0) using Maui hybridization. Invitrogen

version 1.0 chips contain 2 spots for each annotated microRNA across multiple species – since many mouse, rat and human microRNAs have identical sequences, up to 6 spots per array could be averaged for certain microRNAs. We removed from consideration any individual spots with high internal standard deviation (i.e., SD > 3X the median intensity value in either the red or green channel) as well as outlier spots (i.e., cases in which 1 or 2 spots had intensity values < 2X background, and the remaining spots for that microRNA had intensity values > 3X background in either red or green channel). Raw intensity values were adjusted by subtracting local background values from each spot (any spot with resulting intensity < 0 was assigned the value 1). The microarray intensity values, as well as the results of real-time RT-PCR measurements, indicate that the overall concentration of microRNAs relative to total RNA was similar in both the SynN fraction and the total homogenate (fig. 2); the overall profile of intensity values was also similar across the three preps (data not shown). The intensity values were normalized further as described in Results.

10. Immunopurification with anti-PSD95 antibodies (Figure 17). Protein-G and Protein-A agarose beads were rinsed twice with HB buffer containing the cocktail of protease and RNase inhibitors and once with HB diluted 1:1 with RIPA buffer containing inhibitors. Purified synaptosomes (2.3 mg/ml) were lysed by diluting the suspension 1:1 with RIPA buffer (pre-treated with RNAsecure, Ambion and containing the protease and RNase inhibitor cocktail) and pre-cleared with Protein-A agarose beads (Amersham) or with Protein-G agarose beads (Amersham) for 60 min at 4C. Anti-PSD95 monoclonal antibody (Univ. California-Davis, clone 28/86, 1 mg/ml) or anti-Synapsin I affinity purified polyclonal antibody (Chemicon, AB1543P, 0.1 mg/ml) was added to pre-cleared synaptosomes and

incubated over night at 4C with gentle agitation. These were then mixed with protein-G beads (anti-PSD95 sample) or protein-A beads (anti-Synapsin I sample) for 4 h, then the beads were rinsed twice with HB (diluted 1:1 with RIPA containing the inhibitor cocktail), once with HB, and once with 50 mM Tris pH 7.0. To analyze proteins associated with the immunoprecipitates, 40 μl Laemmli loading buffer was added, the beads were heated at 100C for 5 min, and DTT was added (final concentration 1%). As negative controls, assays were conducted in the absence of primary antibodies and in the absence of synaptosomes. To analyze RNA associated with the immunoprecipitates, Trizol 1 ml (Invitrogen) was added to rinsed beads and total RNA was extracted.

11. Western blotting. Western blotting was performed as in Lugli (2005). Blots were blocked in 1% nonfat dry milk for 1 h, room temp, incubated with primary antibody anti-PSD95 monoclonal antibody (Clontech, 1:30,000), anti-PSD95 rabbit polyclonal antibody (Cell signaling D74D3 1:30,000), anti-Synapsin I affinity purified polyclonal antibody (Chemicon, AB1543P, 0.1 μg/μl), anti-Drosha chicken antibody (1,2500), anti-Drosha polyclonal goat antibody (Sigma 1:2,000), anti-DGCR8 monoclonal antibody (Proteintech 60084-1 1:5,000), anti-DGCR8 polyclonal antibody (Proteintech 1: 5,000), anti-spinophilin rabbit polyclonal antibody (Sigma N-5162 1:5,000), anti-Kinesin heavy chain monoclonal antibody (Millipore MAB1614 1:1000), Kinesin light chain (was a generous gift from Brady S. 1:1000) overnight with rocking at 4C and rinsed; goat anti-mouse IgG (peroxidase conjugated; Chemicon) or goat anti-rabbit IgG (peroxidase conjugated; Sigma A0545), sheep anti-mouse IgG (peroxidase conjugates; GE healthcare NA931), goat anti-chicken IgY (peroxidase conjugated; Sigma A9046) was added at 1:30,000-50,000 for 2 h

and rinsed; finally, blots were incubated in ECL-Plus reagent (Amersham) and exposed to film (Hyperfilm ECL, Amersham).

12. siRNA Drosha Knock-down. N2a cells were grown in DMEM (high glucose, Sodium Piruvate, Glutamate) supplemented with Gentamicin and 10% FBS. The media was changed the day before transfection. siRNA sequences were purchased from Ambion (siRNA Drosha: cat.# 4390771 siRNA negative control: cat#4390843). Just before siRNA transfection the media was replaced to Optimem I and the cells were suspended in fresh Optimem I media. RNAi Max mix and the siRNA mix were placed in the dish at 50 nM and after 20 min the Optimem I - N2A cell suspension was added to the plates. They were kept in the incubator at 37C and the day after the media was replaced with Neurobasal Media supplemented with B27.Three days after the transfection the cells were first rinsed with 50mM Hepes (pH=7.5), 125 mM NaCl, 2 mM KAcetate and then collected and homogenized with same buffer supplemented with 0.1% triton X-100, 10 mM EDTA, 2 mM PMSF, 10 mM NEM, 10 μg/μl leupeptin, 1 μg/μl pepstatin A, 2 μg/μl aprotinin. After spinning down at 20,000g for 20 min at 4C, the supernatant was collected and part of it was saved for protein concentration evaluation and aliquots were Methanol precipitated at -20C o/n. After spinning down 20,000g for 20 min at 4C the precipitates, they were air dried and then dissolved in SDS-Laemmeli buffer and DTT was present at a 1% final concentration. The samples were loaded (20ug) in a 4-15% Tris-HCL Criterion Gel (Bio-Rad) and transferred to PVDF membranes (GE Healthcare).The blots were incubated with primary antibodies o/n at 4C and for 2 hours in secondary antibody. They were then incubated with ECL-plus (GE Healthcare) for 5 min, and exposed to Hyperfilm ECL (GE Healthcare).Primary antibodies used were

chicken anti-Drosha antibody (1:20,000), anti-DGCR8 monoclonal antibody (Proteintech, 1:20, 000); rabbit anti-Dicer polyclonal antibody (1:10, 000).

13. Immunoprecipitation with magnetic Dynabeads. All the antibodies, mentioned in the western blotting section but mouse monoclonal anti-BrdU antibody (Sigma B-8434), were concentrated with the Amicon Ultra 10K centrifugal filters, buffer exchanged in PBS, and coupled to the magnetic Dynabeads utilizing the Dynabeads Antibody coupling kit (Invitrogen) following the manufacturer's instructions. Antibody-coupled magnetic beads (1 mg) were coated with bovine serum albumin in HB with Triton X-100 (0.1%) for 1 h and incubated with S2 fraction, P2 fraction, or synaptosomes overnight at 4°C on a rotor. When RIPA was used, samples were diluted 1:1 with RIPA buffer, and when Triton X-100 was used, they were diluted with 1:1 HB supplemented with 0.2% triton X-100. Beads were then washed twice with HB plus either Trion x-100 or RIPA, twice with HB, and once with 50 mM Tris-HCl (pH 7.0). Protein were eluted boiling the beads with SDS-Laemmeli loading buffer for 5 min at 100C and carried out Western blotting as described above.

14. Pri-122 synthetic RNA. To make synthetic intergenic pri-122 hairpin RNA synthetic oligos (forward and reverse) were custom made (IDT DNA) and annealed in 20 mM Tris-HCl and 1 mM EDTA to form double-stranded DNA. This corresponds to the sequence of the endogenous mouse pri-122 flanking the hairpin plus a T7 promoter sequence. The forward sequence is 5′- TAATACGACTCACTATAGGG ACGGAGGAATGTGAAGGGAAGGTTAATACCCTTGTGCCTGACAGACTTTCCTTA GCAGAGCTGTGGAGTGTGACAATGGTGTTTGTGTCCAAACCATCAAACGCCATT

ATCACACTAAATAGCTACTGCTAGGCAATCCGTCCACTCCACGCGTGACTTGACG TCTGTTCTCTCCGAGCA -3′. The DNA was transcribed into RNA using the MEGAshortscript kit (Ambion) following the manufacturer's instructions and DNase treated using TURBO DNA-free DNase (Ambion) for 30 min. The RNA was gel purified in a 15% TBE polyacrylamide gel and eluted overnight in elution buffer as described in the kit. After Trizol purification of the precipitated RNA, OD was measured and purification confirmed by running an aliquot on a 6% agarose gel, on a 15%TBE polyacrylamide gel (Bio-Rad) and on a 15% TBE-UREA gel (Bio-Rad).

15. Immunohistochemistry. Male 2-3 month old wild-type mice were maintained in climate-controlled group housing under a 14:10h light:dark cycle with free access to food and water. Mice were transcardially perfused with ice cold Phosphate Buffered Saline (PBS) followed by 4% paraformaldehyde. Brains were removed and post-fixed in 4% paraformaldehyde. Following 48hr in paraformaldehyde, brains were moved to 30% sucrose solution for 3 days and then sectioned on a freezing stage microtome at 50μm. Sections were stored in a cryopreservant solution (47.6 % PBS, 28.57% Ethylene Glycol and 25% Glycerin v/v) at -20°C until use. Free floating sections were washed 5 times in TBS and then directly placed into blocking solution containing 5% normal donkey serum in TBS with 0.25% TX-100. Following blocking, sections were stained with mouse anti-NeuN (1:400; Millipore), goat anti-Drosha (1:200), rabbit anti-PSD-95 (1:200; Cell Signaling), for 72 hrs at 4°C. Following 72hr incubation in primary antibodies, sections were blocked 2X 1hr in 5% normal donkey serum in TBS with 0.25% TX-100 at room temperature. If necessary, sections were placed into biotin incubation for 1hr. Sections were then incubated in

fluorescent secondary antibodies anti-mouse cy3 (1:500), anti-rabbit cy3 (1:500), anti-goat cy5 (1:250), all from Jackson Immunoresearch (West Grove, PA) for 2hr at room temperature in the dark. Following incubation, sections were washed 3X in TBS and mounted using PVA-DABCO mounting medium. Negative controls employing secondary antibodies only were used to assess antibody specificity. The picture were taken using a Zeiss AX10 microscope (Carl Zeiss Ltd., Hertfordshire, England)

CITED LITERATURE

Abu-Elneel, K., Liu, T., Gazzaniga, F.S., Nishimura, Y., Wall, D.P., Geschwind, D.H., Lao, K., and Kosik K.S.: Heterogeneous dysregulation of microRNAs across the autism spectrum. *Neurogenetics*, 9:153–161, 2008.

Allen, P.B., Ouimet, C.C., and Greengard, P.: Spinophilin, a novel protein phosphatase 1 binding protein localized to dendritic spines. *Proc. Natl. Acad. Sci. USA*, 94:9956-61, 1997.

Asaki, C., Usuda, N., Nakazawa, A., Kametani, K., and Suzuki, T.: Localization of translational components at the ultramicroscopic level at postsynaptic sites of the rat brain. *Brain Res.*, 972:168–176, 2003.

Ashraf, S.I., McLoon, A.L., Sclarsic, S.M. and Kunes, S.: Synaptic protein synthesis associated with memory is regulated by the RISC pathway in Drosophila. *Cell,* 124:191–205, 2006.

Bartel, D.P.: MicroRNAs: target recognition and regulatory functions. *Cell,* 36:15-33, 2009.

Barthelson, R.A., Lambert, G.M., Vanier, C., Lynch, R.M., and Galbraith, D.W.: Comparison of the contributions of the nuclear and cytoplasmic compartments to global gene expression in human cells. *B.M.C. Genomics,* 8:340, 2007.

Berezikov, E., Chung, W.J., Willis, J., Cuppen, E., and Lai, E.C.: Mammalian mirtron genes. *Mol. Cell,* 28:328-36, 2007.

Bernstein, E., Caudy, A.A., Hammond, S.M., and Hannon, G.J.: Role for a bidentate ribonuclease in the initiation step of RNA interference. *Nature,* 409:363−366, 2001.

Beveridge, N.J., Tooney, P.A., Carroll, A.P., Gardiner, E., Bowden, N., Scott, R.J., Tran, N., Dedova, I., and Cairns, M.J.: Dysregulation of miRNA 181b in the temporal cortex in schizophrenia. *Hum. Mol. Genet.,* 17:1156-1168, 2008.

Bourne, J.N., Sorra, K.E., Hurlburt, J., and Harris, K.M.: Polyribosomes are increased in spines of CA1 dendrites 2 h after the induction of LTP in mature rat hippocampal slices. *Hippocampus*, 17:1-4, 2007.

Brady, S.T.: A novel brain ATPase with properties expected for the fast axonal transport motor. *Nature,* 317:73-75, 1985.

Brownawell, A.M., and Macara, I.G.: Exportin-5, a novel karyopherin, mediates nuclear export of double-stranded RNA binding proteins. *J. Cell Biol.,* 156:53-64, 2002.

Bushati, N., and Cohen, S.M.: MicroRNA functions. *Annu. Rev. Cell Dev. Biol.*, 23:175–205, 2007.

Cai, X., Hagedorn, C.H., and Cullen, B.R.: Human microRNAs are processed from capped, polyadenylated transcripts that can also function as mRNAs. *RNA*, 10:1957-1966, 2004.

Cai, Y., Singh, B.B., Aslanukov, A., Zhao, H., and Ferreira, P.A.: The docking of kinesins, KIF5B and KIF5C, to Ran-binding protein 2 (RanBP2) is mediated via a novel RanBP2 domain. *J. Biol. Chem.,* 276:41594–41602, 2001.

Carmell, M.A., Xuan, Z., Zhang, M.Q., and Hannon, G.J.: The Argonaute family: tentacles that reach into RNAi, developmental control, stem cell maintenance, and tumorigenesis. *Genes Dev.,* 16:2733-42, 2001.

Caudy, A.A., Myers, M., Hannon, G.J., and Hammond, S.M.: Fragile X-related protein and VIG associate with the RNA interference machinery. *Genes Dev.,* 16:2491–2496, 2002.

Ceman, S., O'Donnell, W.T., Reed, M., Patton, S., Pohl, J., and Warren, S.T.: Phosphorylation influences the translation state of FMRP-associated polyribosomes. *Hum. Mol. Genet.,* 12:3295-3305, 2003.

Chan, S.L., and Mattson, M.P.: Caspase and calpain substrates: roles in synaptic plasticity and cell death. *J. Neurosci. Res.,* 58:167–190, 1999.

Cheever, A., and Ceman, S.: Phosphorylation of FMRP inhibits association with Dicer. *RNA,* 15:362-366, 2009.

Chekulaeva, M., and Filipowicz, W.: Mechanisms of miRNA-mediated post-transcriptional regulation in animal cells. *Curr. Opin. Cell Biol.,* 21:452-460, 2009.

Clark, A.M., Goldstein, L.D., Tevlin, M., Tavaré, S., Shaham, S., Miska, E.A.: The microRNA miR-124 controls gene expression in the sensory nervous system of Caenorhabditis elegans. *Nucleic Acids Res.,* 38:3780-3793, 2010.

Chendrimada, T.P., Gregory, R.I., Kumaraswamy, E., Norman, J., Cooch, N., Nishikura, K., and Shiekhattar, R.: TRBP recruits the Dicer complex to Ago2 for microRNA processing and gene silencing. *Nature*, 436:740-744, 2005.

Davidovic, L., Jaglin, X.H., Lepagnol-Bestel, A.M., Tremblay, S., Simonneau, M., Bardoni, B., and Khandjian, E.W.: The fragile X mental retardation protein is a molecular adaptor between the neurospecific KIF3C kinesin and dendritic RNA granules. *Hum. Mol. Genet.,* 16:3047–3058, 2007.

DeBoer, S.R., You, Y., Szodorai, A., Kaminska, A., Pigino, G., Nwabuisi, E., Wang, B., Estrada-Hernandez, T., Kins, S., Brady, S.T., and Morfini, G.: Conventional kinesin holoenzymes are composed of heavy and light chain homodimers. *Biochemistry,* 47:4535-4543, 2008.

Dictenberg, J.B., Swanger, S.A., Antar, L.N., Singer, R.H., and Bassell, G.J.: A direct role for FMRP in activity-dependent dendritic mRNA transport links filopodial-spine morphogenesis to fragile X syndrome. *Dev. Cell,* 14:926-939, 2008.

Doi, N., Zenno, S., Ueda, R., Ohki-Hamazaki, H., Ui-Tei, K., and Saigo, K.: Short-interfering-RNA-mediated gene silencing in mammalian cells requires Dicer and eIF2C translation initiation factors. *Curr. Biol.,* 13:41-46, 2003.

Dosemeci, A., Makusky, A.J., Jankowska-Stephens, E., Yang, X., Slotta, D.J., and Markey, S.P.: Composition of the synaptic PSD-95 complex. *Mol. Cell Proteomics,* 6:1749-1760, 2007.

Dostie, J., Mourelatos, Z., Yang, M., Sharma, A., and Dreyfuss, G.: Numerous microRNPs in neuronal cells containing novel microRNAs. *RNA,* 9:180–186, 2003.

Dwivedi, Y.: Evidence demonstrating role of microRNAs in the etiopathology of major depression., *J. Chem. Neuroanat.,* Apr 14, 2011.

Eberwine, J., Miyashiro, K., Kacharmina, J.E., and Job, C.: Local translation of classes of mRNAs that are targeted to neuronal dendrites. *Proc. Natl. Acad. Sci. USA*, 98:7080-7085, 2001.

Eis, P.S., Tam, W., Sun, L., Chadburn, A., Li, Z., Gomez, M.F., Lund, E., and Dahlberg, J.E.: Accumulation of miR-155 and BIC RNA in human B cell lymphomas. *Proc. Natl Acad. Sci. USA,* 102:3627–3632, 2005.

Elbashir, S.M., Lendeckel, W., and Tuschl, T.: RNA interference is mediated by 21- and 22-nucleotide RNAs. *Genes Dev.*, 15:188−200, 2001.

Eyman, M., Cefaliello, C., Ferrara, E., De Stefano, R., Crispino, M., and Giuditta, A.: Synaptosomal protein synthesis is selectively modulated by learning. *Brain Res.,* 1132:148-157, 2007.

Fabian, M.R., Mathonnet, G., Sundermeier, T., Mathys, H., Zipprich, J.T., Svitkin, Y.V., Rivas, F., Jinek, M., Wohlschlegel, J., Doudna, J.A., Chen, C.Y., Shyu, A.B., Yates, J.R. 3rd, Hannon, G.J., Filipowicz, W., Duchaine, T.F., and Sonenberg, N.: Mammalian miRNA RISC recruits CAF1 and PABP to affect PABP-dependent deadenylation. *Mol. Cell,* 35:868-880, 2009.

Feng, J., Yan, Z., Ferreira, A., Tomizawa, K., Liauw, J.A., Zhuo, M., Allen, P.B., Ouimet, C.C., and Greengard, P.: Spinophilin regulates the formation and function of dendritic spines. *Proc. Natl. Acad. Sci. USA,* 97:9287-9292, 2000.

Ferrari, F., Mercaldo, V., Piccoli, G., Sala, C., Cannata, S., Achsel, T., and Bagni, C.: The fragile X mental retardation protein-RNP granules show an mGluR-dependent localization in the post-synaptic spines. *Mol. Cell. Neurosci.,* 34:343–354, 2007.

Filipowicz, W., Bhattacharyya, S.N., and Sonenberg, N.: Mechanisms of post-transcriptional regulation by microRNAs: are the answers in sight?. *Nat. Rev. Genet.,* 9:102-114, 2008.

Fire, A., Xu, S., Montgomery, M.K., Kostas, S.A., Driver, S.E., and Mello, C.C.: Potent and specific genetic interference by double-stranded RNA in Caenorhabditis elegans. *Nature,* 391:806-811, 1998.

Friedman, R.C., Farh, K.K., Burge, C.B., and Bartel, D.P.: Most mammalian mRNAs are conserved targets of microRNAs. *Genome Res.,* 19:92-105, 2008.

Fiore, R., and Schratt, G.: MicroRNAs in synapse development: tiny molecules to remember. *Expert. Opin. Biol. Ther.,* 7:1823-1831, 2007.

Fiore, R., Siegel, G., and Schratt, G.: MicroRNA function in neuronal development, plasticity and disease. *Biochim. Biophys. Acta,* 1779:471-478, 2008.

Fiore, R., Khudayberdiev, S., Christensen, M., Siegel, G., Flavell, S.W., Kim, T.K., Greenberg, M.E., and Schratt, G.: Mef2-mediated transcription of the miR379-410 cluster regulates activity-dependent dendritogenesis by fine-tuning Pumilio2 protein levels. *EMBO J.,* 28:697-710, 2009.

Fortin, K.R., Nicholson, R.H., and Nicholson, A.W.: Mouse ribonuclease III. cDNA structure, expression analysis, and chromosomal location. *B.M.C. Genomics,* 3:26, 2002.

Gao, J., Wang, W.Y., Mao, Y.W., Gräff, J., Guan, J.S., Pan, L., Mak, G., Kim, D., Su, S.C., and Tsai, L.H.: A novel pathway regulates memory and plasticity via SIRT1 and miR-134. *Nature*, 466:1105-1109, 2010.

Ghildiyal, M., and Zamore, P.D.: Small silencing RNAs: an expanding universe. *Nat. Rev. Genet.,* 10:94-108, 2009.

Grishok, A., Pasquinelli, A.E., Conte, D., Li N., Parrish, S., Ha, I., Baillie, D.L., Fire, A., Ruvkun, G., and Mello, C.C.: Genes and mechanisms related to RNA interference regulate expression of the small temporal RNAs that control C. elegans developmental timing. *Cell,* 106:23-34, 2001.

Guillaud, L., Setou, M., and Hirokawa, N.: KIF17 dynamics and regulation of NR2B trafficking in hippocampal neurons. *J. Neurosci.,* 23:131-140, 2003.

Hammond, S.M., Bernstein, E., Beach, D., and Hannon, G.J.: An RNA-directed nuclease mediates post-transcriptional gene silencing in Drosophila cells. *Nature,* 404:293-296, 2000.

Hammond, S.M., Boettcher, S., Caudy, A.A., Kobayashi, R., and Hannon, G.J.: Argonaute2, a link between genetic and biochemical analyses of RNAi. *Science,* 293:1146-1150, 2001.

Han, J., Lee, Y., Yeom, K.H., Kim, Y.K., Jin, H., and Kim, V.N.: The Drosha-DGCR8 complex in primary microRNA processing. *Genes Dev.,* 18:3016-3027, 2004.

Han, J., Lee, Y., Yeom, K.H., Nam, J.W., Heo, I., Rhee, J.K., Sohn, S.Y., Cho, Y., Zhang, B.T., and Kim, V.N.: Molecular basis for the recognition of primary microRNAs by the Drosha-DGCR8 complex. *Cell,* 125:887-901, 2006.

Han, J., Pedersen, J.S., Kwon, S.C., Belair, C.D., Kim, Y.K., Yeom, K.H., Yang, W.Y., Haussler, D., Blelloch, R., and Kim, V.N.: Posttranscriptional crossregulation between Drosha and DGCR8. *Cell,* 136:75-84, 2009.

Henke, J.I., Goergen, D., Zheng, J., Song, Y., Schüttler, C.G., Fehr, C., Jünemann, C., and Niepmann, M.: MicroRNA-122 stimulates translation of hepatitis C virus RNA. *EMBO J.,* 27:3300-3310, 2008.

Hirokawa, N.: mRNA transport in dendrites: RNA granules, motors, and tracks. *J. Neurosci.,* 26:7139-7142, 2006.

Hirokawa, N., and Noda, Y.: Intracellular transport and kinesin superfamily proteins, KIFs: structure, function, and dynamics. *Physiol. Rev.,* 88:1089-1118, 2008.

Hutvágner, G., McLachlan, J., Pasquinelli, A.E., Bálint, E., Tuschl, T., and Zamore, P.D.: A cellular function for the RNA-interference enzyme Dicer in the maturation of the let-7 small temporal RNA. *Science,* 293:834−838, 2001.

Ishizuka, A., Siomi, M.C. and Siomi, H.: A Drosophila fragile X protein interacts with components of RNAi and ribosomal proteins. *Genes Dev.,* 16:2497–2508, 2002.

Jiang, J., Lee, E.J., Gusev, Y. and Schmittgen, T.D.: Real-time expression profiling of microRNA precursors in human cancer cell lines. *Nucleic Acids Res.,* 33:5394-5403, 2005.

Jin, P., Zarnescu, D.C., Ceman, S., Nakamoto, M., Mowrey, J., Jongens, T.A., Nelson, D.L., Moses, K. and Warren, S.T.: Biochemical and genetic interaction between the

fragile X mental retardation protein and the microRNA pathway. *Nature Neurosci.,* 7:113–117, 2004.

Ju, W., Morishita, W., Tsui, J., Gaietta, G., Deerinck, T.J., Adams, S.R., Garner, C.C., Tsien, R.Y., Ellisman, M.H., and Malenka, R.C.: Activity-dependent regulation of dendritic synthesis and trafficking of AMPA receptors. *Nature Neurosci.,* 7:244-253, 2004.

Kanai, Y., Okada, Y., Tanaka, Y., Harada, A., Terada, S., and Hirokawa, N.: KIF5C, a novel neuronal kinesin enriched in motor neurons. *J. Neurosci.,* 20:6374-6384, 2000.

Kanai, Y., Dohmae, N., and Hirokawa, N.: Kinesin transports RNA: isolation and characterization of an RNA-transporting granule. *Neuron,* 43:513-525, 2004.

Ketting, R.F., Fischer, S.E., Bernstein, E., Sijen, T., Hannon, G.J., and Plasterk, R.H.: Dicer functions in RNA interference and in synthesis of small RNA involved in developmental timing in C. elegans. *Genes Dev.,* 15:2654−2659, 2001.

Kim, J., Krichevsky, A., Grad, Y., Hayes, G.D., Kosik, K.S., Church, G.M. and Ruvkun, G.: Identification of many microRNAs that copurify with polyribosomes in mammalian neurons. *Proc. Natl Acad. Sci. USA,* 101:360–365, 2004.

Klein, M.E., Lioy, D.T., Ma, L., Impey, S., Mandel, G., and Goodman, R.H.: Homeostatic regulation of MeCP2 expression by a CREB-induced microRNA. *Nat. Neurosci.,* 10:1513-1514, 2007.

Kosik, K.S.: The neuronal microRNA system. *Nat. Rev. Neurosci.,* 7:911–920, 2006.

Krichevsky, A.M., and Kosik, K.S.: Neuronal RNA granules: a link between RNA localization andstimulation-dependent translation. *Neuron,* 32:683-696, 2001.

Krichevsky, A.M., King, K.S., Donahue, C.P., Khrapko, K. and Kosik, K.S.: A microRNA array reveals extensive regulation of microRNAs during brain development. *RNA,* 9:1274–1281, 2003.

Kye, M.J., Liu, T., Levy, S.F., Xu, N.L., Groves, B.B., Bonneau, R., Lao, K. and Kosik, K.S.: Somatodendritic microRNAs identified by laser capture and multiplex RT-PCR. *RNA,* 13:1224–1234, 2007.

Landthaler, M., Yalcin, A., and Tuschl, T.: The human DiGeorge syndrome critical region gene 8 and its D. melanogaster homolog are required for miRNA biogenesis. *Curr. Biol.,* 14:2162-2167, 2004.

Lau, N.C., Lim, L.P., Weinstein, E.G., and Bartel, D.P.: An abundant class of tiny RNAs with probable regulatoryroles in Caenorhabditis elegans. *Science,* 294:858-862, 2001.

Lagos-Quintana, M., Rauhut, R., Lendeckel, W., and Tuschl, T.: Identification of novel genes coding for small expressed RNAs. *Science,* 294:853-858, 2001.

Lagos-Quintana, M., Rauhut, R., Yalcin, A., Meyer, J., Lendeckel, W. and Tuschl, T.: Identification of tissue-specific microRNAs from mouse. *Curr. Biol.,* 12:735–739, 2002.

Lagos-Quintana, M., Rauhut, R., Meyer, J., Borkhardt, A., and Tuschl, T.: New microRNAs from mouse and human. *RNA,* 9:175-179, 2003.

Lee, R.C., Feinbaum, R.L., and Ambros, V.: The C. elegans heterochronic gene lin-4 encodes small RNAs with antisense complementarity to lin-14. *Cell,* 75:843-854, 1993.

Lee, Y., Jeon, K., Lee, J.T., Kim, S., and Kim, V.N.: MicroRNA maturation: stepwise processing and subcellular localization. *EMBO J.,* 21:4663–4670, 2002.

Lee, Y., Ahn, C., Han, J., Choi, H., Kim, J., Yim, J., Lee, J., Provost, P., Rådmark, O., Kim, S., and Kim, V.N.: The nuclear RNase III Drosha initiates microRNA processing. *Nature,* 425:415–419, 2003.

Lee, Y., Kim, M., Han, J., Yeom, K.H., Lee, S., Baek, S.H., and Kim, V.N.: MicroRNA genes are transcribed by RNA polymerase II. *EMBO J.,* 23:4051-4056, 2004.

Lee, Y., Hur, I., Park, S.Y., Kim, Y.K., Suh, M.R., and Kim, V.N.: The role of PACT in the RNA silencing pathway. *EMBO J.,* 25:522-532, 2006.

Leopold, P.L., McDowall, A.W., Pfister, K.K., Bloom, G.S., and Brady, S.T.: Association of kinesin with characterized membrane-bounded organelles. *Cell Motil. Cytoskeleton,* 23:19–33, 1992.

Li, F., Pallan, P.S., Maier, M.A., Rajeev, K.G., Mathieu, S.L., Kreutz, C., Fan, Y., Sanghvi, J., Micura, R., Rozners, E., Manoharan, M., and Egli, M.: Crystal structure, stability and in vitro RNAi activity of oligoribonucleotides containing the ribo-difluorotoluyl nucleotide: insights into substrate requirements by the human RISC Ago2 enzyme. *Nucleic Acids Res.,* 35:6424-6438, 2007.

Li, H.L., Chelladurai, B.S., Zhang, K., and Nicholson, A.W.: Ribonuclease III cleavage of a bacteriophage T7 processing signal. Divalent cation specificity, and specific anion effects. *Nucleic Acids Res.,* 21:1919-1925, 1993.

Lugli, G., Larson, J., Martone, M.E., Jones, Y., and Smalheiser, N.R.: Dicer and eIF2c are enriched at postsynaptic densities in adult mouse brain and are modified by neuronal activity in a calpain-dependent manner. *J. Neurochem.,* 94:896–905, 2005.

Lugli, G., Torvik, V.I., Larson, J., and Smalheiser, N.R.: Expression of microRNAs and their precursors insynaptic fractions of adult mouse forebrain. *J. Neurochem.,* 106:650-661, 2008.

Lynch, G., and Baudry, M.: Brain spectrin, calpain and long-term changes in synaptic efficacy. *Brain Res. Bull.,* 18:809–815, 1987.

Lynch, D.R., Gleichman, A.J.: Picking up the pieces: the roles of functional remnants of calpainmediatedproteolysis. *Neuron,* 53:317-319, 2007.

Ma, E., MacRae, I.J., Kirsch, J.F., and Doudna, J.A.: Autoinhibition of human dicer by its internal helicase domain. *J. Mol. Biol.,* 380:237-243, 2008.

Miska, E.A., Alvarez-Saavedra, E., Townsend, M., Yoshii, A., Sestan, N., Rakic, P., Constantine-Paton M. and Horvitz H.R.: Microarray analysis of microRNA expression in the developing mammalian brain. *Genome Biol.,* 5:R68, 2004.

Mourelatos, Z., Dostie, J., Paushkin, S., Sharma, A., Charroux, B., Abel, L., Rappsilber, J., Mann, M., and Dreyfuss, G.: miRNPs: a novel class of ribonucleoproteins containing numerous microRNAs. *Genes Dev.,* 16:720-728, 2002.

Mullen, R.J., Buck, C.R., and Smith, A.M.: NeuN, a neuronal specific nuclear protein in vertebrates. *Development,* 116:201-211, 1992.

Nicholson, A.W.: Function, mechanism and regulation of bacterial ribonucleases. *FEMS Microbiol Rev.,* 23:371-390, 1999.

Nicoloso, M., Qu, L.H., Michot, B., and Bachellerie, J.P.: Intron-encoded, antisense small nucleolar RNAs: the characterization of nine novel species points to their direct role as guides for the 2'-O-ribose methylation of rRNAs. *J. Mol. Biol.,* 260:178-195, 1996.

Ostroff, L.E., Fiala, J.C., Allwardt, B., and Harris, K.M.: Polyribosomes redistribute from dendritic shafts intospines with enlarged synapses during LTP in developing rat hippocampal slices. *Neuron,* 35:535-545, 2002.

Ørom, U.A., Nielsen, F.C., and Lund, A.H.: MicroRNA-10a binds the 5'UTR of ribosomal protein mRNAs and enhances their translation. *Mol. Cell,* 30:460-71, 2008.

Pasquinelli, A.E., Reinhart, B.J., Slack, F., Martindale, M.Q., Kuroda, M.I., Maller, B., Hayward, D.C., Ball, E.E., Degnan, B., Müller, P., Spring, J., Srinivasan, A., Fishman, M., Finnerty, J., Corbo, J., Levine, M., Leahy, P., Davidson, E., and Ruvkun, G.: Conservation of the sequence and temporal expression of let-7 heterochronic regulatory RNA. *Nature,* 408: 86-89, 2000.

Park, C.S., and Tang, S.J.: Regulation of microRNA Expression by Induction of Bidirectional Synaptic Plasticity. *Journal of Molecular Neuroscience,* 38:50–66, 2008.

Perkins, D.O., Jeffries, C.D., Jarskog, L.F., Thomson, J.M., Woods, K., Newman, M.A., Parker, J.S., Jin, J., and Hammond, S.M.: microRNA expression in the prefrontal cortex of individuals with schizophrenia and schizoaffective disorder. *Genome Biol.,* 8:R27, 2007.

Plante, I., Davidovic, L., Ouellet, D.L., Gobeil, L.A., Tremblay, S., Khandjian, E.W. and Provost, P.: Dicer-Derived MicroRNAs Are Utilized by the Fragile X Mental Retardation Protein for Assembly on Target RNAs. *J. Biomed. Biotechnol.,* 2006:64347, 2006

Provost, P., Dishart, D., Doucet, J., Frendewey, D., Samuelsson, B., and Radmark, O.: Ribonuclease activity and RNA binding of recombinant human Dicer. *EMBO J.,* 21:5864–5874, 2002.

Rajasethupathy, P., Fiumara, F., Sheridan, R., Betel, D., Puthanveettil, S.V., Russo, J.J., Sander, C., Tuschl, T., and Kandel, E..: Characterization of small RNAs in Aplysia reveals a role for miR-124 in constraining synaptic plasticity through CREB. *Neuron,* 63:803-817, 2009.

Rodriguez, A., Griffiths-Jones, S., Ashurst, J.L., and Bradley, A.: Identification of mammalian microRNA host genes and transcription units. *Genome Res.,* 14:1902–1910, 2004.

Ryu, S., Joshi, N., McDonnell, K., Woo, J., Choi, H., Gao, D., McCombie, W.R., and Mittal, V.: Discovery of novel human breast cancer microRNAs from deep sequencing data by analysis of pri-microRNA secondary structures. *PLoS One,* 6:e16403, 2011.

Saini, H.K., Griffiths-Jones, S., and Enright, A.J.: Genomic analysis of human microRNA transcripts. *Proc. Natl. Acad. Sci. USA,* 104:17719–17724, 2007.

Sánchez-Carbente Mdel, R., and Desgroseillers, L.: Understanding the importance of mRNA transport inmemory. *Prog. Brain Res.,* 169:41-58, 2008.

Schad, A., Fahimi, H.D., Völkl, A., and Baumgart, E.: Expression of catalase mRNA and protein in adult rat brain: detection by nonradioactive in situ hybridization with signal amplification by catalyzed reporter deposition (ISH-CARD) and immunohistochemistry (IHC)/immunofluorescence (IF). *J. Histochem. Cytochem.,* 51:751-760, 2003.

Schmittgen, T.D., Lee, E.J., Jiang, J., Sarkar, A., Yang, L., Elton, T.S. and Chen, C.: Real-time PCR quantification of precursor and mature microRNA. *Methods,* 44:31-38, 2008.

Schratt, G.M., Tuebing, F., Nigh, E.A., Kane, C.G., Sabatini, M.E., Kiebler, M., and Greenberg, M.E.: A brain-specific microRNA regulates dendritic spine development. *Nature,* 439:283–289, 2006.

Schratt, G.: microRNAs at the synapse. *Nat. Rev. Neurosci.,* 10:842-849, 2009.

Sempere, L.F., Freemantle, S., Pitha-Rowe, I., Moss, E., Dmitrovsky, E. and Ambros, V.: Expression profiling of mammalian microRNAs uncovers a subset of brain-expressed microRNAs with possible roles in murine and human neuronal differentiation. *Genome Biol.,* 5:R13, 2004.

Setou, M., Seog, D.H., Tanaka, Y., Kanai, Y., Takei, Y., Kawagishi, M., and Hirokawa, N.: Glutamate-receptorinteracting protein GRIP1 directly steers kinesin to dendrites. *Nature,* 417:83-87, 2002.

Siegel, G., Obernosterer, G., Fiore, R., Oehmen, M., Bicker, S., Christensen, M., Khudayberdiev, S., Leuschner, P.F., Busch, C.J., Kane, C., Hübel, K., Dekker, F., Hedberg, C., Rengarajan, B., Drepper, C., Waldmann, H., Kauppinen, S., Greenberg, M.E., Draguhn, A., Rehmsmeier, M., Martinez J., and Schratt, G.M.: A functional screen implicates microRNA-138-dependent regulation of the depalmitoylation enzyme APT1 in dendritic spine morphogenesis. *Nat. Cell Biol.,* 11:705-716, 2009.

Smalheiser, N.R. and Collins, B.J.: Coordinate enrichment of cranin (dystroglycan) subunits in synaptic membranes of sheep brain. *Brain Res.,* 887:469–471, 2000.

Smalheiser, N.R., Manev, H., and Costa, E.: RNAi and brain function: Was McConnell on the right track? *Trends in Neurosciences,* 24:216–218, 2001.

Smalheiser, N.R., Lugli, G., Rizavi, H.S., Zhang, H., Torvik, V.I., Pandey, G.N., Davis, J.M., and Dwivedi, Y.: MicroRNA expression in rat brain exposed to repeated inescapable shock: differential alterations in learned helplessness vs. non-learned helplessness. *Int. J. Neuropsychopharmacol.,* 28:1-11, 2011.

Smirnova, L., Gräfe, A., Seiler, A., Schumacher, S., Nitsch, R. and Wulczyn, F.G.: Regulation of miRNA expression during neural cell specification. *Eur. J. Neurosci.*, 21:1469–1477, 2005.

Song, J.J., Liu, J., Tolia, N.H., Schneiderman, J., Smith, S.K., Martienssen, R.A., Hannon, G.J., and Joshua-Tor, L.: The crystal structure of the Argonaute2 PAZ domain reveals an RNA binding motif in RNAi effector complexes. *Nat. Struct. Biol.,* 10:1026-1032, 2003.

Song, J.J., Smith, S.K., Hannon, G.J., and Joshua-Tor, L.: Crystal structure of Argonaute and its implications for RISC slicer activity. *Science,* 305:1434-1437, 2004.

Sossin, W.S., and DesGroseillers, L.: Intracellular trafficking of RNA in neurons. *Traffic.,* 7:1581-1589, 2006.

Stark, K.L., Xu, B., Bagchi, A., Lai, W.S., Liu, H., Hsu, R., Wan, X., Pavlidis, P., Mills, A.A., Karayiorgou, M., and Gogos, J.A.: Altered brain microRNA biogenesis contributes to phenotypicdeficits in a 22q11-deletion mouse model. *Nat. Genet.,* 40:751-760, 2008.

Sutton, M.A., and Schuman, E.M.: Local translational control in dendrites and its role in long-term synaptic plasticity. *J. Neurobiol.,* 64:116, 2005.

Suzuki, T., Tian, Q.B., Kuromitsu, J., Kawai, T. and Endo, S.: Characterization of mRNA species that are associated with postsynaptic density fraction by gene chip microarray analysis. *Neurosci. Res.,* 57:61–85, 2007.

Tai, H.C., and Schuman, E.M.: MicroRNA: microRNAs reach out into dendrites. *Curr. Biol.,* 16:R121–123, 2006.

Talebizadeh, Z., Butler, M.G., and Theodoro, M.F.: Feasibility and relevance of examining lymphoblastoid cell lines to study role of microRNAs in autism. *Autism Research,* 1:240-250, 2008.

Tang, X., Zhang, Y., Tucker, L., and Ramratnam, B.: Phosphorylation of the RNase III enzyme Drosha at Serine300 or Serine302 is required for its nuclear localization. *Nucleic Acids Res.,* 38:6610-6619, 2010.

Todd, P.K., Mack, K.J., Malter, J.S.: The fragile X mental retardation protein is required for type-I metabotropic glutamate receptor-dependent translation of PSD-95. *Proc. Natl. Acad. Sci. USA,* 100:14374-14378, 2003.

Triboulet, R., Chang, H.M., Lapierre, R.J., and Gregory, R.I.: Post-transcriptional control of DGCR8 expression by the Microprocessor. *RNA*, 15:1005-1011, 2009.

Tsurudome, K., Tsang, K., Liao, E.H., Ball, R., Penney, J., Yang, J.S., Elazzouzi, F., He, T., Chishti, A., Lnenicka, G., Lai, E.C., and Haghighi, A.P.: The Drosophila miR-310 cluster negatively regulates synaptic strength at the neuromuscular junction. *Neuron*, 68:879-893, 2010.

Tucker, R.P., Garner, C.C., and Matus, A.: In situ localization of microtubule-associated protein mRNA in the developing and adult rat brain. *Neuron,* 2:1245-1256, 1989.

Vasudevan, S., Tong, Y., and Steitz, J.A.: Switching from repression to activation: microRNAs can up-regulate translation. *Science,* 318:1931–1934, 2007.

Vasudevan, S., Tong, Y., and Steitz, J.A.: Cell-cycle control of microRNA-mediated translation regulation. *Cell Cycle,* 7:1545-1549, 2008.

Velleca, M.A., Wallace, M.C., and Merlie, J.P.: A novel synapse-associated noncoding RNA. *Mol. Cell. Biol.,* 14:7095–7104, 1994.

Vessey, J.P., Vaccani, A., Xie, Y., Dahm, R., Karra, D., Kiebler, M.A., and Macchi, P.: Dendritic localization of the translational repressor Pumilio 2 and its contribution to dendritic stress granules. *J. Neurosci.,* 26:6496–6508, 2006.

Vinade, L., Chang, M., Schlief, M.L., Petersen, J.D., Reese, T.S., Tao-Cheng, J.H., and Dosemeci, A.: Affinity purification of PSD-95-containing postsynaptic complexes. *J. Neurochem.,* 87:1255–1261, 2003.

Vitali, P., Royo, H., Marty, V., Bortolin-Cavaillé, M.L., and Cavaillé J.: Long nuclear-retained non-coding RNAs and allele-specific higher-order chromatin organization at imprinted snoRNA gene arrays. *J. Cell Sci.,* 123:70-83, 2010.

Vo, N., Klein, M.E., Varlamova, O., Keller, D.M., Yamamoto, T., Goodman, R.H., and Impey, S.: A cAMP-response element binding protein-induced microRNA regulates neuronal morphogenesis. *Proc. Natl. Acad. Sci. USA,* 102:16426-16431, 2005.

Wang, Y., Medvid, R., Melton, C., Jaenisch, R., and Blelloch, R.: DGCR8 is essential for microRNA biogenesis and silencing of embryonic stem cell self-renewal. *Nat. Genet.,* 39:380-385, 2007.

Weiler, I.J., Irwin, S.A., Klintsova, A.Y., Spencer, C.M., Brazelton, A.D., Miyashiro, K., Comery, T.A., Patel, B., Eberwine, J., and Greenough, W.T.: Fragile X mental retardation protein is translated near synapses in response to neurotransmitter activation. *Proc. Natl. Acad. Sci. USA,* 94:5395–5400, 1997.

Welker, N.C., Maity, T.S., Ye, X., Aruscavage, P.J., Krauchuk, A.A., Liu, Q., and Bass, B.L.: Dicer's helicase domain discriminates dsRNA termini to promote an altered reaction mode. *Mol. Cell,* 41:589-599, 2011.

Wibrand, K., Panja, D., Tiron, A., Ofte, M.L., Skaftnesmo, K.O., Lee, C.S., Pena, J.T., Tuschl, T., and Bramham, C.R.: Differential regulation of mature and precursor microRNA expression by NMDA and metabotropic glutamate receptor activation during LTP in the adult dentate gyrus in vivo. *Eur. J. Neurosci.,* 31:636-645, 2010.

Wu, H., Xu, H., Miraglia, L.J., and Crooke, S.T.: Human RNase III is a 160-kDa protein involved in preribosomal RNA processing. *J. Biol. Chem.,* 275:36957−36965, 2000.

Wulczyn, F.G., Smirnova, L., Rybak, A., Brandt, C., Kwidzinski, E., Ninnemann, O., Strehle, M., Seiler, A., Schumacher, S. and Nitsch, R.: Post-transcriptional regulation of the let-7 microRNA during neural cell specification. *FASEB J.,* 21:415–426, 2007.

Xu, X.L., Li, Y., Wang, F., Gao, F.B.: The steady-state level of the nervous-system-specific microRNA-124a is regulated by dFMR1 in Drosophila. *J. Neurosci*., 28:11883-11889, 2008.

Yi, R., Qin, Y., Macara, I.G., and Cullen, B.R.: Exportin-5 mediates the nuclear export of pre-microRNAs and short hairpin RNAs. *Genes Dev.,* 17:3011-3016, 2003.

Yu, J.Y., Chung, K.H., Deo, M., Thompson, R.C., and Turner, D.L.: MicroRNA miR-124 regulates neurite outgrowth during neuronal differentiation. *Exp. Cell Res.,* 314: 2618-2633, 2008.

Zamore, P.D., Tuschl, T., Sharp, P.A., and Bartel, D.P.: RNAi: double-stranded RNA directs the ATP-dependent cleavage of mRNA at 21 to 23 nucleotide intervals. *Cell,* 101:25-33, 2000.

Zhang, H., Kolb, F.A., Brondani, V., Billy, E., and Filipowicz, W.: Human Dicer preferentially cleaves dsRNAs at their termini without a requirement for ATP. *EMBO J.,* 21:5875–5885, 2002.

VITA

NAME: Giovanni Lugli

EDUCATION: B.S., Pharmacy, University of Modena, Italy, 1994

M.S., Pharmaceutical science, University of Modena, Italy, 1994

Ph.D. Neuroscience, University of Illinois at the Medical Center, Chicago, Illinois, 2011

WORKING: Pharmacist, Farmacia Berni, Reggio Emilia, Italy, 1996-2001

Technical director (Doctor) of "Afford cosmetic diffusion", Modena, Italy, 2000-2001

Research specialist in health science, University of Illinois, Psychiatric Institute, Chicago, Illinois, 2001- present

HONORS: Fellowship from "ENRICO and ENRICA SOVENA foundation, University of Modena, Italy, 2001

PROFESSIONAL MEMBERSHIP: Pharmacists association of the province of Modena, (Italy)
Society of Neuroscience

ABSTRACTS: Ferioli, V., Rustichelli, C., Vezzalini, F., Gamberini, G., and Lugli, G.: Determination of Zinc Pyrithione and related compounds in hair care formulation by HPLC. *VI Meeting recent development and Application in the Pharmaceutical Analysis,* Milan 21-23, June 1995.

Ferioli, V., Vezzalini, F., Rustichelli, C., Gamberini, G., and Lugli, G.: HPLC structural characterization of Dihydroxyacetone as its bis-2,4-dinitrophenylhydrazone derivative. *VI Meeting recent development and Application in the Pharmaceutical Analysis,* Milan 21-23 June 1995.

Rustichelli, C., Vezzalini, F., Rossi, M.C., Ferioli, V., Lugli, G., and Gamberini G.: Investigation of cannabis constituent by HPLC/MS. *II Meeting Italian-Spanish of Therapeutical Chemistry,* Ferrara (Italy), 30 August - 3 September, 1995.

Avallone, R., Corsi, L., Lugli, G., and Baraldi, M.: Natural modulators of anxiety and sleep disturbances in food. *Euroffodchem XI*, Norwich, UK, 26-28 September, 2001.

Pappas, G.D., Kriho, V., Caruncho, H., Lugli, G., Smalheiser, N.R., Liu, W.S., and Costa, E.: Reelin in the olphactory bulb of the mouse: a model for schizophrenia research. *Neuroscience meeting*, Orlando, Nov. 2002.

Lugli, G., Larson, J., Martone, M.E., Jones, Y., and Smalheiser, N.R.: Dicer and eIF2c are enriched at PSDs in adult mouse brain and are modified by neuronal activity in a calpain-dependent manner. *Neuroscience meeting,* Washington D.C., Nov. 2005.

Lugli, G., Torvik, V.I., Larson, J., Smalheiser, N.R.: Expression of microRNAs and their precursors in synaptic fractions of adult mouse forebrain. *Neuroscience meeting*, Washington D.C., Nov. 2008.

Smalheiser, N.R., Lugli, G., Lenon, A.L., and Larson J.: Olfactory discrimination training increases expression of microRNAs in mouse hippocampus. *Neuroscience meeting,* Chicago, Nov. 2009.

Smalheiser, N.R., Lugli, G., Cook, E.H., Larson, J.: Endogenous siRNAs and noncoding RNA-derived small RNAs are expressed in adult mouse hippocampus and are up-regulated in olfactory discrimination training. *Neuroscience meeting,* San Diego, Nov. 2010.

PUBLICATIONS:

Lugli, G., Krueger, J.M., Davis, J.M., Persico, A., Keller, F. and Smalheiser, N.R.: Methodological factors influencing measurement and processing of plasma reelin in humans. *B.M.C. Biochem.,* 7:4-9, 2003.

Pappas, G.D., Kriho, V., Liu, W.S., Tremolizzo, L., Lugli, G., and Larson, J.: Immunocytochemical localization of reelin in the olfactory bulb of the heterozygous reel mouse: An animal model for schizophrenia. *Neurologiacal research,* 25:819-830, 2003.

Lugli, G., Larson, J., Martone, M.E., Jones, Y., and Smalheiser, N.R.: Dicer and eIF2c are Enriched at Postsynaptic Densities in Adult Mouse Brain and are Modified by Neuronal Activity in a Calpain-dependent Manner. *J. of Neurochemistry,* 94:896-905, 2005.

Lugli, G., Torvik, V.I., Larson, J., and Smalheiser, N.R.: Expression of microRNAs and their precursors in synaptic fractions of adult mouse forebrain. *J. of Neurochememistry,* 106:650-661, 2008.

Smalheiser, N.R., Lugli, G., Torvik, V.I., Mise, N., Ikeda, R., and Abe, K.: Natural antisense transcripts are co-expressed with sense mRNAs in synaptoneurosomes of adult mouse forebrain. *Neurosci Res.,* 62:236-239, 2008.

Smalheiser, N.R., and Lugli, G.: microRNA regulation of synaptic plasticity. *Neuromolecular Med.,* 11:133-140, 2009.

Smalheiser, N.R., Lugli, G., Lenon, A.L., Davis, J.M., Torvik, V.I. and Larson, J.R.: Olfactory discrimination training up-regulates and reorganizes expression of microRNAs in adult mouse hippocampus. *A.S.N. Neuro,* 2:28, 2010.

Smalheiser, N.R., Lugli, G., Thimmapuram, J., Cook, E.H., and Larson, J.: Endogenous siRNAs and noncoding RNA-derived small RNAs are expressed in adult mouse hippocampus and are up-regulated in olfactory discrimination training. *RNA,* 17:166-181, 2011.

Smalheiser, N.R., Lugli, G., Rizavi, H.S., Zhang, H., Torvik, V.I., Pandey, G.N., Davis, J.M., and Dwivedi, Y.: MicroRNA expression in rat brain exposed to repeated inescapable shock: differential alterations in learned helplessness vs. non-learned helplessness. *Int. J. Neuropsychopharmacol.,* 28:1-11, 2011.